TECHNISCHE UNIVERSITÄT WIEN

DIPLOMARBEIT

Momentum Broadening in a Highly Diluted Glasma

zur Erlangung des akademischen Grades

Diplom-Ingenieur

im Rahmen des Studiums

Technische Physik

eingereicht von

Daniel Schuh

Matrikelnummer: 01226227

ausgeführt am Institut für Theoretische Physik
der Fakultät für Physik der Technischen Universität Wien

Betreuung
Betreuer: Privatdoz. Dipl.-Ing. Dr.techn. Andreas Ipp
Mitbetreuer: Dipl.-Ing. Dr.techn. David Müller BSc

Wien, 5. August 2019

Unterschrift Daniel Schuh *Unterschrift Dr. Andreas Ipp*

Abstract

The Colour Glass Condensate is a model that describes high energy nuclei in the framework of a classical field theory. When two such nuclei collide, they can create the Glasma, which is the non-equilibrium precursor state of the Quark Gluon Plasma.

Jet quenching occurs when a jet or the parton that produces the jet interacts strongly with a medium so that a part of the jet cannot escape to reach the detector. The jet is therefore highly suppressed. Such interactions can be investigated by analysing momentum changes of the parton or the jet. Momentum broadening characterises changes in momentum of the parton that produces the jet. It describes the change in time of the average momentum squared of a test particle in said medium and has already been investigated in various media. It is the central part of this master's thesis.

After a review of the description of the colliding high energy nuclei in the Colour Glass Condensate framework, the boost invariant Yang-Mills equations are stated. Together with the corresponding initial conditions, they determine the dynamics of the Glasma. Then, their known solution up to second order is verified. This solution serves as the basis for the following analysis of the momentum broadening in the Glasma, which is the focus of the remaining part of this work.

Zusammenfassung

Das „Colour Glass Condensate“ ist ein Modell, das hochenergetische Kerne im Rahmen einer klassischen Feldtheorie beschreibt. Bei der Kollision zweier solcher Kerne entsteht das sogenannte Glasma. Es ist ein Nichtgleichgewichtszustand, aus dem sich nach kurzer Zeit das „Quark Gluon Plasma“ entwickelt.

Wenn durch starke Wechselwirkungen eines Teilchenstrahles oder des ihn erzeugenden Partons mit einem Medium der Strahl nicht vollständig aus dem Medium entkommen und somit den Detektor nur teilweise erreichen kann, spricht man von „jet quenching“. Diese Wechselwirkungen können durch die Untersuchung von Impulsänderungen des Strahles oder des Partons analysiert werden. Die Impulsverbreiterung charakterisiert die Impulsänderung des Partons, das den Strahl erzeugt. Sie beschreibt die zeitliche Änderung des gemittelten Impulsquadrates eines Testteilchens im betrachteten Medium und bildet den zentralen Teil dieser Arbeit.

Nach einer Wiederholung der bereits bekannten Beschreibung hochenergetischer Kerne im Rahmen des „Colour Glass Condensate“ werden die boostinvarianten Yang-Mills-Gleichungen vorgestellt, die gemeinsam mit den zugehörigen Anfangsbedingungen die Dynamik des Glasmas festlegen. Danach wird ihre bereits bekannte Lösung bis zur zweiten Ordnung verifiziert. Diese Lösung dient als Ausgangsbasis für die Analyse der Impulsverbreiterung eines Testteilchens im Glasma, der sich der restliche Teil der Arbeit widmet.

Contents

Chapter 1

Introduction

Nucleus-nucleus interactions are governed by the strong force. QCD calculations can be inaccessible, which is why models are developed that describe some aspects of QCD. One such model is the Colour Glass Condensate (CGC). It is an effective theory that describes high energy scattering in QCD [1] and will be used in this work to analyse high energy collisions of two nuclei. "Colour" in CGC states that the theory describes partons, which are coloured. They are also disordered and frozen, like in a "Glass". This system contains many gluons. For a saturated gluon density, it corresponds to a multi-particle Bose "Condensate".

A main idea of the CGC is the distinction between hard partons that carry high momentum, i.e. valence quarks and high energy gluons, and soft partons with lower momentum, i.e. lower energy gluons. The effective degrees of freedom in this classical field theory are therefore the colour charge density ρ, which describes the former, and the gauge field A_μ, which describes the latter [2]. The hard partons are affected by time dilation. Therefore, their colour configuration does not change much and is considered to be frozen with respect to QCD time scales. It is specified by some distribution function, for which the MV model is chosen in this master's thesis. It is presented in Section 2.3.

High-energy nuclei are strongly Lorentz contracted [3], hence usually they are treated as infinitely thin [4]. This assumption leads to boost invariance and consequently an effectively $2+1$ dimensional system, in which all observable quantities are independent of the spacetime rapidity η. In this work, *all* quantities are taken to be rapidity independent, not only the observable ones.

After a high energy nucleus-nucleus collision a state called "Glasma" is created [5]. It is described by a classical field and treated in terms of classical field theory. Its name originates from the "Glass" in CGC and the "Plasma" in Quark Gluon Plasma (QGP), which is the successor state of the Glasma [6]. The classical field that describes the Glasma is the vector potential A_μ. In [7], it is expanded in orders of the particle density ρ in a certain gauge and solved for the lowest non-vanishing order. The lowest non-vanishing order itself is a good approximation for a strongly diluted Glasma, whereas higher order terms become more significant for a denser Glasma.

In a high energy nuclei collision, high momentum parton pairs can be created, which move in opposite directions and lose energy whilst travelling through the Glasma. They produce jets of particles, which can be observed by particle detectors. If such a high momentum parton pair is created near the edge of a medium, it is possible that one parton and its corresponding jet lose much energy so that only a part of the jet escapes the medium. The jet produced by the other parton loses less energy, thus a higher portion of it is detected. Due to the jet of the former parton being partially missing, this phenomenon is called jet quenching. The interaction between such a parton, which will be called test parton, and the medium in question is therefore of interest. The momentum broadening of a test particle is a quantity of interest in the study of said interaction. [8] and [9] explore interactions between particle jets and the Quark Gluon Plasma, whereas the focus of this work is the Glasma.

The field A_μ determines the strong force acting on test particles in the Glasma. One parameter that can be extracted from this information is the transport coefficient $\hat{q}$, which is also called "momentum broadening" parameter and describes the radiative energy loss of a test particle [10]. It is discussed in two different media in [11], namely in a QED plasma and in a QCD plasma.

In Chapter 2, I will explain how one high energy nucleus is described in the CGC framework. Then, I will discuss two high energy nuclei moving in opposite directions, which resemble the system that creates the Glasma. Afterwards, I will present the equations of motion that govern the evolution of the Glasma and their boundary conditions. At the end of this chapter, I will give a short overview of the MV model, which is used to solve occurring ensemble averages. The content of Chapter 2 has already been well established by former works and is only to be taken as a foundation for the rest of this master's thesis. More information on this topic can be found e.g. in [12, 13].

In Chapter 3, I will expand the equations of motion and the corresponding initial conditions given in the previous chapter and solve them in close analogy to [7]. Afterwards, I will discuss whether the choice of gauge of ρ that is used as expansion parameter is special or interchangeable.

In Chapter 4, I will use the solution of the previous chapter and discuss the momentum broadening of a test parton in the Glasma. It depends on the trajectory of the test particle, hence I will start by deriving a formula for $\langle p^2 \rangle$ that depends on the trajectory. Then I will discuss two different trajectories, leading to the two momentum broadening parameters $\hat{q}$ and κ.

In Appendix A, I clarify my notations and conventions, in Appendix B, I discuss the coordinates that I use in this work and derive the Yang-Mills equations in Milne coordinates. In Appendix C, I list some properties of the Bessel differential equation and explain how they are applicable in this master's thesis, and Appendix D contains a detailed analysis of some integrals that arise during the calculation.

Chapter 2

Description of the Glasma

The Colour Glass Condensate is the description of choice of nuclei at high energy in this work. Their partons are described by classical colour fields and currents, and their dynamics is governed by the classical Yang-Mills equations. In this chapter, I will discuss one such high energy nucleus moving in z direction, then two nuclei moving in opposite directions, $+z$ and $-z$, so that they collide at $z = 0$, $t = 0$. Afterwards, I will present the equations of motion of the Glasma, which is produced by this collision, in the appropriate coordinates as well as the corresponding initial conditions. Finally, I will give an overview of the MV model.

2.1 Single Nucleus

The focus of this section is the description of one nucleus moving at the speed of light c in z direction. The four current $J_a^\mu(x)$ of particles, of which such a nucleus consists, has only one non-vanishing component in light cone coordinates, namely the J_a^+ component. Different coordinate systems are discussed in Appendix B. The current can be written in terms of the particle density $\rho_a(x)$ as

$$J_a^\mu(x) = \delta^{\mu+}\rho_a(x), \tag{2.1}$$

or equivalently, with the generators t_a of the associated symmetry group in the fundamental representation

$$J^\mu(x) = \delta^{\mu+}\rho_a(x)t_a. \tag{2.2}$$

Said symmetry group is $SU(3)$, nevertheless the formulas in this work will also be given for $SU(N_c)$ with arbitrary N_c.

Due to the assumption that the particles move at the constant speed c in z direction, their dynamics is infinitely time dilated. They are thus considered to be static in x^+, which means that $J^\mu(x)$ does not depend on x^+

$$J^\mu(x^-, x_T) = \delta^{\mu+}\rho_a(x^-, x_T)t_a. \tag{2.3}$$

Furthermore, the particles are infinitely Lorentz contracted and the current can be written as

$$J^\mu(x^-, x_T) = \delta^{\mu+}\delta(x^-)\rho_a(x_T)t_a. \tag{2.4}$$

Their distribution in the transversal plane is described by a probability functional introduced in Section 2.3.

The Yang-Mills equations

$$D_\mu F^{\mu\nu} = J^\nu \tag{2.5}$$

provide the link between the particles in question and the fields they create. The definitions of the covariant derivative D_μ and the field strength tensor $F_{\mu\nu}$ are given in Appendix A. To solve these equations of motion, a gauge and an ansatz are chosen, viz. the Lorentz gauge

$$\partial_\mu A^\mu = 0, \tag{2.6}$$

which is also known as covariant gauge, and

$$A^\mu(x^-, x_T) = \delta^{\mu+} A^+_a(x^-, x_T) t_a. \tag{2.7}$$

This ansatz turns out to be general enough because it does not lead to any conditions for $J^\mu(x^-, x_T)$.

The only non-zero component of A^μ is the + component, hence the imposed gauge condition becomes

$$\partial_+ A^+ = 0. \tag{2.8}$$

It is already respected by the chosen ansatz and thus does not lead to any additional conditions.

The field strength tensor is needed, so that the ansatz can be inserted into the Yang-Mills equations. Due to the fact that A^+ is the only non-zero component, the only possibly non-vanishing independent components of the field strength tensor are F^{+-} and F^{+i}

$$\begin{aligned} F^{+-} &= -\partial^- A^+ = -\eta^{-+}\partial_+ A^+ = 0, \\ F^{+i} &= -\partial^i A^+, \quad i = 1, 2 \end{aligned} \tag{2.9}$$

with the metric $\eta_{\mu\nu}$, which is defined in Appendix B.

The left-hand side of the Yang-Mills equations for the + component is

$$D_\mu F^{\mu+} = D_i F^{i+} = \partial_i F^{i+} + ig\left[A_i, F^{i+}\right] = \partial_i \partial^i A^+ = -\Delta_T A^+, \tag{2.10}$$

again with $i = 1, 2$. The definition of the Laplace operator in the transverse plane Δ_T can be found in Appendix A, as well as the definition of the partial Fourier transform, which will be used in the following. The resulting Yang-Mills equation is

$$-\Delta_T A^+(x^-, x_T) = \delta(x^-)\rho(x_T), \tag{2.11}$$

and its solution reads

$$A^+(x^-, x_T) = \int \frac{\mathrm{d}^2 k_T}{(2\pi)^2} \frac{\delta(x^-)\widetilde{\rho}(k_T)}{k_T^2} e^{ik_T x_T}. \tag{2.12}$$

Due to the form of Eq. (2.12), $A^+(x^-, x_T)$ can be split up and $A^{+,cov}(x_T)$ is defined via

$$A^{+,cov}(x^-, x_T) = \delta(x^-) A^{+,cov}(x_T). \tag{2.13}$$

Now, the solution is transformed into the light cone gauge

$$A_\mu^{cov}(x^-, x_T) \to A_\mu^{LC}(x^-, x_T) = V(x^-, x_T)\left(A_\mu^{cov}(x^-, x_T) + \frac{1}{ig}\partial_\mu\right)V^\dagger(x^-, x_T). \tag{2.14}$$

The covariant gauge and the light cone gauge are denoted by the superscripts *cov* and *LC*, respectively. The light cone gauge condition is

$$A^{+,LC} = 0 \Leftrightarrow A_-^{LC} = 0. \tag{2.15}$$

The transformation matrix $V(x)$ is chosen to be independent of x^+ because then

$$A^{-,LC} = A_+^{LC} = 0, \tag{2.16}$$

as can be seen by inserting V into Eq. (2.14) and by keeping in mind that $A^{-,cov}$ vanishes. Note that Eq. (2.16) is the light cone gauge condition of the second nucleus, which will be introduced in Section 2.2, and that Eq. (2.15) follows from the choice of an x^- independent transformation matrix for the second nucleus.

V can be calculated using Eq. (2.15)

$$\begin{aligned} 0 &= V(x^-, x_T)\left(A_-^{cov}(x^-, x_T) + \frac{1}{ig}\partial_-\right)V^\dagger(x^-, x_T), \\ \partial_- V^\dagger(x^-, x_T) &= -igA_-^{cov}(x^-, x_T)V^\dagger(x^-, x_T) \\ &= -igA^{+,cov}(x^-, x_T)V^\dagger(x^-, x_T), \\ V^\dagger(x^-, x_T) &= \mathcal{P}e^{-ig\int_{-\infty}^{x^-}\mathrm{d}x'^- A^{+,cov}(x'^-, x_T)}. \end{aligned} \tag{2.17}$$

$\mathcal{P}$ denotes the path ordering operator. Equation (2.17) can be simplified further by inserting Eq. (2.13) and integrating the δ function

$$V^\dagger(x^-, x_T) = e^{-ig\theta(x^-)A^{+,cov}(x_T)}. \tag{2.18}$$

The two components of A_μ^{LC} that are yet to be calculated are

$$A_i^{LC}(x^-, x_T) = V(x^-, x_T)\frac{1}{ig}\partial_i V^\dagger(x^-, x_T). \tag{2.19}$$

Equation (2.19) can be rewritten using the result of Eq. (2.18) as

$$\begin{aligned} A_i^{LC}(x^-, x_T) &= \frac{1}{ig}V(x^-, x_T)\partial_i\Big(-ig\theta(x^-)A^{+,cov}(x_T)\Big)V^\dagger(x^-, x_T) \\ &= \frac{\theta(x^-)}{ig}V(x^-, x_T)\partial_i\Big(-ig\theta(x^-)A^{+,cov}(x_T)\Big)V^\dagger(x^-, x_T) \\ &= \frac{\theta(x^-)}{ig}V(x^-, x_T)\partial_i V^\dagger(x^-, x_T). \end{aligned} \tag{2.20}$$

If $x^- < 0$, $A_i^{LC} = 0$. If $x^- \geq 0$, the θ function in the exponents of V and $V^\dagger$ equals to one. Therefore, A_i^{LC} can be expressed by

$$A_i^{LC}(x^-, x_T) = \frac{\theta(x^-)}{ig}V(x_T)\partial_i V^\dagger(x_T). \tag{2.21}$$

$V(x_T)$ equals to $V(x^-, x_T)$ in Eq. (2.18) with the θ function omitted.

A_i^{LC} consists of one factor that only depends on x^- and of one that only depends on x_T, so it can be split up

$$A^{i,LC}(x^-, x_T) = \theta(x^-)\alpha^i(x_T), \tag{2.22}$$

with

$$\alpha^i(x_T) = \frac{1}{ig} V(x_T)\partial^i V^\dagger(x_T). \tag{2.23}$$

The colour current Eq. (2.4) obeys the transformation law

$$J^{\mu,LC}(x^-, x_T) = V(x_T)J^{\mu,cov}(x^-, x_T)V^\dagger(x_T). \tag{2.24}$$

The relation between $J^{+,LC}$ and ρ^{LC} is the same as the one between $J^{+,cov}$ and ρ^{cov}

$$\begin{aligned} J^{+,LC}(x^-, x_T) &= V(x_T)J^{+,cov}(x^-, x_T)V^\dagger(x_T) \\ &= \delta(x^-)V(x_T)\rho^{cov}(x_T)V^\dagger(x_T) \\ &= \delta(x^-)\rho^{LC}(x_T). \end{aligned} \tag{2.25}$$

The components $F^{-+,LC}$ and $F^{i+,LC}$ are needed to obtain the + component of the Yang-Mills equations in the light cone gauge. The former vanishes because $A^{+,LC}$ and $A^{-,LC}$ vanish. The latter reads

$$F^{i+,LC} = -\partial^+ A^{i,LC}, \tag{2.26}$$

where again $i = 1, 2$. The left-hand side of the aforementioned Yang-Mills equation is

$$\begin{aligned} D_\mu F^{\mu+,LC} &= \partial_\mu F^{\mu+,LC} + ig\left[A_\mu^{LC}, F^{\mu+,LC}\right] \\ &= -\partial_i\partial^+ A^{i,LC} \\ &= -\partial_i\partial_- A^{i,LC} \\ &= -\partial_i\Big(\partial_-\theta(x^-)\alpha^i(x_T)\Big) \\ &= -\delta(x^-)\partial_i\alpha^i(x_T). \end{aligned} \tag{2.27}$$

The commutator term vanishes because of

$$\left[A_\mu^{LC}, F^{\mu+,LC}\right] = \left[A_i^{LC}, -\partial_- A^{i,LC}\right] = \theta(x^-)\delta(x^-)[\alpha_i, \alpha_i] = 0. \tag{2.28}$$

Combining the right-hand side of Eq. (2.27) and the right-hand side of Eq. (2.25) of the + component of the Yang-Mills equations in the light cone gauge yields

$$\partial_i\alpha^i(x_T) = -\rho^{LC}(x_T). \tag{2.29}$$

Summing up, one nucleus viewed as CGC moving at c in z direction can be described by the vector potential Eq. (2.12) in the covariant gauge. In the light cone gauge, the vector potential produced by this nucleus is given by Eq. (2.21). The other components vanish.

2.2 Two Nuclei

In this section, a second nucleus enters the picture. It moves at c in $-z$ direction. The resulting system thus consists of two nuclei, one moving in $+z$ direction, which is discussed in Section 2.1, and one moving in $-z$ direction. The formulas associated with the latter are analogous to the ones for the former. As an example, the current describing only the second nucleus is given by

$$J^{\mu}(x^{+}, x_T) = \delta^{\mu -}\delta(x^{+})\rho(x_T). \tag{2.30}$$

The only non-zero component of the vector field in the covariant gauge describing the second nuclei is

$$A^{-,cov}(x^{+}, x_T) = \int \frac{\mathrm{d}^2 k_T}{(2\pi)^2} \frac{\delta(x^{+})\tilde{\rho}(k_T)}{k_T^2} e^{ik_T x_T}, \tag{2.31}$$

and the non-vanishing components in the light cone gauge are

$$A_i^{LC}(x^{+}, x_T) = \frac{\theta(x^{+})}{ig} V(x_T)\partial_i V^{\dagger}(x_T), \tag{2.32}$$

with

$$V^{\dagger}(x_T) = e^{-igA^{-,cov}(x_T)}. \tag{2.33}$$

Note that Eq. (2.29) also holds for the second nucleus.

The currents for both nuclei can be obtained by superimposing the single nucleus currents. The subscripts denote the nucleus, 1 refers to the one moving in $+z$ direction, 2 to the one moving in $-z$ direction. The current for both nuclei thus reads

$$J^{\mu}(x) = J_1^{\mu}(x^{-}, x_T) + J_2^{\mu}(x^{+}, x_T). \tag{2.34}$$

In the abelian case the vector potential A_μ is simply the sum of the vector potentials of the single nuclei. To obtain the field describing both nuclei in the non-abelian case, which is the relevant one in this calculation, consider the spacetime diagram drawn in Figure 2.1. Nucleus 1 moves along the x^{+} axis, nucleus 2 along the x^{-} axis. The collision takes place at the intersection point of these two axes.

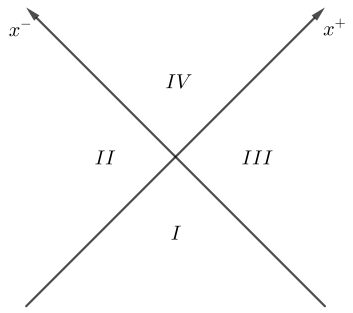

Figure 2.1: Spacetime diagram for the nuclei collision. The x_T coordinates are suppressed.

The collision splits the spacetime diagram into four regions. Region I is its past. The two nuclei cannot influence anything in this region and the vector field vanishes. Region II is only influenced by the nucleus travelling along the x^+ axis. The vector field can therefore be described by Eq. (2.21). Likewise, region III is only influenced by the nucleus moving along the x^- axis and the vector field is described by Eq. (2.32). Region IV is the future of the collision, it is the region in which the Glasma is created. There the vector potential depends on the currents of both nuclei, which move along the boundary of the forward light cone, and is yet to be calculated.

In regions II and III, $A^+ = 0$ and $A^- = 0$ are selected as conditions. In region II, the former equation is the light cone condition and the latter holds because the transformation matrix V is chosen to be independent of x^+. In region III, they change their roles. The latter equation is the light cone condition, whereas the former holds because the transformation matrix is chosen to be independent of x^-. In region IV, the Fock-Schwinger gauge

$$x^+ A^- + x^- A^+ = 0 \tag{2.35}$$

is the gauge of choice. At the boundaries from region IV to the regions II and III, this gauge can be connected smoothly to the light cone gauge in these two regions.

Coordinates that reflect the symmetries of the problem at hand are the Milne coordinates, to which will also be referred as (τ, η) or (τ, η, x_T) coordinates. They are introduced in Appendix B. In these coordinates, the Fock-Schwinger gauge condition becomes

$$A^\tau = 0. \tag{2.36}$$

A boost invariant ansatz for the whole spacetime reads

$$\begin{aligned} A^i(x) &= \theta(x^+)\theta(x^-)\alpha^i(\tau, x_T) + \underbrace{\theta(-x^+)\theta(x^-)\alpha_1^i(x_T)}_{\text{region } II} + \underbrace{\theta(x^+)\theta(-x^-)\alpha_2^i(x_T)}_{\text{region } III}, \\ A^\eta(x) &= \underbrace{\theta(x^+)\theta(x^-)\alpha^\eta(\tau, x_T)}_{\text{region } IV}, \end{aligned} \tag{2.37}$$

with

$$\begin{aligned} \alpha_m^i(x_T) &= \frac{1}{ig} V_m(x_T)\partial^i V_m^\dagger(x_T), \\ V_1^\dagger(x_T) &= e^{-igA_1^{+,cov}(x_T)}, \\ V_2^\dagger(x_T) &= e^{-igA_2^{-,cov}(x_T)}, \\ m &= 1, 2. \end{aligned} \tag{2.38}$$

$\alpha^i(\tau, x_T)$ and $\alpha^\eta(\tau, x_T)$ describe the Glasma, which only exists in region IV. They are determined by the Yang-Mills equations (B.28), (B.30) and (B.31)

$$\begin{aligned} \frac{1}{\tau^3}\partial_\tau(\tau^3\partial_\tau\alpha^\eta) + D_i D^i\alpha^\eta &= 0, \\ ig\tau^2[\alpha^\eta, \partial_\tau\alpha^\eta] - D_i\partial_\tau\alpha^i &= 0, \\ -\partial_\tau(\tau\partial_\tau\alpha^i) + \tau D_j F^{ij} + ig\tau^3[\alpha^\eta, D_i\alpha^\eta] &= 0 \end{aligned} \tag{2.39}$$

and the boundary conditions [12]

$$\begin{aligned}
\alpha^i(\tau \to 0^+, x_T) &= \alpha_1^i(x_T) + \alpha_2^i(x_T), \\
\partial_\tau \alpha^i(\tau \to 0^+, x_T) &= 0, \\
\alpha^\eta(\tau \to 0^+, x_T) &= \frac{ig}{2}\Big[\alpha_1^i(x_T), \alpha_2^i(x_T)\Big], \\
\partial_\tau \alpha^\eta(\tau \to 0^+, x_T) &= 0.
\end{aligned} \tag{2.40}$$

They are matching conditions at the boundary between regions II and IV and regions III and IV. Due to the fact that (τ, η) coordinates are used and the fact that this boundary corresponds to the equal time surface $\tau \to 0^+$, they are also called initial conditions. The Yang-Mills equations (2.39) are source-free in this region because all the sources are located on its boundary. They are derived in Appendix B.

2.3 MV Model

The so-called MV model was developed by McLerran and Venugopalan [14, 15]. It requires the particle density in the nucleus to be large compared to the QCD-scale $\rho \gg \Lambda_{QCD}$, so that weak coupling methods are applicable and a classical approximation is valid. The valence quarks are treated as recoilless classical charge sources $\rho(x)$ that move at the speed of light. They are called hard partons. The soft partons are represented by a classical colour field $A_\mu(x)$. The link between the hard partons and the soft ones is given by the classical Yang-Mills equations.

Due to the assumption that the velocity of the hard partons is c, the corresponding current has only a $+$ component in light cone coordinates if it moves in z direction. In the transverse plane, the nuclei are considered to be infinitely large. There, the exact position of each hard parton is unknown, which is why they are described by a probability functional $W[\rho]$

$$W[\rho] = \frac{1}{Z} e^{-\frac{1}{2g^2\mu^2}\int \mathrm{d}^2x_T\, \rho_a(x_T)\rho_a(x_T)}, \tag{2.41}$$

with the average charge density squared per unit area μ^2 and the normalisation constant Z

$$Z = \int \mathcal{D}\rho\, e^{-\frac{1}{2g^2\mu^2}\int \mathrm{d}^2x_T \rho_a(x_T)\rho_a(x_T)}. \tag{2.42}$$

The particle density ρ can be given in any gauge because $W[\rho]$ is gauge invariant [1].

Ensemble averages of observables O can be calculated via

$$\langle O[A_\mu]\rangle = \int \mathcal{D}\rho\, O[A_\mu] W[\rho]. \tag{2.43}$$

This leads to

$$\begin{aligned}
\langle \rho_a(x_T)\rangle &= 0, \\
\langle \rho_a(x_T)\rho_b(y_T)\rangle &= g^2\mu^2\delta_{ab}\delta^{(2)}(x_T - y_T), \\
\langle \widetilde{\rho}_a(k_T)\rangle &= 0, \\
\langle \widetilde{\rho}_a(k_T)\widetilde{\rho}_b(l_T)\rangle &= (2\pi)^2 g^2\mu^2\delta_{ab}\delta^{(2)}(k_T + l_T).
\end{aligned} \tag{2.44}$$

Equation (2.44) needs to be modified to yield finite results for the momentum broadening parameters, which are introduced in Section 4.2 and then used throughout the rest of the chapter.

$$\begin{aligned}
\widetilde{\rho}'_a(k_T) &= \frac{k_T^2}{k_T^2+m^2}\widetilde{\rho}_a(k_T)\Theta(\Lambda_{UV}-|k_T|),\\
\langle\widetilde{\rho}'_a(k_T)\widetilde{\rho}'_b(l_T)\rangle &= \frac{k_T^2}{k_T^2+m^2}\frac{l_T^2}{l_T^2+m^2}\langle\widetilde{\rho}_a(k_T)\widetilde{\rho}_b(l_T)\rangle\Theta(\Lambda_{UV}-|k_T|)\Theta(\Lambda_{UV}-|l_T|)\\
&= \frac{k_T^4}{(k_T^2+m^2)^2}(2\pi)^2g^2\mu^2\delta_{ab}\delta(k_T+l_T)\Theta(\Lambda_{UV}-|k_T|). \qquad (2.45)
\end{aligned}$$

Λ_{UV} is an ultraviolet cut-off, m is an infrared regulator.

Chapter 3

Solution of the Equations of the Glasma up to Second Order

In this chapter, I will analytically expand the initial conditions of the Glasma, which are given by Eq. (2.40), and the Yang-Mills equations that govern its propagation. They are listed in Eq. (2.39). Both expansions will be in the particle density ρ^{LC}. Then, I will solve them up to second order, i.e. I will give an analytical solution for $\alpha^i(\tau, x_T)$ and $\alpha^\eta(\tau, x_T)$ up to second order. Finally, I will discuss the choice of ρ^{LC} as expansion parameter and examine if particle densities in other gauges could have been chosen instead. Large parts of this calculation are analogous to [7].

Before starting with the expansions, some formulas will be rewritten in a useful way. The first four ones have already been given in Eq. (2.38) in a different way

$$\alpha_m^i(x_T) = \frac{1}{ig} V_m(x_T) \partial^i V_m^\dagger(x_T), \tag{3.1}$$

$$V_m(x_T) = e^{ig\phi_m^{cov}(x_T)}, \tag{3.2}$$

$$\phi_1^{cov}(x_T) = A_1^{+,cov}(x_T), \tag{3.3}$$

$$\phi_2^{cov}(x_T) = A_2^{-,cov}(x_T), \tag{3.4}$$

$$\phi = \phi_1 + \phi_2, \tag{3.5}$$

$$\rho = \rho_1 + \rho_2, \tag{3.6}$$

$$\phi_m = -\frac{1}{\Delta_T} \rho_m, \tag{3.7}$$

$$\widetilde{\phi}_m = \frac{1}{k_T^2} \widetilde{\rho}_m. \tag{3.8}$$

The last four formulas are valid in any gauge. Equation (3.7) contains the inverse Laplace operator $\Delta_T^{-1} = 1/\Delta_T$, Eq. (3.8) is the same relation, but in momentum space. $m = 1, 2$ and refers to the quantities of the first or second nucleus. Note that in Section 2.1 only one nucleus was discussed and therefore there was no index needed to distinguish between different nuclei. From now on ϕ and ρ without indices refer to the whole system of nuclei, indicated by Eqs. (3.5) and (3.6).

3.1 Expansion of the Initial Conditions

In the following expansion, there will be terms containing factors of ϕ or its derivatives. It is assumed that these factors are of order ρ, which is why the expansion can also be thought to be in orders of ϕ. With the help of Eq. (3.8), this assumption can be translated to one for k_T. When the results of this expansion are used in Chapter 4, one introduces an infrared regulator m and and ultraviolet cut-off Λ_{UV}, with which one can fulfil said assumption.

According to Eq. (3.1), one can find an expansion for α^i in terms of ρ^{LC} by seeking an expansion for V_m first. Equation (3.2) gives V_m in terms of ϕ^{cov}. With the transformation law for ρ, which is used in Eq. (2.27), one finds

$$\phi_m^{cov} = \phi_m^{LC} + \mathcal{O}(\phi_m^{2\,LC}). \tag{3.9}$$

With this relation one can start with an expansion of V_m in terms of ϕ_m^{cov}

$$V_m = 1 + ig\phi_m^{cov} - \frac{g^2}{2}\phi_m^{2\,cov} + \mathcal{O}(\phi_m^{3\,cov}), \tag{3.10}$$

$$V_m^\dagger = 1 - ig\phi_m^{cov} - \frac{g^2}{2}\phi_m^{2\,cov} + \mathcal{O}(\phi_m^{3\,cov}), \tag{3.11}$$

$$\partial^i V_m^\dagger = -ig\partial^i\phi_m^{cov} - \frac{g^2}{2}\left\{\partial^i\phi_m^{cov}, \phi_m^{cov}\right\} + \mathcal{O}(\phi_m^{3\,cov}) \tag{3.12}$$

and later translate it to one in ϕ_m^{LC}. Inserting Eqs. (3.10) and (3.12) into Eq. (3.1), one obtains

$$\alpha_m^i = -\partial^i\phi_m^{cov} + \frac{ig}{2}\left[\partial^i\phi_m^{cov}, \phi_m^{cov}\right] + \mathcal{O}(\phi_m^{3\,cov}). \tag{3.13}$$

Calculating the divergence of α_m^i yields

$$\partial_i\alpha_m^i = \Delta_T\phi_m^{cov} + \frac{ig}{2}\partial_i\left[\partial^i\phi_m^{cov}, \phi_m^{cov}\right] + \mathcal{O}(\phi_m^{3\,cov}). \tag{3.14}$$

Here, Eq. (A.3) was used. Equations (2.29) and (3.14) lead to

$$-\rho_m^{LC} = \Delta_T\phi_m^{cov} + \frac{ig}{2}\partial_i\left[\partial^i\phi_m^{cov}, \phi_m^{cov}\right] + \mathcal{O}(\phi_m^{3\,cov}), \tag{3.15}$$

and after applying the inverse Laplace operator $\Delta_T^{-1} = 1/\Delta_T$ and taking advantage of Eq. (3.7), one obtains

$$\phi_m^{LC} = \phi_m^{cov} + \frac{ig}{2}\frac{1}{\Delta_T}\partial_i\left[\partial^i\phi_m^{cov}, \phi_m^{cov}\right] + \mathcal{O}(\phi_m^{3\,cov}). \tag{3.16}$$

From Eq. (3.16), the negative gradient of ϕ_m^{cov} can be calculated

$$-\partial^i\phi_m^{cov} = -\partial^i\phi_m^{LC} + \frac{ig}{2}\partial^i\frac{1}{\Delta_T}\partial_j\left[\partial^j\phi_m^{cov}, \phi_m^{cov}\right] + \mathcal{O}(\phi_m^{3\,cov}). \tag{3.17}$$

After inserting Eq. (3.17) into Eq. (3.13), one gets

$$\alpha_m^i = -\partial^i\phi_m^{LC} + \frac{ig}{2}\left(\eta^{ij} + \partial^i\frac{1}{\Delta_T}\partial^j\right)[\partial_j\phi_m^{cov}, \phi_m^{cov}] + \mathcal{O}(\phi_m^{3\,cov}), \tag{3.18}$$

and after making use of Eq. (3.16), the desired expansion of α_m^i in terms of ϕ_m^{LC} is found

$$\alpha_m^i = -\partial^i\phi_m^{LC} + \frac{ig}{2}\left(\eta^{ij} + \partial^i\frac{1}{\Delta_T}\partial^j\right)\left[\partial_j\phi_m^{LC}, \phi_m^{LC}\right] + \mathcal{O}(\phi_m^{3\,LC}). \tag{3.19}$$

Now, it is possible to write the right-hand side of Eq. (2.40) in orders of ϕ^{LC}, but not yet the left-hand side. To change that, an expansion of the vector fields in powers of ϕ^{LC} is made

$$\begin{aligned}\alpha^i(\tau, x_T) &= \sum_{n=1}^{\infty} \alpha^i_{(n)}(\tau, x_T),\\ \alpha^\eta(\tau, x_T) &= \sum_{n=1}^{\infty} \alpha^\eta_{(n)}(\tau, x_T).\end{aligned} \tag{3.20}$$

Thus, the initial conditions to first order are

$$\begin{aligned}\alpha^i_{(1)}(\tau = 0, x_T) &= -\partial^i \phi^{LC},\\ \partial_\tau \alpha^i_{(1)}(\tau = 0, x_T) &= 0,\end{aligned} \tag{3.21}$$

$$\begin{aligned}\alpha^\eta_{(1)}(\tau = 0, x_T) &= 0,\\ \partial_\tau \alpha^\eta_{(1)}(\tau = 0, x_T) &= 0,\end{aligned} \tag{3.22}$$

and the ones to second order read

$$\begin{aligned}\alpha^i_{(2)}(\tau = 0, x_T) &= \frac{ig}{2}(\eta^{ij} + \partial^i \frac{1}{\Delta_T} \partial^j) \sum_{m=1}^{2} \left[\partial_j \phi^{LC}_m, \phi^{LC}_m\right],\\ \partial_\tau \alpha^i_{(2)}(\tau = 0, x_T) &= 0,\end{aligned} \tag{3.23}$$

$$\begin{aligned}\alpha^\eta_{(2)}(\tau = 0, x_T) &= \frac{ig}{2}\left[\partial^i \phi^{LC}_1, \partial^i \phi^{LC}_2\right],\\ \partial_\tau \alpha^\eta_{(2)}(\tau = 0, x_T) &= 0.\end{aligned} \tag{3.24}$$

3.2 Expansion of the Equations of Motion

With the help of Eqs. (2.39) and (3.20), the equations of motion can be written in powers of ϕ^{LC}. The first order equations are

$$\frac{1}{\tau^3}\partial_\tau\left(\tau^3 \partial_\tau \alpha^\eta_{(1)}\right) - \Delta_T \alpha^\eta_{(1)} = 0, \tag{3.25}$$

$$\partial_i \partial_\tau \alpha^i_{(1)} = 0, \tag{3.26}$$

$$-\partial_\tau\left(\tau \partial_\tau \alpha^i_{(1)}\right) + \tau\left(\delta^i_j \Delta_T + \partial_j \partial^i\right)\alpha^j_{(1)} = 0. \tag{3.27}$$

Note that they are decoupled. Equation (3.25) is a differential equation for $\alpha^\eta_{(1)}$, whereas Eqs. (3.26) and (3.27) are differential equations for $\alpha^i_{(1)}$.

For the second order equations, one obtains

$$\begin{aligned}\frac{1}{\tau^3}\partial_\tau\left(\tau^3 \partial_\tau \alpha^\eta_{(2)}\right) - \Delta_T \alpha^\eta_{(2)} + ig\left(\left[\alpha^i_{(1)}, \alpha^\eta_{(1)}\right] - \left[\alpha^i_{(1)}, \partial^i \alpha^\eta_{(1)}\right]\right) &= 0,\\ \partial_i \partial_\tau \alpha^i_{(2)} - ig\tau^2\left[\alpha^\eta_{(1)}, \partial_\tau \alpha^\eta_{(1)}\right] - ig\left[\alpha^i_{(1)}, \partial_\tau \alpha^i_{(1)}\right] &= 0,\\ -\partial_\tau\left(\tau \partial_\tau \alpha^i_{(2)}\right) + \tau\left(\delta^i_j \Delta_T + \partial_j \partial^i\right)\alpha^j_{(2)} + ig\tau \partial_j\left[\alpha^i_{(1)}, \alpha^j_{(1)}\right]&\\ - ig\left(\left[\alpha^j_{(1)}, \partial^i \alpha^j_{(1)}\right] - \left[\alpha^j_{(1)}, \partial^j \alpha^i_{(1)}\right]\right) + ig\tau^3\left[\alpha^\eta_{(1)}, \partial_i \alpha^\eta_{(1)}\right] &= 0.\end{aligned} \tag{3.28}$$

Using the solution of the first order, which will be discussed in Subsection 3.3.1, this simplifies to

$$\frac{1}{\tau^3}\partial_\tau\left(\tau^3\partial_\tau\alpha^\eta_{(2)}\right) - \Delta_T\alpha^\eta_{(2)} = 0, \tag{3.29}$$

$$\partial_i\partial_\tau\alpha^i_{(2)} = 0, \tag{3.30}$$

$$-\partial_\tau\left(\tau\partial_\tau\alpha^i_{(2)}\right) + \tau\left(\delta^i_j\Delta_T + \partial_j\partial^i\right)\alpha^j_{(2)} + ig\tau\partial_j\left[\alpha^i_{(1)}, \alpha^j_{(1)}\right] = 0. \tag{3.31}$$

Equations (3.29) and (3.30) have the same structure as their respective first order counterpart, but Eq. (3.31) contains an extra term of first order fields.

3.3 Solution of the Equations of Motion

3.3.1 Solution to First Order

The problem at hand can be solved via Fourier transformation. The Fourier transform of Eq. (3.25) is

$$\frac{1}{\tau^3}\partial_\tau(\tau^3\partial_\tau\tilde{\alpha}^\eta_{(1)}) + k_T^2\tilde{\alpha}^\eta_{(1)} = 0. \tag{3.32}$$

The Fourier transforms of the first order initial conditions for α^η, which are given by Eq. (3.22), are

$$\begin{aligned}\tilde{\alpha}^\eta_{(1)}(\tau = 0, k_T) &= 0,\\ \partial_\tau\tilde{\alpha}^\eta_{(1)}(\tau = 0, k_T) &= 0.\end{aligned} \tag{3.33}$$

The unique solution of Eq. (3.32) with the initial conditions given by Eq. (3.33) is

$$\tilde{\alpha}^\eta_{(1)}(\tau, k_T) = 0, \tag{3.34}$$

and the solution of the original equation, which is nothing but the inverse Fourier transform of Eq. (3.34), is therefore

$$\alpha^\eta_{(1)}(\tau, x_T) = 0. \tag{3.35}$$

The Fourier transform of Eq. (3.26) reads

$$\partial_\tau(k_1\tilde{\alpha}^1_{(1)} + k_2\tilde{\alpha}^2_{(1)}) = 0. \tag{3.36}$$

This leads to

$$\begin{aligned}\partial_\tau\tilde{\alpha}^1_{(1)} &= -\frac{k_2}{k_1}\partial_\tau\tilde{\alpha}^2_{(1)},\\ \tilde{\alpha}^1_{(1)}(\tau, k_T) &= -\frac{k_2}{k_1}\tilde{\alpha}^2_{(1)}(\tau, k_T) + C(k_T).\end{aligned} \tag{3.37}$$

The Fourier transforms of the first order initial conditions for α^i, which are given by Eq. (3.21), read

$$\begin{aligned}\tilde{\alpha}^i_{(1)}(\tau = 0, k_T) &= ik_i\tilde{\phi}^{LC},\\ \partial_\tau\tilde{\alpha}^i_{(1)}(\tau = 0, k_T) &= 0.\end{aligned} \tag{3.38}$$

With the help of Eqs. (3.37) and (3.38), C can be determined

$$C = -i\left(k_1 + \frac{(k_2)^2}{k_1}\right)\tilde{\phi}^{LC}. \tag{3.39}$$

Equation (3.27) becomes

$$\begin{aligned} -\partial_\tau(\tau\partial_\tau\tilde{\alpha}^1_{(1)}) + \tau(-(k_2)^2\tilde{\alpha}^1_{(1)} + k_2k_1\tilde{\alpha}^2_{(1)}) = 0, \\ -\partial_\tau(\tau\partial_\tau\tilde{\alpha}^2_{(1)}) + \tau(-(k_1)^2\tilde{\alpha}^2_{(1)} + k_1k_2\tilde{\alpha}^1_{(1)}) = 0. \end{aligned} \tag{3.40}$$

Inserting Eq. (3.37) into Eq. (3.40) yields the same equation twice

$$-\partial_\tau(\tau\partial_\tau\tilde{\alpha}^2_{(1)}) + \tau(-(k_2)^2\tilde{\alpha}^2_{(1)} + k_1k_2C - (k_1)^2\tilde{\alpha}^2_{(1)}) = 0. \tag{3.41}$$

The unique solution of Eq. (3.41) with the initial conditions given by Eq. (3.38) can be written as

$$\tilde{\alpha}^2_{(1)}(\tau, k_T) = ik_2\tilde{\phi}^{LC}(k_T). \tag{3.42}$$

Due to the symmetry of the equations and their associated initial conditions, one obtains the solution of $\tilde{\alpha}^1_{(1)}$ by exchanging $1 \leftrightarrow 2$ in Eq. (3.42). Hence, the solution of the original equation reads

$$\alpha^i_{(1)}(\tau, x_T) = -\partial^i\phi^{LC}(x_T). \tag{3.43}$$

This solution is pure gauge, as will be shown explicitly in Subsection 3.3.2 by choosing the residual gauge freedom in a way that the new field in Eq. (3.43) vanishes.

3.3.2 Solution to Second Order

There is still some residual gauge freedom left in the chosen Fock-Schwinger gauge. It will be fixed in this subsection. Not only will the first order solution turn out to be pure gauge, but also the second order equations will become easier to solve with said gauge fixing. Thus, a gauge transformation of the fields α^i and α^η is done

$$\epsilon^\mu = U(x_T)(\alpha^\mu + \frac{1}{ig}\partial^\mu)U^\dagger(x_T), \tag{3.44}$$

with a transformation matrix $U(x_T)$ that is independent of τ so that the τ component vanishes in the new gauge as well and independent of η because there shall be no rapidity dependencies in this problem, as explained in Chapter 1. The new field is

$$\begin{aligned} \epsilon^\tau &= 0, \\ \epsilon^\eta &= U(x_T)\alpha^\eta U^\dagger(x_T), \\ \epsilon^i &= U(x_T)(\alpha^i + \frac{1}{ig}\partial^i)U^\dagger(x_T). \end{aligned} \tag{3.45}$$

The next thing to do is to expand ϵ^μ and $U(x_T)$ in powers of ϕ^{LC}

$$\begin{aligned} \epsilon^\eta &= \sum_{n=1}^{\infty}\epsilon^\eta_{(n)}, \\ \epsilon^i &= \sum_{n=1}^{\infty}\epsilon^i_{(n)}, \\ U(x_T) &= e^{ig\phi_\perp(x_T)}, \end{aligned} \tag{3.46}$$

with

$$\phi_\perp(x_T) = \sum_{n=1}^{\infty} \phi_{\perp(n)}(x_T), \tag{3.47}$$

which is also expanded in powers of ϕ^{LC}.

Making use of

$$\begin{aligned} U &= 1 + ig\phi_{\perp(1)} + ig\phi_{\perp(2)} - \frac{g^2}{2}\phi^2_{\perp(1)} + \mathcal{O}(\phi^{3\,LC}), \\ U^\dagger &= 1 - ig\phi_{\perp(1)} - ig\phi_{\perp(2)} - \frac{g^2}{2}\phi^2_{\perp(1)} + \mathcal{O}(\phi^{3\,LC}), \\ U\partial^i U^\dagger &= -ig\partial^i\phi_{\perp(1)} - ig\partial^i\phi_{\perp(2)} + \frac{g^2}{2}\Big[\phi_{\perp(1)}, \partial^i\phi_{\perp(1)}\Big] + \mathcal{O}(\phi^{3\,LC}), \end{aligned} \tag{3.48}$$

Eq. (3.45) can be written in orders of ϕ^{LC}. The first order reads

$$\begin{aligned} \epsilon^\eta_{(1)} &= \alpha^\eta_{(1)} = 0, \\ \epsilon^i_{(1)} &= \alpha^i_{(1)} - \partial^i\phi_{\perp(1)}, \end{aligned} \tag{3.49}$$

and the second order is

$$\epsilon^\eta_{(2)} = \alpha^\eta_{(2)}, \tag{3.50}$$

$$\epsilon^i_{(2)} = \alpha^i_{(2)} - \partial^i\phi_{\perp(2)} + \frac{ig}{2}\Big[\phi_{\perp(1)}, \partial^i\phi_{\perp(1)}\Big]. \tag{3.51}$$

Now, part of the residual gauge freedom is used, i.e. the first order of $\phi_\perp$ is chosen. The equations of motion are gauge invariant, so they can be written in terms of ϵ^μ by replacing α^μ in the old equations by ϵ^μ. Equation (3.31) contains a commutator term of first order terms. Equation (3.49) states that one can set $\epsilon^i_{(1)}$ to 0 if one finds a $\phi_{\perp(1)}$ that satisfies

$$\partial^i\phi_{\perp(1)} = \alpha^i_{(1)}. \tag{3.52}$$

This would show that the first order solution is in fact pure gauge and it would make the second order equations easier to solve.

$$\begin{aligned} \partial^i\phi_{\perp(1)} &\stackrel{!}{=} \alpha^i_{(1)} = -\partial^i\phi^{LC}, \\ \phi_{\perp(1)} &= -\phi^{LC}. \end{aligned} \tag{3.53}$$

In the last step, the fact that $\phi_\perp$ depends neither on η nor on τ is used. Overall constants are ignored as usual.

The new second order equations of motion are

$$\frac{1}{\tau^3}\partial_\tau(\tau^3\partial_\tau\epsilon^\eta_{(2)}) - \Delta_T\epsilon^\eta_{(2)} = 0, \tag{3.54}$$

$$\partial_i\partial_\tau\epsilon^i_{(2)} = 0, \tag{3.55}$$

$$-\partial_\tau(\tau\partial_\tau\epsilon^i_{(2)}) + \tau(\delta^i_j\Delta_T + \partial_j\partial^i)\epsilon^j_{(2)} = 0. \tag{3.56}$$

The initial conditions, given by Eq. (3.24), remain the same for $\epsilon^{\eta}_{(2)}$ because of Eq. (3.50), but Eq. (3.23) changes. One obtains with the help of Eq. (3.51)

$$\epsilon^{i}_{(2)}(\tau=0,x_T) = \alpha^{i}_{(2)}(\tau=0,x_T) + \frac{ig}{2}\Big[\phi_{\perp(1)},\partial^i\phi_{\perp(1)}\Big] - \partial^i\phi_{\perp(2)}, \tag{3.57}$$

$$\partial_\tau\epsilon^{i}_{(2)}(\tau=0,x_T) = 0, \tag{3.58}$$

$$\epsilon^{\eta}_{(2)}(\tau=0,x_T) = \frac{ig}{2}\Big[\partial^i\phi_1^{LC},\partial^i\phi_2^{LC}\Big], \tag{3.59}$$

$$\partial_\tau\epsilon^{\eta}_{(2)}(\tau=0,x_T) = 0. \tag{3.60}$$

Note that

$$\partial_\tau\epsilon^{\mu} = \partial_\tau\alpha^{\mu} \tag{3.61}$$

for the first and the second order because $\phi_\perp$ does not depend on τ.

With the last gauge condition, $\phi_{\perp(2)}$ will be fixed. One demands

$$\partial_i\epsilon^{i}(\tau=0,x_T) = 0, \tag{3.62}$$

which means that

$$\partial_i\epsilon^{i}_{(2)}(\tau=0,x_T) = 0 \tag{3.63}$$

and obtains the following equation for $\phi_{\perp(2)}$ by calculating the divergence of Eq. (3.57)

$$\begin{aligned} 0 &= \frac{ig}{2}\partial_i\Big[\phi_{\perp(1)},\partial^i\phi_{\perp(1)}\Big] + \Delta_T\phi_{\perp(2)}, \\ \phi_{\perp(2)} &= -\frac{ig}{2}\frac{1}{\Delta_T}\partial^i\Big[\phi_{\perp(1)},\partial_i\phi_{\perp(1)}\Big]. \end{aligned} \tag{3.64}$$

Inserting Eq. (3.64) into Eq. (3.57) yields

$$\begin{aligned} \epsilon^{i}_{(2)}(\tau=0,x_T) &= \alpha^{i}_{(2)}(\tau=0,x_T) + \frac{ig}{2}\Big(\eta^{ij}+\partial^i\frac{1}{\Delta_T}\partial^j\Big)\Big[\phi_{\perp(1)},\partial_j\phi_{\perp(1)}\Big] \\ &= \frac{ig}{2}\Big(\eta^{ij}+\partial^i\frac{1}{\Delta_T}\partial^j\Big)\Big(\Big[\partial_j\phi_1^{LC},\phi_1^{LC}\Big]+\Big[\partial_j\phi_2^{LC},\phi_2^{LC}\Big] \\ &\quad + \Big[\phi_1^{LC}+\phi_2^{LC},\partial_j\Big(\phi_1^{LC}+\phi_2^{LC}\Big)\Big]\Big) \\ &= \frac{ig}{2}\Big(\eta^{ij}+\partial^i\frac{1}{\Delta_T}\partial^j\Big)\Big(\Big[\phi_1^{LC},\partial_j\phi_2^{LC}\Big]+\Big[\phi_2^{LC},\partial_j\phi_1^{LC}\Big]\Big) \\ &= ig\Big(\eta^{ij}+\partial^i\frac{1}{\Delta_T}\partial^j\Big)\Big[\phi_1^{LC},\partial_j\phi_2^{LC}\Big]. \end{aligned} \tag{3.65}$$

In the last step, the fact that

$$\Big(\eta^{ij}+\partial^i\frac{1}{\Delta_T}\partial^j\Big)\partial_j\Big[\phi_2^{LC},\phi_1^{LC}\Big] = \Big(\partial^i-\partial^i\Big)\Big[\phi_2^{LC},\phi_1^{LC}\Big] = 0 \tag{3.66}$$

and the product rule were used. Equation (3.55) is an ordinary differential equation for $\partial_i\epsilon^{i}_{(2)}$. Together with the initial condition Eq. (3.58), one can deduce that

$$\partial_i\epsilon^{i}_{(2)} = 0 \quad \forall\tau. \tag{3.67}$$

Therefore, $\epsilon^{i}_{(2)}$ can be written as rotation of another field $\chi(\tau,x_T)$

$$\epsilon^{i}_{(2)} = \epsilon^{ij}\partial_j\chi, \tag{3.68}$$

with the two dimensional epsilon tensor ϵ^{ij}.

Equation (3.56) can be rewritten in terms of χ

$$\begin{aligned}\epsilon^{ij}\partial_j\Big(-\frac{1}{\tau}\partial_\tau(\tau\partial_\tau\chi)+\Delta_T\chi\Big)&=0,\\ \partial_j\Big(-\frac{1}{\tau}\partial_\tau(\tau\partial_\tau\chi)+\Delta_T\chi\Big)&=0,\\ \frac{1}{\tau}\partial_\tau(\tau\partial_\tau\chi)-\Delta_T\chi&=a(\tau).\end{aligned}\tag{3.69}$$

The function $a(\tau)$, which is nothing but an integration constant with respect to x_T, is set to 0 now. The reason why this is possible without changing the observables is explained in detail in Appendix C. The initial condition that is given by Eq. (3.65) becomes in terms of χ

$$\begin{aligned}\epsilon^{ij}\partial_j\chi(\tau=0,x_T)&=ig\Big(\eta^{ij}+\partial^i\frac{1}{\Delta_T}\partial^j\Big)\Big[\phi_1^{LC},\partial_j\phi_2^{LC}\Big],\\ \partial_k\chi(\tau=0,x_T)&=ig\epsilon_{ik}\Big(\eta^{ij}+\partial^i\frac{1}{\Delta_T}\partial^j\Big)\Big[\phi_1^{LC},\partial_j\phi_2^{LC}\Big],\\ \Delta_T\chi(\tau=0,x_T)&=ig\epsilon^{ij}\Big[\partial_i\phi_1^{LC},\partial_j\phi_2^{LC}\Big],\\ \chi(\tau=0,x_T)&=\frac{ig}{\Delta_T}\epsilon^{ij}\Big[\partial_i\phi_1^{LC},\partial_j\phi_2^{LC}\Big].\end{aligned}\tag{3.70}$$

The first line was multiplied by ϵ_{ik} to get the second one, on which was acted by $-\partial^k$ to come to the third. Finally the inverse Laplace operator Δ_T^{-1} was applied to both sides. The initial condition that is given by Eq. (3.58) can be written as

$$\begin{aligned}\epsilon^{ij}\partial_j\partial_\tau\chi(\tau=0,x_T)&=0,\\ \partial_i\partial_\tau\chi(\tau=0,x_T)&=0,\\ \partial_\tau\chi(\tau=0,x_T)&=0.\end{aligned}\tag{3.71}$$

In the last step, an overall constant was ignored again. The remaining equations of motion are given by

$$\frac{1}{\tau^3}\partial_\tau(\tau^3\partial_\tau\epsilon^\eta_{(2)})-\Delta_T\epsilon^\eta_{(2)}=0,\tag{3.72}$$

$$\frac{1}{\tau}\partial_\tau(\tau\partial_\tau\chi)-\Delta_T\chi=0,\tag{3.73}$$

and their initial conditions read

$$\begin{aligned}\epsilon^\eta_{(2)}(\tau=0,x_T)&=\frac{ig}{2}\Big[\partial_i\phi_1^{LC},\partial_i\phi_2^{LC}\Big],\\ \partial_\tau\epsilon^\eta_{(2)}(\tau=0,x_T)&=0,\\ \chi(\tau=0,x_T)&=\frac{ig}{\Delta_T}\epsilon^{ij}\Big[\partial_i\phi_1^{LC},\partial_j\phi_2^{LC}\Big],\\ \partial_\tau\chi(\tau=0,x_T)&=0.\end{aligned}\tag{3.74}$$

The solution is obtained by Fourier transforming the spatial part of the problem. The equations of motion become

$$\frac{1}{\tau^3}\partial_\tau(\tau^3\partial_\tau\tilde{\epsilon}^\eta_{(2)})+k_T^2\tilde{\epsilon}^\eta_{(2)}=0,\tag{3.75}$$

$$\frac{1}{\tau}\partial_\tau(\tau\partial_\tau\tilde{\chi})+k_T^2\tilde{\chi}=0,\tag{3.76}$$

and the associated initial conditions are

$$\begin{aligned}\tilde{\epsilon}^{\eta}_{(2)}(\tau=0,k_T) &= \frac{ig}{2}\mathcal{F}\Big(\big[\partial_i\phi_1^{LC},\partial_i\phi_2^{LC}\big]\Big)\\ &= -\frac{ig}{2}\frac{1}{(2\pi)^2}\int \mathrm{d}^2k'_T\,(k_i-k'_i)k'_i\Big[\tilde{\phi}_1^{LC}(k_T-k'_T),\tilde{\phi}_2^{LC}(k'_T)\Big],\\ \partial_\tau\tilde{\epsilon}^{\eta}_{(2)}(\tau=0,k_T) &= 0\end{aligned} \tag{3.77}$$

and

$$\begin{aligned}k_T^2\tilde{\chi}(\tau=0,k_T) &= \frac{ig\epsilon^{ij}}{(2\pi)^2}\int \mathrm{d}^2k'_T\,(k_i-k'_i)k'_j\Big[\tilde{\phi}_1^{LC}(k_T-k'_T),\tilde{\phi}_2^{LC}(k'_T)\Big],\\ \partial_\tau\tilde{\chi}(\tau=0,k_T) &= 0.\end{aligned} \tag{3.78}$$

$\mathcal{F}$ denotes the Fourier transform. The solution of the problem in Fourier space is, as is shown in Appendix C,

$$\tilde{\epsilon}^{\eta}_{(2)}(\tau,k_T) = -\frac{2J_1(\omega\tau)}{\omega\tau}\tilde{\epsilon}^{\eta}_{(2)}(\tau=0,k_T), \tag{3.79}$$

$$\tilde{\chi}(\tau,k_T) = J_0(\omega\tau)\tilde{\chi}(\tau=0,k_T), \tag{3.80}$$

with the Bessel functions of the first kind J_n and

$$\omega = \sqrt{(k_1)^2+(k_2)^2}. \tag{3.81}$$

The solution of the original problem is therefore

$$\epsilon^{\eta}_{(2)}(\tau,x_T) = \int \mathrm{d}^2k_T\,\frac{J_1(\omega\tau)}{\omega\tau}e^{ik_Tx_T}f_\epsilon(k_T), \tag{3.82}$$

$$\chi(\tau,x_T) = \int \mathrm{d}^2k_T\,\frac{J_0(\omega\tau)}{\omega^2}e^{ik_Tx_T}f_\chi(k_T), \tag{3.83}$$

with

$$f_\epsilon(k_T) = \frac{ig}{(2\pi)^4}\int \mathrm{d}^2k'_T\,(k_i-k'_i)k'_i\Big[\tilde{\phi}_1^{LC}(k_T-k'_T),\tilde{\phi}_2^{LC}(k'_T)\Big], \tag{3.84}$$

$$f_\chi(k_T) = \frac{ig\epsilon^{ij}}{(2\pi)^4}\int \mathrm{d}^2k'_T\,(k_i-k'_i)k'_j\Big[\tilde{\phi}_1^{LC}(k_T-k'_T),\tilde{\phi}_2^{LC}(k'_T)\Big]. \tag{3.85}$$

3.4 Expansions in ρ in Other Gauges

The expansions that were made in the preceding sections were in ρ^{LC}. Although this may be motivated by the fact that one could make use of Eq. (2.29), it was still an arbitrary choice. One could expand all quantities in ρ^{cov} or in ρ in any other gauge. In this section, the differences between these choices will be investigated.

Any expansion of fields, e.g. $\alpha^i_{(1)}(\tau,x_T)$, was of the form

$$\alpha^i_{(1)}(\tau,x_T) = \sum_{n=1}^{\infty}\alpha^i_{(n)}(\tau,x_T), \tag{3.86}$$

i.e. ρ^{LC} did not explicitly appear, but the fields $\alpha^i_{(n)}(\tau, x_T)$ are understood to be of order n in ρ^{LC}. If the expansions shall be in ρ^{cov} or any other ρ, the form of the formulas does not change, only the interpretation of the fields, as they are to be understood to be of order n in the particular ρ that is used as expansion parameter. The only thing that changes if another ρ is used as expansion parameter are the initial conditions because there, ρ^{LC}, or equivalently ϕ^{LC}, appears explicitly.

Before investigating a general ρ, the initial conditions are expanded in ρ^{cov}, or equivalently ϕ^{cov}, because this particle density appears naturally due to Eq. (3.2).

3.4.1 Expansion in ρ^{cov}

Because of $\rho^{cov} = \rho^{LC} + \mathcal{O}(\rho^{2\,LC})$, the interpretation of the first order of the fields does not need to change. Also, the initial conditions in first order can be obtained by replacing ϕ^{LC} with ϕ^{cov}. Due to the fact that the initial condition for $\alpha^\eta_{(2)}$ only depends on the first order of α^i_m, it can also be obtained via $\phi^{LC} \to \phi^{cov}$. The only initial condition that remains to be calculated is therefore the one for $\alpha^i_{(2)}$. In order to do that, the expansion of α^i_m in terms of ϕ^{cov} is needed. Conveniently, it has already been found during the search for an expansion of α^i_m in terms of ϕ^{LC}, namely in Eq. (3.13). The missing initial condition becomes

$$\alpha^i_{(2)}(\tau = 0, x_T) = \frac{ig}{2} \sum_{m=1}^{2} \Big[\partial^i \phi^{cov}_m, \phi^{cov}_m\Big]. \tag{3.87}$$

Now, one performs the same gauge transformation as before, namely the one given in Eq. (3.44). The field $\phi_{\perp(1)}$ can be obtained by $\phi^{LC} \to \phi^{cov}$ because it is of first order. For the second order, the starting point is Eq. (3.57)

$$\begin{aligned}
\epsilon^i_{(2)}(\tau = 0, x_T) &= \alpha^i_{(2)}(\tau = 0, x_T) + \frac{ig}{2}\Big[\phi_{\perp(1)}, \partial^i \phi_{\perp(1)}\Big] - \partial^i \phi_{\perp(2)} \\
&= \frac{ig}{2}\Big(\Big[\partial^i \phi^{cov}_1, \phi^{cov}_1\Big] + \Big[\partial^i \phi^{cov}_2, \phi^{cov}_2\Big] \\
&\quad + \Big[\phi^{cov}_1 + \phi^{cov}_2, \partial^i(\phi^{cov}_1 + \phi^{cov}_2)\Big]\Big) - \partial^i \phi_{\perp(2)} \\
&= \frac{ig}{2}\Big(\Big[\phi^{cov}_1, \partial^i \phi^{cov}_2\Big] + \Big[\phi^{cov}_2, \partial^i \phi^{cov}_1\Big]\Big) - \partial^i \phi_{\perp(2)}.
\end{aligned} \tag{3.88}$$

The result for $\phi_{\perp(2)}$ can be obtained by imposing the same gauge condition as before, Eq. (3.62). It states that the divergence of Eq. (3.88) has to vanish

$$\begin{aligned}
\Delta_T \phi_{\perp(2)} &= -\frac{ig}{2}\partial_i\Big(\Big[\phi^{cov}_1, \partial^i \phi^{cov}_2\Big] + \Big[\phi^{cov}_2, \partial^i \phi^{cov}_1\Big]\Big), \\
\phi_{\perp(2)} &= -\frac{ig}{2}\frac{1}{\Delta_T}\partial_i\Big(\Big[\phi^{cov}_1, \partial^i \phi^{cov}_2\Big] + \Big[\phi^{cov}_2, \partial^i \phi^{cov}_1\Big]\Big).
\end{aligned} \tag{3.89}$$

The initial condition becomes

$$\epsilon^i_{(2)}(\tau = 0, x_T) = ig\left(\eta^{ij} + \partial^i \frac{1}{\Delta_T}\partial^j\right)[\phi^{cov}_1, \partial_j \phi^{cov}_2]. \tag{3.90}$$

This is the same initial condition for $\epsilon^i_{(2)}$ expanded in ρ^{cov} as for $\epsilon^i_{(2)}$ expanded in ρ^{LC}, Eq. (3.65).

Summing up, the equations of motion and all the initial conditions have the same form in both considered expansions up to second order. Hence, the solutions have the same form as well up to that order. However, their interpretation is different because one is an expansion in terms of ρ^{LC}, whereas the other is an expansion in terms of ρ^{cov}. Now the question arises if the solution up to second order might be the same for expansions in ρ in other gauges as well.

3.4.2 Expansion in a More General ρ

For an expansion in some other $\widehat{\rho}$, one can gauge transform ρ^{LC}

$$\widehat{\rho}_m = W_m \rho_m^{LC} W_m^\dagger, \tag{3.91}$$

with

$$\begin{aligned} W(x^\mu) &= e^{iga_m(x^\mu)}, \\ a_m &= \mathcal{O}(\rho_m). \end{aligned} \tag{3.92}$$

One obtains

$$\widehat{\rho}_m = \rho_m^{LC} + ig\Big[a_m, \rho_m^{LC}\Big] + \mathcal{O}(\rho_m^{3\,LC}), \tag{3.93}$$

and from Eqs. (2.29) and (3.13) one can conclude

$$\begin{aligned} \widehat{\rho}_m &= -\Delta_T \phi_m^{cov} - \frac{ig}{2}\partial_i\Big[\partial^i\phi_m^{cov}, \phi_m^{cov}\Big] + ig[a_m, -\Delta_T\phi_m^{cov}] + \mathcal{O}(\phi_m^{3\,cov}) \\ &= -\Delta_T \phi_m^{cov} - \frac{ig}{2}\partial_i\Big[\partial^i\phi_m^{cov}, \phi_m^{cov}\Big] + ig\partial_i\Big[a_m, \partial^i\phi_m^{cov}\Big] + \mathcal{O}(\phi_m^{3\,cov}) \\ &= -\Delta_T \phi_m^{cov} - \frac{ig}{2}\partial_i\Big[\partial^i\phi_m^{cov}, \phi_m^{cov} + 2a_m\Big] + \mathcal{O}(\phi_m^{3\,cov}) \\ \widehat{\phi}_m &= \phi_m^{cov} + \frac{ig}{2}\frac{1}{\Delta_T}\partial^j[\partial_j\phi_m^{cov}, \phi_m^{cov} + 2a_m] + \mathcal{O}(\phi_m^{3\,cov}). \end{aligned} \tag{3.94}$$

In the last step, Eq. (3.7) was used. Note that

$$a_m = \mathcal{O}(\phi_m^{2\,cov}) \tag{3.95}$$

leads to

$$\widehat{\rho}_m = \rho_m^{LC} + \mathcal{O}(\phi_m^{3\,cov}) \tag{3.96}$$

and

$$a_m = -\frac{1}{2}\phi_m^{cov} + \mathcal{O}(\phi_m^{2\,cov}) \tag{3.97}$$

to

$$\widehat{\phi}_m = \phi_m^{cov} + \mathcal{O}(\phi_m^{3\,cov}). \tag{3.98}$$

Calculating the gradient of Eq. (3.94) one can deduce

$$-\partial^i\phi_m^{cov} = -\partial^i\widehat{\phi}_m + \frac{ig}{2}\partial^i\frac{1}{\Delta_T}\partial^j[\partial_j\phi_m^{cov}, \phi_m^{cov} + 2a_m] + \mathcal{O}(\phi_m^{3\,cov}). \tag{3.99}$$

Inserting Eq. (3.99) into Eq. (3.13), one gets

$$\alpha_m^i = -\partial^i\widehat{\phi}_m + \frac{ig}{2}\eta^{ij}[\partial_j\phi_m^{cov}, \phi_m^{cov}] + \frac{ig}{2}\partial^i\frac{1}{\Delta_T}\partial^j[\partial_j\phi_m^{cov}, \phi_m^{cov} + 2a_m] + \mathcal{O}(\phi_m^{3\,cov}), \tag{3.100}$$

and due to

$$\phi_m^{cov} = \widehat{\phi}_m + \mathcal{O}(\widehat{\phi}_m^2) \tag{3.101}$$

one finds

$$\alpha_m^i = -\partial^i \widehat{\phi}_m + \frac{ig}{2}\Big(\eta^{ij}\Big[\partial_j\widehat{\phi}_m, \widehat{\phi}_m\Big] + \partial^i \frac{1}{\Delta_T}\partial^j\Big[\partial_j\widehat{\phi}_m, \widehat{\phi}_m + 2a_m\Big]\Big) + \mathcal{O}(\widehat{\phi}_m^3). \tag{3.102}$$

With the same argument as for ϕ^{cov}, only one initial condition needs to be calculated, the rest can be obtained by replacing ϕ^{LC} with $\widehat{\phi}$

$$\begin{aligned}
\alpha^i_{(2)}(\tau = 0, x_T) &= \frac{ig}{2}\Big(\eta^{ij}\Big(\Big[\partial_j\widehat{\phi}_1, \widehat{\phi}_1\Big] + \Big[\partial_j\widehat{\phi}_2, \widehat{\phi}_2\Big]\Big) + \partial^i\frac{1}{\Delta_T}\partial^j b_j\Big),\\
b_j &= \Big[\partial_j\widehat{\phi}_1, \widehat{\phi}_1 + 2a_m\Big] + \Big[\partial_j\widehat{\phi}_2, \widehat{\phi}_2 + 2a_m\Big],\\
\epsilon^i_{(2)}(\tau = 0, x_T) &= \alpha^i_{(2)}(\tau = 0, x_T) + \frac{ig}{2}\Big[\phi_{\perp(1)}, \partial^i\phi_{\perp(1)}\Big] - \partial^i\phi_{\perp(2)}\\
&= \frac{ig}{2}\Big(\eta^{ij}\Big(\Big[\widehat{\phi}_1, \partial_j\widehat{\phi}_2\Big] + \Big[\widehat{\phi}_2, \partial_j\widehat{\phi}_1\Big]\Big) + \partial^i\frac{1}{\Delta_T}\partial^j b_j\Big) - \partial^i\phi_{\perp(2)}.
\end{aligned} \tag{3.103}$$

Again, one imposes the gauge condition Eq. (3.62) and finds

$$\begin{aligned}
\Delta_T\phi_{\perp(2)} &= -\frac{ig}{2}\Big(\partial^j\Big(\Big[\widehat{\phi}_1, \partial_j\widehat{\phi}_2\Big] + \Big[\widehat{\phi}_2, \partial_j\widehat{\phi}_1\Big]\Big) - \partial^j b_j\Big),\\
-\partial^i\phi_{\perp(2)} &= \frac{ig}{2}\partial^i\frac{1}{\Delta_T}\partial^j\Big(\Big[\widehat{\phi}_1, \partial_j\widehat{\phi}_2\Big] + \Big[\widehat{\phi}_2, \partial_j\widehat{\phi}_1\Big] - b_j\Big),\\
\epsilon^i_{(2)}(\tau = 0, x_T) &= ig\Big(\eta^{ij} + \partial^i\frac{1}{\Delta_T}\partial^j\Big)\Big[\widehat{\phi}_1, \partial_j\widehat{\phi}_2\Big].
\end{aligned} \tag{3.104}$$

This is once again the same initial condition as Eq. (3.65).

In conclusion, the expansion can be made in any $\widehat{\rho}$ for which one can write $\widehat{\rho}_m = W_m\rho_m^{LC}W_m^\dagger$ with $W_m = e^{iga_m}$ and for which it is possible to expand a_m in powers of ϕ_m^{cov}. This means that the solution found in this chapter is not restricted to an expansion in ρ in one specific gauge, but more general.

Chapter 4

Momentum Broadening in the Glasma

The momentum broadening of a test parton is a quantity of interest in the study of jet quenching, which is a phenomenon that can happen after a high energy nuclei collision. When two high energy nuclei collide, the creation of high momentum partons can occur. They move in opposite directions and lose energy on their way through the Glasma, while they also produce jets of particles, which can be observed by particle detectors. If such a high momentum parton pair is created near the edge of the Glasma, it is possible that one parton and its corresponding jet lose much energy so that only a part of the jet escapes the Glasma and the jet produced by the other parton predominates. Due to one jet being partially missing, this phenomenon is called jet quenching.

In addition to the momentum broadening parameters $\hat{q}$ and κ in a medium themselves, the quantity p^2 of a test particle in said medium, more precisely some average $\langle p^2 \rangle$, is of interest. It changes in time $\langle p^2 \rangle(t)$ and the aforementioned momentum broadening parameters can be derived by performing its time derivative $\mathrm{d}\langle p^2 \rangle(t)/\mathrm{d}t$. In the Glasma, the test particle can be a quark or a gluon. The vector potentials that exist in the Glasma are calculated in Chapter 3. They lead to forces that act on the test parton and consequently influence its momentum. These forces depend on its trajectory, which is why the latter has to be specified to calculate its momentum broadening.

In this chapter, I will derive a formula for $\langle p^2 \rangle$ before choosing a particular trajectory for the test parton. Then, I will study two special trajectories. The first one describes a resting quark or gluon; I will refer to the corresponding quantity as $\langle p^2 \rangle_\kappa$ because its time derivative is κ. The second trajectory describes the test parton moving at the speed of light in some direction in the plane perpendicular to the axis of the two colliding nuclei, which remains the z axis. This transverse plane is then the (x, y) plane and the interior coordinate system is chosen in a way that the x axis coincides with the direction of the test parton. I will refer to the quantity $\langle p^2 \rangle$ corresponding to this trajectory as $\langle p^2 \rangle_{\hat{q}}$ because its time derivative is $\hat{q}$.

The formulas corresponding to the aforementioned parameters that describe the momentum broadening of a test parton contain the vector potentials calculated in Chapter 3. These vector potentials are the result of an expansion in the particle density ρ. Therefore, the results of the momentum broadening parameters in this chapter will also be in some order of the chosen ρ. Due to the fact that the smallest non-vanishing order of the vector potentials in Chapter 3 is two, the smallest non-vanishing order of the momentum broadening parameters will be four. This will be explained as soon as I present the relevant formulas. Higher orders are not considered in this master's thesis, thus the results are only valid for a highly diluted Glasma.

The average $\langle \ldots \rangle$ that is used in this chapter is explained in detail in Section 2.3. The infrared parameter and the ultraviolet cut-off parameter that are introduced to obtain final results are also discussed in Section 2.3. In this chapter, I will analyse the dependence of the momentum broadening parameters on them. Then, I will give the asymptotic behaviour of $\langle p^2 \rangle_{\kappa\,(4)}$ for large t. The subscript (4) refers to the order in ρ. Afterwards, I will discuss numerical results of the momentum broadening parameters. Finally, I will present an alternative way of calculating the momentum broadening parameters, namely with the help of correlators.

4.1 Formula for $\langle p^2 \rangle$

The equations of motion for a test parton in a non-Abelian background field are the Wong equations [16]

$$\frac{\mathrm{d}p^\mu}{\mathrm{d}\tau} = gQ_a F_a^{\mu\nu} u_\nu, \tag{4.1}$$

$$\frac{\mathrm{d}Q_a}{\mathrm{d}\tau} = -gf_{abc} u_\mu A_b^\mu Q_c, \tag{4.2}$$

with the four momentum p^μ, the proper time τ, the coupling constant g, the colour charge Q_a, the field strength tensor $F_a^{\mu\nu}$, the four velocity u^μ, the structure constants f_{abc} of $SU(N_c)$ and the vector potential A_a^μ. In terms of algebra elements, Eqs. (4.1) and (4.2) can be written as

$$\frac{\mathrm{d}p^\mu}{\mathrm{d}\tau} = 2g\,\mathrm{Tr}(QF^{\mu\nu}u_\nu), \tag{4.3}$$

$$\frac{\mathrm{d}Q}{\mathrm{d}\tau} = ig[u_\mu A^\mu, Q]. \tag{4.4}$$

To get the momentum broadening in terms of t, instead of τ, one makes use of

$$\frac{\mathrm{d}}{\mathrm{d}\tau} = \gamma \frac{\mathrm{d}}{\mathrm{d}t},$$
$$u^\mu = \gamma v^\mu, \tag{4.5}$$

with

$$v^\mu = \begin{pmatrix} 1 \\ \frac{\mathrm{d}x^i}{\mathrm{d}t} \end{pmatrix}^\mu \tag{4.6}$$

and obtains

$$\frac{\mathrm{d}p^\mu}{\mathrm{d}t} = 2g\,\mathrm{Tr}(QF^{\mu\nu}v_\nu), \tag{4.7}$$

$$\frac{\mathrm{d}Q}{\mathrm{d}t} = ig[v_\mu A^\mu, Q]. \tag{4.8}$$

Equation (4.8) is an ordinary differential equation. Together with a given $Q(t_0)$ as initial condition, it has a unique solution. The ansatz

$$Q(t) = U(t,t_0)Q(t_0)U^\dagger(t,t_0). \tag{4.9}$$

is made to translate said differential equation to one for $U(t,t_0)$, namely

$$\frac{\mathrm{d}U}{\mathrm{d}t} = igv_\mu A^\mu U. \tag{4.10}$$

This can be obtained by plugging Eq. (4.9) into Eq. (4.8). The initial condition reads

$$U(t_0,t_0) = 1. \tag{4.11}$$

It ensures that Eq. (4.9) is consistent. This new differential equation, Eq. (4.10), together with its initial condition, Eq. (4.11), has the unique solution

$$U(t,t_0) = \mathcal{T}e^{ig\int_{t_0}^{t}\mathrm{d}t'\,v_\mu(t')A^\mu(t')}, \tag{4.12}$$

with the time ordering operator $\mathcal{T}$. Note that this solution states that the colour charge $Q(t)$ rotates in charge space.

The Lorentz force

$$F^i = F^{i\mu}v_\mu \tag{4.13}$$

and its parallel transported version

$$f^i(x^j(t'),t') = U(t_0,t')F^i(x^j(t'),t')U(t',t_0) \tag{4.14}$$

permit the solution of the spatial components of Eq. (4.7) to be written as

$$\begin{aligned} p^i(t) &= 2g\int_{t_0}^{t}\mathrm{d}t'\ \mathrm{Tr}(Q(t')F^i(x^j(t'),t')) \\ &= 2g\int_{t_0}^{t}\mathrm{d}t'\ \mathrm{Tr}(U(t',t_0)Q(t_0)U^\dagger(t',t_0)F^i(x^j(t'),t')) \\ &= 2gQ_a(t_0)\int_{t_0}^{t}\mathrm{d}t'\ \mathrm{Tr}(t_aU(t_0,t')F^i(x^j(t'),t')U(t',t_0)) \\ &= 2gQ_a(t_0)\int_{t_0}^{t}\mathrm{d}t'\ \mathrm{Tr}(t_af^i). \end{aligned} \tag{4.15}$$

In the first step, Eq. (4.9) was used.

One obtains for the square of one component of the momentum

$$p^{\underline{i}}p^{\underline{i}} = 4g^2 Q_a(t_0)Q_b(t_0)\int_{t_0}^{t}\mathrm{d}t'\int_{t_0}^{t}\mathrm{d}t''\ \mathrm{Tr}(t_a f^{\underline{i}})\,\mathrm{Tr}(t_b f^{\underline{i}}), \tag{4.16}$$

where the summation convention is not applied to underlined indices. This expression depends on the colour of the test parton, which is not an observable quantity. The quantity of interest is therefore an average over the colours

$$A\int \mathrm{d}Q\, p^{\underline{i}}p^{\underline{i}} = 4g^2 A\int \mathrm{d}Q\, Q_a(t_0)Q_b(t_0)\int_{t_0}^{t}\mathrm{d}t'\int_{t_0}^{t}\mathrm{d}t''\ \mathrm{Tr}(t_a f^{\underline{i}})\,\mathrm{Tr}(t_b f^{\underline{i}}). \tag{4.17}$$

A is a normalisation constant that depends on whether the test parton in question is a quark or a gluon. More precisely, as is stated in [17],

$$A = \begin{cases} \dfrac{1}{N_c} = \dfrac{1}{3} & \text{for quarks,} \\ \dfrac{1}{N_c^2-1} = \dfrac{1}{8} & \text{for gluons.} \end{cases} \tag{4.18}$$

where N_c corresponds to the gauge group $SU(N_c)$. Performing the average yields, as is shown in [18],

$$\int \mathrm{d}Q\, Q_a Q_b = C_2\delta_{ab}, \tag{4.19}$$

with the quadratic Casimir C_2,

$$C_2 = \begin{cases} \dfrac{1}{2} & \text{for quarks,} \\ N_c = 3 & \text{for gluons.} \end{cases} \tag{4.20}$$

One defines

$$\widetilde{A} = AC_2, \tag{4.21}$$

hence

$$\widetilde{A} = \begin{cases} \dfrac{1}{2N_c} = \dfrac{1}{6} & \text{for quarks,} \\ \dfrac{N_c}{N_c^2-1} = \dfrac{3}{8} & \text{for gluons.} \end{cases} \tag{4.22}$$

With Eqs. (4.14), (4.19) and (4.21), Eq. (4.17) becomes

$$\begin{aligned} A\int \mathrm{d}Q\, p^{\underline{i}}p^{\underline{i}} &= 4g^2\widetilde{A}\int_{t_0}^{t}\mathrm{d}t'\int_{t_0}^{t}\mathrm{d}t''\ \mathrm{Tr}(t_a f^{\underline{i}})\,\mathrm{Tr}(t_a f^{\underline{i}}) \\ &= 2g^2\widetilde{A}\int_{t_0}^{t}\mathrm{d}t'\int_{t_0}^{t}\mathrm{d}t''\ \mathrm{Tr}(f^{\underline{i}}f^{\underline{i}}) \\ &= 2g^2\widetilde{A}\int_{t_0}^{t}\mathrm{d}t'\int_{t_0}^{t}\mathrm{d}t''\ \mathrm{Tr}(U(t_0,t')F^{\underline{i}}(x^j(t'),t')U(t',t'')F^{\underline{i}}(x^j(t''),t'')U(t'',t_0)). \end{aligned} \tag{4.23}$$

In the first step, Eq. (A.11) was used. The fact that $U(t',t_0)U(t_0,t'') = U(t',t'')$ was exploited in the last step.

In Chapter 3, the quantities in question were expanded in powers of the particle density ρ. In order to use those results, one needs to do the same here. The only order of interest in this master's thesis is the lowest non-vanishing one. The vector fields are of order two in a specific gauge, so the field strength tensor is of order two in this gauge as well. Due to the fact that Eq. (4.23) is gauge invariant, one can plug the previous results in without the need to transform them to another gauge. $U(t_0, t)$ needs to be expanded as well

$$U(t_0, t) = 1 + \mathcal{O}(A^\mu) = 1 + \mathcal{O}(\rho^2). \tag{4.24}$$

The lowest non-vanishing order is therefore four

$$A \int \mathrm{d}Q \, p^i p^i_{(4)} = 2g^2 \widetilde{A} \int_{t_0}^{t} \mathrm{d}t' \int_{t_0}^{t} \mathrm{d}t'' \, \mathrm{Tr}(F^i_{(2)}(x^j(t'), t') F^i_{(2)}(x^j(t''), t'')). \tag{4.25}$$

The field strength tensors and consequently the forces in Eq. (4.25) depend on the specific ρ that is chosen. However, one does not want to work with *one* configuration of particle densities, but use an ensemble of them. Thus, one is interested in ensemble averages of the left-hand side of Eq. (4.25). Here, the MV model, which was developed in [14, 15], is used and adapted by introducing an infrared regulator and an ultraviolet cut-off. This leads to Eq. (2.45), which is used to perform these averages. One defines

$$\langle p^i p^i \rangle = \langle A \int \mathrm{d}Q \, p^i p^i \rangle, \tag{4.26}$$

that means, when talking about $\langle p^2 \rangle$, the already colour averaged quantity is always meant. One obtains

$$\langle p^i p^i \rangle_{(4)}(t) = 2g^2 \widetilde{A} \int_{t_0}^{t} \mathrm{d}t' \int_{t_0}^{t} \mathrm{d}t'' \, \langle \mathrm{Tr}(F^i_{(2)}(x^j(t'), t') F^i_{(2)}(x^j(t''), t'')) \rangle. \tag{4.27}$$

The next step is to calculate the forces in Eq. (4.27). Equation (B.10) together with

$$F_i = E_i + \epsilon_i{}^{jk} \dot{x}_j B_k \tag{4.28}$$

makes it possible to calculate the force in terms of the field strength tensor in (τ, η, x_T) coordinates; the convention of the epsilon tensor is specified in Appendix A. The result is

$$\begin{aligned} F_i &= F_{\tau i}(\cosh\eta - \dot{x}_3 \sinh\eta) - \frac{1}{\tau} F_{\eta i}(\sinh\eta - \dot{x}_3 \cosh\eta) - \epsilon_{ij3} \dot{x}_j F_{12}, \\ F_3 &= \frac{1}{\tau} F_{\tau\eta} - \sum_{i=1}^{2} \dot{x}_i \Big(F_{i\tau} \sinh\eta + \frac{1}{\tau} F_{\eta i} \cosh\eta \Big). \end{aligned} \tag{4.29}$$

Note that $\dot{x}$ denotes $\mathrm{d}x/\mathrm{d}t$, not $\mathrm{d}x/\mathrm{d}\tau$ and that $i = 1, 2$ because there are only two dimensions in the transverse plane.

After the collision of the two nuclei, which are moving in $+z$ and $-z$ direction, the created particles propagate in every direction. The test parton in question is

considered to be and to remain in the (x, y) plane, which can also be described by $\eta = 0$ and $\tau = t$. There, Eq. (4.29) becomes

$$\begin{aligned} F_i &= F_{\tau i} + \frac{\dot{x}_3}{\tau} F_{\eta i} - \epsilon_{ij3}\dot{x}_j F_{12}, \\ F_3 &= \frac{1}{\tau} F_{\tau\eta} - \sum_{i=1}^{2} \frac{\dot{x}_i}{\tau} F_{\eta i}, \end{aligned} \tag{4.30}$$

where again $i = 1, 2$. The field strength tensor in terms of the fields ϵ^i and ϵ^η reads

$$\begin{aligned} F_{\tau i} &= \partial_\tau \epsilon_i - \partial_i \epsilon_\tau + ig[\epsilon_\tau, \epsilon_i] &&= -\partial_\tau \epsilon^i, \\ F_{\eta i} &= \partial_\eta \epsilon_i - \partial_i \epsilon_\eta + ig[\epsilon_\eta, \epsilon_i] &&= \tau^2 \partial_i \epsilon^\eta + ig\tau^2 \left[\epsilon^\eta, \epsilon^i\right], \\ F_{12} &= \partial_1 \epsilon_2 - \partial_2 \epsilon_1 + ig[\epsilon_1, \epsilon_2] &&= \partial_1 \epsilon_2 - \partial_2 \epsilon_1 + ig\left[\epsilon^1, \epsilon^2\right], \\ F_{\tau\eta} &= \partial_\tau \epsilon_\eta - \partial_\eta \epsilon_\tau + ig[\epsilon_\tau, \epsilon_\eta] &&= -\partial_\tau \left(\tau^2 \epsilon^\eta\right). \end{aligned} \tag{4.31}$$

With Eq. (3.68), the field strength tensor to second order in terms of ϵ and χ can be written as

$$\begin{aligned} F_{\tau i\,(2)} &= -\epsilon_{ij}\partial_\tau \partial_j \chi, \\ F_{\eta i\,(2)} &= \tau^2 \partial_i \epsilon^\eta_{(2)}, \\ F_{12\,(2)} &= \Delta_T \chi, \\ F_{\tau\eta\,(2)} &= -\partial_\tau(\tau^2 \epsilon^\eta_{(2)}). \end{aligned} \tag{4.32}$$

To further calculate Eq. (4.30), the trajectory has to be specified. A resting test parton yields $\langle p^2 \rangle$ pertaining to κ, which will be called $\langle p^2 \rangle_\kappa$, a test parton propagating at the speed of light perpendicular to the axis of the colliding nuclei, which will be the x axis, yields $\langle p^2 \rangle$ corresponding to $\hat{q}$, which will be called $\langle p^2 \rangle_{\hat{q}}$.

4.2 Resting Test Parton: $\langle p^2 \rangle_\kappa$ and κ

Equations (4.30), (4.32) and the trajectory $x^j(t) = x_0^j$, $\dot{x}^j = 0$ yield

$$\begin{aligned} F_{i\,(2)}(t, x_T) &= -\epsilon_{ij}\partial_\tau \partial_j \chi \Big|_{\tau=t} = -\epsilon_{ij}\partial_t \partial_j \chi, \quad i = 1, 2 \\ F_{3\,(2)}(t, x_T) &= -\frac{1}{\tau}\partial_\tau(\tau^2 \epsilon_{(2)}) \Big|_{\tau=t} = -\frac{1}{t}\partial_t(t^2 \epsilon_{(2)}). \end{aligned} \tag{4.33}$$

Using Eqs. (3.82) to (3.85), Eq. (4.33) becomes

$$\begin{aligned} F_{i\,(2)}(t, x_T) &= -\epsilon_{ij}\partial_t \partial_j \int \mathrm{d}^2 k_T \, \frac{J_0(\omega t)}{\omega^2} e^{ik_T x_T} f_\chi(k_T) \\ &= \epsilon_{ij} \int \mathrm{d}^2 k_T \, \frac{ik_j}{\omega} J_1(\omega t) e^{ik_T x_T} f_\chi(k_T), \end{aligned} \tag{4.34}$$

$$\begin{aligned} F_{3\,(2)}(t, x_T) &= -\frac{1}{t}\partial_t \int \mathrm{d}^2 k_T \, \frac{t}{\omega} J_1(\omega t) e^{ik_T x_T} f_\epsilon(k_T) \\ &= -\int \mathrm{d}^2 k_T \, J_0(\omega t) e^{ik_T x_T} f_\epsilon(k_T). \end{aligned} \tag{4.35}$$

4.2.1 Longitudinal Component: $\langle p_z^2\rangle_\kappa$ and κ_z

The first thing that will be calculated is $\langle p_3^2\rangle_{\kappa\,(4)} = \langle p_z^2\rangle_{\kappa\,(4)}$. Equations (4.27) and (4.35) with $t_0 = 0$ lead to

$$\langle p_z^2\rangle_{\kappa\,(4)}(t;x_0) = 2g^2\tilde{A}\int_0^t \mathrm{d}t'\int_0^t \mathrm{d}t''\int \mathrm{d}^2k_T\int \mathrm{d}^2k'_T\, J_0(\omega t')J_0(\omega' t'') \times e^{ik_Tx_0}e^{ik'_Tx_0}\langle \mathrm{Tr}(f_\epsilon(k_T)f_\epsilon(k'_T))\rangle. \tag{4.36}$$

The trace and the ensemble average commute, as is shown in the following proof, which makes use of Equation (2.43).

Proof:

$$\begin{aligned}\mathrm{Tr}\langle\mathcal{O}[A_\mu]\rangle &= \mathrm{Tr}\Big(\int\mathcal{D}\rho\, O[A_\mu]W[\rho]\Big)\\ &= \int\mathcal{D}\rho\ \mathrm{Tr}(O[A_\mu]W[\rho])\\ &= \int\mathcal{D}\rho\ \mathrm{Tr}(O[A_\mu])W[\rho]\\ &= \langle\mathrm{Tr}(\mathcal{O}[A_\mu])\rangle.\end{aligned} \tag{4.37}$$

□

The next thing that will be calculated is $\langle\mathrm{Tr}(f_\epsilon(k_T)f_\epsilon(k'_T))\rangle$, or equivalently, as shown in Proof (4.37), $\mathrm{Tr}(\langle f_\epsilon(k_T)f_\epsilon(k'_T)\rangle)$. With the definition of f_ϵ, which is given in Eq. (3.84), one gets

$$\langle f_\epsilon(k_T)f_\epsilon(k'_T)\rangle = \left(\frac{ig}{(2\pi)^4}\right)^2\int\mathrm{d}^2l_T\int\mathrm{d}^2l'_T(k_i-l_i)l_i(k'_j-l'_j)l_j \times\Big\langle\Big[\tilde{\phi}_1(k_T-l_T),\tilde{\phi}_2(l_T)\Big]\Big[\tilde{\phi}_1(k'_T-l'_T),\tilde{\phi}_2(l'_T)\Big]\Big\rangle. \tag{4.38}$$

With the help of Eq. (3.8), one obtains

$$\begin{aligned}&\Big\langle\Big[\tilde{\phi}_1(k_T-l_T),\tilde{\phi}_2(l_T)\Big]\Big[\tilde{\phi}_1(k'_T-l'_T),\tilde{\phi}_2(l'_T)\Big]\Big\rangle\\ &= \frac{1}{(k_T-l_T)^2}\frac{1}{(k'_T-l'_T)^2}\frac{1}{l_T^2}\frac{1}{l_T'^2}\langle[\tilde{\rho}'_1(k_T-l_T),\tilde{\rho}'_2(l_T)][\tilde{\rho}'_1(k'_T-l'_T),\tilde{\rho}'_2(l'_T)]\rangle.\end{aligned} \tag{4.39}$$

The two point function can be calculated in the fundamental representation with Eq. (2.45)

$$\begin{aligned}&\langle[\tilde{\rho}'_1(k_T-l_T),\tilde{\rho}'_2(l_T)][\tilde{\rho}'_1(k'_T-l'_T),\tilde{\rho}'_2(l'_T)]\rangle\\ &= \langle\tilde{\rho}'_{1a}(k_T-l_T)\tilde{\rho}'_{2b}(l_T)\tilde{\rho}'_{1c}(k'_T-l'_T)\tilde{\rho}'_{2d}(l'_T)[t_a,t_b][t_c,t_d]\rangle\\ &= i^2f_{abe}f_{cdf}t_et_f\langle\tilde{\rho}'_{1a}(k_T-l_T)\tilde{\rho}'_{1c}(k'_T-l'_T)\rangle\langle\tilde{\rho}'_{2b}(l_T)\tilde{\rho}'_{2d}(l'_T)\rangle\\ &= -f_{abe}f_{cdf}t_et_f\frac{(k_T-l_T)^4}{((k_T-l_T)^2+m^2)^2}\frac{l_T^4}{(l_T^2+m^2)^2}\\ &\quad\times(2\pi)^4g^4\mu^4\delta_{ac}\delta_{bd}\delta(k_T+k'_T)\delta(l_T+l'_T)\theta(\Lambda_{UV}-|k_T-l_T|)\theta(\Lambda_{UV}-|l_T|).\end{aligned} \tag{4.40}$$

From the second to the third line the relation $[t_a,t_b] = if_{abe}t_e$ was used. The trace was omitted until now. It neither affects the prefactor nor the integral on the right-hand side of Eq. (4.38), nor does it affect the prefactor on the right-hand side of

Eq. (4.39). It only acts on the ensemble average of $\widetilde{\rho}'$ and can thus be reinserted now. The relation $\mathrm{Tr}(t_e t_f) = \frac{1}{2}\delta_{ef}$ leads to

$$\begin{aligned}
&\mathrm{Tr}\langle[\widetilde{\rho}_1'(k_T - l_T), \widetilde{\rho}_2'(l_T)][\widetilde{\rho}_1'(k_T' - l_T'), \widetilde{\rho}_2'(l_T')]\rangle \\
&= -f_{abe}f_{cdf}\,\mathrm{Tr}(t_e t_f)\frac{(k_T - l_T)^4}{((k_T - l_T)^2 + m^2)^2}\frac{l_T^4}{(l_T^2 + m^2)^2} \\
&\quad \times (2\pi)^4 g^4 \mu^4 \delta_{ac}\delta_{bd}\delta(k_T + k_T')\delta(l_T + l_T')\theta(\Lambda_{UV} - |k_T - l_T|)\theta(\Lambda_{UV} - |l_T|) \\
&= -\frac{1}{2}f_{abc}f_{abc}\frac{(k_T - l_T)^4}{((k_T - l_T)^2 + m^2)^2}\frac{l_T^4}{(l_T^2 + m^2)^2} \\
&\quad \times (2\pi)^4 g^4 \mu^4 \delta(k_T + k_T')\delta(l_T + l_T')\theta(\Lambda_{UV} - |k_T - l_T|)\theta(\Lambda_{UV} - |l_T|)
\end{aligned} \tag{4.41}$$

and the fully contracted structure constants f_{abc} of $SU(3)$ yield

$$\begin{aligned}
f_{abc}f_{abc} &= 3!\sum_{a<b<c} f_{abc}f_{abc} \\
&= 3!\Big((f_{123})^2 + (f_{147})^2 + (f_{156})^2 + (f_{246})^2 + (f_{257})^2 + (f_{345})^2 + \\
&\quad + (f_{367})^2 + (f_{458})^2 + (f_{678})^2\Big) \\
&= 3!\left(1 + 6\times\frac{1}{4} + 2\times\frac{3}{4}\right) = 24.
\end{aligned} \tag{4.42}$$

Taking advantage of

$$f_{acd}f_{bcd} = N_c\,\delta_{ab}, \tag{4.43}$$

which is stated in [19], one obtains for the fully contracted structure constants for $SU(N_c)$

$$f_{abc}f_{abc} = N_c(N_c^2 - 1). \tag{4.44}$$

Going from the formulation in $\widetilde{\rho}$ back to the one in $\widetilde{\phi}$, the denominator in Eq. (4.39) cancels the numerator in Eq. (4.41) due to the δ functions

$$\begin{aligned}
&\mathrm{Tr}\Big\langle\Big[\widetilde{\phi}_1(k_T - l_T), \widetilde{\phi}_2(l_T)\Big]\Big[\widetilde{\phi}_1(k_T' - l_T'), \widetilde{\phi}_2(l_T')\Big]\Big\rangle \\
&= -\frac{N_c(N_c^2 - 1)}{2}\frac{(2\pi)^4 g^4 \mu^4}{((k_T - l_T)^2 + m^2)^2(l_T^2 + m^2)^2}\delta(k_T + k_T')\delta(l_T + l_T') \\
&\quad \times \theta(\Lambda_{UV} - |k_T - l_T|)\theta(\Lambda_{UV} - |l_T|).
\end{aligned} \tag{4.45}$$

Putting everything together and integrating one δ function, one obtains

$$\begin{aligned}
\mathrm{Tr}\langle f_\epsilon(k_T) f_\epsilon(k_T')\rangle &= \frac{N_c(N_c^2 - 1)g^6\mu^4}{2(2\pi)^4}\delta(k_T + k_T') \\
\times \int \mathrm{d}^2 l_T\, &\frac{(k_i - l_i)l_i(k_j - l_j)l_j}{((k_T - l_T)^2 + m^2)^2(l_T^2 + m^2)^2}\theta(\Lambda_{UV} - |k_T - l_T|)\theta(\Lambda_{UV} - |l_T|).
\end{aligned} \tag{4.46}$$

The definitions

$$g_z(k_T) = \int \mathrm{d}^2 l_T\, \frac{(k_i - l_i)l_i(k_j - l_j)l_j}{((k_T - l_T)^2 + m^2)^2(l_T^2 + m^2)^2}\theta(\Lambda_{UV} - |k_T - l_T|)\theta(\Lambda_{UV} - |l_T|) \tag{4.47}$$

and

$$B = \frac{N_c(N_c^2-1)g^8\mu^4\tilde{A}}{(2\pi)^4} = \frac{24g^8\mu^4\tilde{A}}{(2\pi)^4}, \tag{4.48}$$

together with Eqs. (4.46) and (4.36), lead to

$$\begin{aligned}
\langle p_z^2\rangle_{\kappa\,(4)}(t;x_0) &= B\int \mathrm{d}^2k_T\, g_z(k_T)\int_0^t \mathrm{d}t'\int_0^t \mathrm{d}t''\int \mathrm{d}^2k_T'\, J_0(\omega t')J_0(\omega' t'') \\
&\quad\times e^{ik_Tx_0}e^{ik_T'x_0}\delta(k_T+k_T') \\
&= B\int \mathrm{d}^2k_T\, g_z(k_T)\int_0^t \mathrm{d}t'\int_0^t \mathrm{d}t''\, J_0(\omega t')J_0(\omega t'') \\
&= B\int \mathrm{d}^2k_T\, g_z(k_T)\left(\int_0^t \mathrm{d}t'\, J_0(\omega t')\right)^2 \\
&= B\int \mathrm{d}^2k_T\, g_z(k_T)\frac{t^2}{4}(\pi J_1(\omega t)H_0(\omega t)+J_0(\omega t)(2-\pi H_1(\omega t)))^2,
\end{aligned} \tag{4.49}$$

with the Struve functions H_n. Note that the x_0 dependence drops out, hence $\langle p_z^2\rangle_{\kappa\,(4)}$ and $\kappa_{z\,(4)}$ do not depend on it.

If one defines

$$f_z(\omega t) = \frac{\omega t}{2}(\pi J_1(\omega t)H_0(\omega t)+J_0(\omega t)(2-\pi H_1(\omega t))), \tag{4.50}$$

the quantity $\langle p_z^2\rangle_{\kappa\,(4)}/B$ can be written more concisely

$$\frac{\langle p_z^2\rangle_{\kappa\,(4)}}{B} = \int \mathrm{d}^2k_T\, g_z(k_T)\frac{1}{\omega^2}f_z(\omega t)^2. \tag{4.51}$$

Note that f_z is a function of ωt, not a function of ω and t separately.

Up until now, there was no need for an ultraviolet cut-off or an infrared regulator, but they are key to make the substitution

$$q_i = k_i - l_i \tag{4.52}$$

possible. Afterwards, polar coordinates are introduced

$$\begin{aligned}
\frac{\langle p_z^2\rangle_{\kappa\,(4)}}{B} &= \int \mathrm{d}^2k_T\int \mathrm{d}^2l_T\,\frac{(k_i-l_i)l_i(k_j-l_j)l_j}{((k_T-l_T)^2+m^2)^2(l_T^2+m^2)^2} \\
&\quad\times\theta(\Lambda_{UV}-|k_T-l_T|)\theta(\Lambda_{UV}-|l_T|)\frac{1}{\omega^2}f_z(\omega t)^2 \\
&= \int \mathrm{d}^2l_T\int \mathrm{d}^2q_T\,\frac{q_il_iq_jl_j}{(q_T^2+m^2)^2(l_T^2+m^2)^2} \\
&\quad\times\theta(\Lambda_{UV}-|q_T|)\theta(\Lambda_{UV}-|l_T|)\frac{1}{\omega^2}f_z(\omega t)^2 \\
&= \int_0^{\Lambda_{UV}}\mathrm{d}r_l\int_0^{\Lambda_{UV}}\mathrm{d}r_q\int_0^{2\pi}\mathrm{d}\varphi_l\int_0^{2\pi}\mathrm{d}\varphi_q\,\frac{1}{\omega^2}\frac{r_q^3r_l^3\cos^2(\varphi_q-\varphi_l)}{(r_q^2+m^2)^2(r_l^2+m^2)^2}f_z(\omega t)^2.
\end{aligned} \tag{4.53}$$

Another substitution,

$$\varphi = \varphi_q - \varphi_l, \tag{4.54}$$

is made, which leads to

$$\begin{aligned}\frac{\langle p_z^2\rangle_{\kappa\,(4)}}{B} &= \int_0^{\Lambda_{UV}}\mathrm{d}r_l\int_0^{\Lambda_{UV}}\mathrm{d}r_q\int_0^{2\pi}\mathrm{d}\varphi_l\int_{-\varphi_l}^{2\pi-\varphi_l}\mathrm{d}\varphi\,\frac{(r_q r_l)^3}{\omega^2}\left(\frac{\cos\varphi}{(r_q^2+m^2)(r_l^2+m^2)}f_z(\omega t)\right)^2\\ &= \int_0^{\Lambda_{UV}}\mathrm{d}r_l\int_0^{\Lambda_{UV}}\mathrm{d}r_q\int_0^{2\pi}\mathrm{d}\varphi_l\int_0^{2\pi}\mathrm{d}\varphi\,\frac{(r_q r_l)^3}{\omega^2}\left(\frac{\cos\varphi}{(r_q^2+m^2)(r_l^2+m^2)}f_z(\omega t)\right)^2,\\ \frac{\langle p_z^2\rangle_{\kappa\,(4)}(t)}{2\pi B} &= \int_0^{\Lambda_{UV}}\mathrm{d}r_l\int_0^{\Lambda_{UV}}\mathrm{d}r_q\int_0^{2\pi}\mathrm{d}\varphi\,\frac{(r_q r_l)^3}{\omega^2}\left(\frac{\cos\varphi}{(r_q^2+m^2)(r_l^2+m^2)}f_z(\omega t)\right)^2.\end{aligned}\tag{4.55}$$

Note that the above substitutions change ω in Eq. (3.81) to

$$\omega(r_q, r_l, \varphi) = \sqrt{r_l^2 + r_q^2 + 2r_l r_q\cos\varphi}.\tag{4.56}$$

From Eq. (4.55), one can calculate $\kappa_{z\,(4)} = \mathrm{d}\langle p_z^2\rangle_{\kappa\,(4)}/\mathrm{d}t$

$$\frac{\kappa_{z\,(4)}(t)}{2\pi B} = 2\int_0^{\Lambda_{UV}}\mathrm{d}r_l\int_0^{\Lambda_{UV}}\mathrm{d}r_q\int_0^{2\pi}\mathrm{d}\varphi\,\frac{(r_q r_l)^3}{\omega}\left(\frac{\cos\varphi}{(r_q^2+m^2)(r_l^2+m^2)}\right)^2 J_0(\omega t)f_z(\omega t).\tag{4.57}$$

4.2.2 Transversal Component: $\langle p_T^2\rangle_\kappa$ and κ_T

The next thing that will be calculated is $\langle p_2^2\rangle_{\kappa\,(4)} = \langle p_y^2\rangle_{\kappa\,(4)}$; t_0 is again set to be 0. Equations (4.27) and (4.34) lead to

$$\begin{aligned}\langle p_y^2\rangle_{\kappa\,(4)}(t;x_0) = 2g^2\widetilde{A}\int_0^t\mathrm{d}t'\int_0^t\mathrm{d}t''\int\mathrm{d}^2k_T\int\mathrm{d}^2k_T'\,\frac{ik_1}{\omega}J_1(\omega t')\frac{ik_1'}{\omega'}J_1(\omega' t'')\\ \times e^{ik_T x_0}e^{ik_T' x_0}\langle\mathrm{Tr}(f_\chi(k_T)f_\chi(k_T'))\rangle.\end{aligned}\tag{4.58}$$

A comparison between Eq. (3.84) and Eq. (3.85) leads to the conclusion that Eq. (3.84) can be written as

$$f_\epsilon(k_T) = \frac{ig}{(2\pi)^4}\delta_i^j\int\mathrm{d}^2k_T'\,(k_i-k_i')k_j'\left[\widetilde{\phi}_1^{LC}(k_T-k_T'),\widetilde{\phi}_2^{LC}(k_T')\right]\tag{4.59}$$

and that Eq. (3.85) can be reproduced by $\delta_i^j \to \epsilon^{ij}$. Therefore, the calculation is analogous to the one above and one obtains

$$\begin{aligned}&\mathrm{Tr}\langle f_\chi(k_T)f_\chi(k_T')\rangle = \frac{12g^6\mu^4}{(2\pi)^4}\delta(k_T+k_T')\\ &\times\int\mathrm{d}^2l_T\,\frac{\epsilon^{ij}\epsilon^{mn}(k_i-l_i)(k_m-l_m)l_j l_n}{((k_T-l_T)^2+m^2)^2(l_T^2+m^2)^2}\theta(\Lambda_{UV}-|k_T-l_T|)\theta(\Lambda_{UV}-|l_T|)\\ &= \frac{12g^6\mu^4}{(2\pi)^4}\delta(k_T+k_T')\\ &\times\int\mathrm{d}^2l_T\,\frac{(k_T-l_T)^2l_T^2-(k_i-l_i)l_i(k_j-l_j)l_j}{((k_T-l_T)^2+m^2)^2(l_T^2+m^2)^2}\theta(\Lambda_{UV}-|k_T-l_T|)\theta(\Lambda_{UV}-|l_T|).\end{aligned}\tag{4.60}$$

The definition

$$g_T(k_T) = \int\mathrm{d}^2l_T\,\frac{(k_T-l_T)^2l_T^2-(k_i-l_i)l_i(k_j-l_j)l_j}{((k_T-l_T)^2+m^2)^2(l_T^2+m^2)^2}\theta(\Lambda_{UV}-|k_T-l_T|)\theta(\Lambda_{UV}-|l_T|)\tag{4.61}$$

highlights the similarity of Eq. (4.49) to

$$\begin{aligned}\langle p_y^2 \rangle_{\kappa\,(4)}(t;x_0) &= B \int \mathrm{d}^2 k_T\, g_T(k_T) \int_0^t \mathrm{d}t' \int_0^t \mathrm{d}t'' \int \mathrm{d}^2 k_T' \, \frac{ik_1}{\omega} J_1(\omega t') \frac{ik_1'}{\omega'} J_1(\omega' t'') \\ &\quad \times e^{ik_T x_0} e^{ik_T' x_0} \delta(k_T + k_T') \\ &= B \int \mathrm{d}^2 k_T\, g_T(k_T) \int_0^t \mathrm{d}t' \int_0^t \mathrm{d}t'' \, \frac{(k_1)^2}{\omega^2} J_1(\omega t') J_1(\omega t'') \\ &= B \int \mathrm{d}^2 k_T\, g_T(k_T) \frac{(k_1)^2}{\omega^2} \left(\int_0^t \mathrm{d}t'\, J_1(\omega t') \right)^2 \\ &= B \int \mathrm{d}^2 k_T\, g_T(k_T) \frac{(k_1)^2}{\omega^4} (1 - J_0(\omega t))^2. \end{aligned} \tag{4.62}$$

The x_0 dependence drops out again. Therefore, $\langle p_y^2 \rangle_{\kappa\,(4)}$ does not depend on it as well. Due to the fact that one gets $\langle p_x^2 \rangle_{\kappa\,(4)}$ by replacing $k_1 \to k_2$, $\langle p_x^2 \rangle_{\kappa\,(4)}$ does not depend on x_0 either and consequently their sum

$$\langle p_T^2 \rangle_{\kappa\,(4)} = \langle p_x^2 \rangle_{\kappa\,(4)} + \langle p_y^2 \rangle_{\kappa\,(4)} \tag{4.63}$$

and its time derivative $\kappa_{T\,(4)} = \mathrm{d}\langle p_T^2 \rangle_{\kappa\,(4)} / \mathrm{d}t$ neither. The definition

$$f_T(\omega t) = 1 - J_0(\omega t) \tag{4.64}$$

permits to write $\langle p_T^2 \rangle_{\kappa\,(4)} / B$ in a similar way to Eq. (4.51), namely

$$\frac{\langle p_T^2 \rangle_{\kappa\,(4)}}{B} = \int \mathrm{d}^2 k_T\, g_T(k_T) \frac{1}{\omega^2} f_T(\omega t)^2. \tag{4.65}$$

The same coordinate changes as before lead to the results

$$\frac{\langle p_T^2 \rangle_{\kappa\,(4)}(t)}{2\pi B} = \int_0^{\Lambda_{UV}} \mathrm{d}r_l \int_0^{\Lambda_{UV}} \mathrm{d}r_q \int_0^{2\pi} \mathrm{d}\varphi \, \frac{(r_q r_l)^3}{\omega^2} \left(\frac{\sin\varphi}{(r_q^2 + m^2)(r_l^2 + m^2)} f_T(\omega t) \right)^2 \tag{4.66}$$

and

$$\frac{\kappa_{T\,(4)}(t)}{2\pi B} = 2 \int_0^{\Lambda_{UV}} \mathrm{d}r_l \int_0^{\Lambda_{UV}} \mathrm{d}r_q \int_0^{2\pi} \mathrm{d}\varphi \, \frac{(r_q r_l)^3}{\omega} \left(\frac{\sin\varphi}{(r_q^2 + m^2)(r_l^2 + m^2)} \right)^2 J_1(\omega t) f_T(\omega t). \tag{4.67}$$

4.2.3 Dependence on Ultraviolet Cut-Off and Infrared Regulator

An ultraviolet cut-off Λ_{UV} and an infrared regulator m were introduced to provide finite results. Ultimately, the limit $\Lambda_{UV} \to \infty$ or the limit $m \to 0$ are desired to be taken, if possible. At least the dependence of the results on these two parameters should be explored. The integrand of Eq. (4.55) can be made independent of m by

substituting $r'_{q,l} = r_{q,l}/m$

$$\begin{aligned}
\frac{\langle p_z^2\rangle_{\kappa\,(4)}(t)}{2\pi B} &= \int_0^{\Lambda_{UV}} \mathrm{d}r_l \int_0^{\Lambda_{UV}} \mathrm{d}r_q \int_0^{2\pi} \mathrm{d}\varphi\, \frac{(r_q r_l)^3}{\omega^2} \left(\frac{\cos\varphi}{(r_q^2+m^2)(r_l^2+m^2)} f_z(\omega t) \right)^2 \\
&= \int_0^{\frac{\Lambda_{UV}}{m}} m\,\mathrm{d}r'_l \int_0^{\frac{\Lambda_{UV}}{m}} m\,\mathrm{d}r'_q \int_0^{2\pi} \mathrm{d}\varphi\, \frac{m^6 (r'_q r'_l)^3}{m^2 \omega'^2} \left(\frac{\cos\varphi}{m^4 (r_q'^2+1)(r_l'^2+1)} f_z(m\omega' t) \right)^2, \\
\frac{\langle p_z^2\rangle_{\kappa\,(4)}(t')}{2\pi B} &= \frac{1}{m^2} \int_0^{\frac{\Lambda_{UV}}{m}} \mathrm{d}r'_l \int_0^{\frac{\Lambda_{UV}}{m}} \mathrm{d}r'_q \int_0^{2\pi} \mathrm{d}\varphi\, \frac{(r'_q r'_l)^3}{\omega'^2} \left(\frac{\cos\varphi}{(r_q'^2+1)(r_l'^2+1)} f_z(\omega' t') \right)^2,
\end{aligned} \tag{4.68}$$

with $\omega' = \omega(r'_q, r'_l, \varphi)$, analogous to Eq. (4.56), and $t' = mt$. That means that if the limit $\Lambda_{UV} \to \infty$ is taken, $\langle p_z^2\rangle_{\kappa\,(4)} m^2$ becomes independent of not only the ultraviolet cut-off but also the infrared regulator if the rescaled time t' is used. The same thing is done with $\langle p_T^2\rangle_{\kappa\,(4)}$, $\kappa_{z\,(4)}$ and $\kappa_{T\,(4)}$. The integration variables are renamed and the result is

$$\frac{\langle p_z^2\rangle_{\kappa\,(4)}(t')}{2\pi B} m^2 = \int_0^{\infty} \mathrm{d}r_l \int_0^{\infty} \mathrm{d}r_q \int_0^{2\pi} \mathrm{d}\varphi\, \frac{(r_q r_l)^3}{\omega^2} \left(\frac{\cos\varphi}{(r_q^2+1)(r_l^2+1)} f_z(\omega t') \right)^2, \tag{4.69}$$

$$\frac{\kappa_{z\,(4)}(t')}{2\pi B} m = 2 \int_0^{\infty} \mathrm{d}r_l \int_0^{\infty} \mathrm{d}r_q \int_0^{2\pi} \mathrm{d}\varphi\, \frac{(r_q r_l)^3}{\omega} \left(\frac{\cos\varphi}{(r_q^2+1)(r_l^2+1)} \right)^2 J_0(\omega t') f_z(\omega t'), \tag{4.70}$$

$$\frac{\langle p_T^2\rangle_{\kappa\,(4)}(t')}{2\pi B} m^2 = \int_0^{\infty} \mathrm{d}r_l \int_0^{\infty} \mathrm{d}r_q \int_0^{2\pi} \mathrm{d}\varphi\, \frac{(r_q r_l)^3}{\omega^2} \left(\frac{\sin\varphi}{(r_q^2+1)(r_l^2+1)} f_T(\omega t') \right)^2, \tag{4.71}$$

$$\frac{\kappa_{T\,(4)}(t')}{2\pi B} m = 2 \int_0^{\infty} \mathrm{d}r_l \int_0^{\infty} \mathrm{d}r_q \int_0^{2\pi} \mathrm{d}\varphi\, \frac{(r_q r_l)^3}{\omega} \left(\frac{\sin\varphi}{(r_q^2+1)(r_l^2+1)} \right)^2 J_1(\omega t') f_T(\omega t'). \tag{4.72}$$

4.2.4 Asymptotic Behaviour for Large Times

To determine the behaviour of $\langle p_z^2\rangle_{\kappa\,(4)}$ and $\langle p_T^2\rangle_{\kappa\,(4)}$ for large t, the limit $t \to \infty$ is taken in Eqs. (4.49) and (4.62) by replacing $\int_0^t$ with $\int_0^\infty$

$$\begin{aligned}
\left(\int_0^{\infty} \mathrm{d}t'\, J_0(\omega t') \right)^2 &= \frac{1}{\omega^2}, \\
\left(\int_0^{\infty} \mathrm{d}t'\, J_1(\omega t') \right)^2 &= \frac{1}{\omega^2}.
\end{aligned} \tag{4.73}$$

The rest of the calculation works as before, thus one can simply replace $f_z \to 1$ and $f_T \to 1$ in the result. One obtains

$$\lim_{t\to\infty} \frac{\langle p_z^2\rangle_{\kappa\,(4)}}{2\pi B} m^2 = \int_0^{\infty} \mathrm{d}r_l \int_0^{\infty} \mathrm{d}r_q \int_0^{2\pi} \mathrm{d}\varphi\, \frac{(r_q r_l)^3}{\omega^2} \left(\frac{\cos\varphi}{(r_q^2+1)(r_l^2+1)} \right)^2, \tag{4.74}$$

$$\lim_{t\to\infty} \frac{\langle p_T^2\rangle_{\kappa\,(4)}}{2\pi B} m^2 = \int_0^{\infty} \mathrm{d}r_l \int_0^{\infty} \mathrm{d}r_q \int_0^{2\pi} \mathrm{d}\varphi\, \frac{(r_q r_l)^3}{\omega^2} \left(\frac{\sin\varphi}{(r_q^2+1)(r_l^2+1)} \right)^2. \tag{4.75}$$

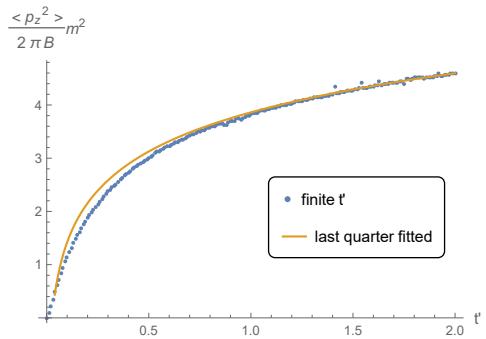

(a) $\langle p_z^2 \rangle_{\kappa\,(4)}$

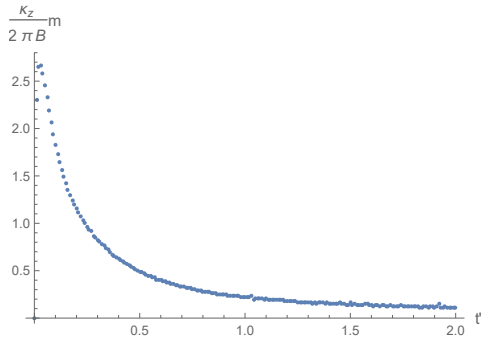

(b) $\kappa_{z\,(4)}$

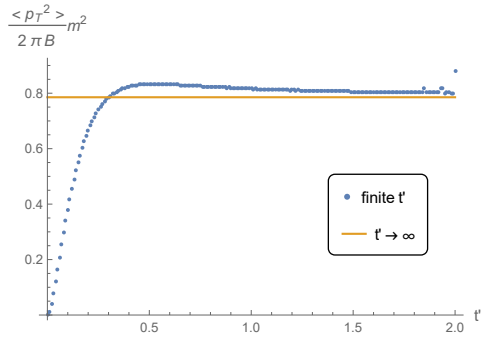

(c) $\langle p_T^2 \rangle_{\kappa\,(4)}$

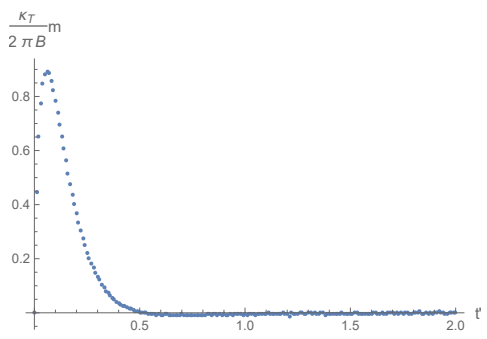

(d) $\kappa_{T\,(4)}$

Figure 4.1: $\langle p_z^2 \rangle_{\kappa\,(4)}$, $\kappa_{z\,(4)}$, $\langle p_T^2 \rangle_{\kappa\,(4)}$ and $\kappa_{T\,(4)}$, $\Lambda_{UV} \to \infty$

In Appendix D, it is shown that Eq. (4.74) diverges whereas Eq. (4.75) has a finite result. If the limit $\Lambda_{UV} \to \infty$ is not taken, but only $t \to \infty$, this result is given by Eq. (D.17) and if the former is taken as well, one obtains

$$\lim_{t\to\infty} \frac{\langle p_T^2 \rangle_{\kappa\,(4)}}{2\pi B} m^2 = \frac{\pi}{4}. \tag{4.76}$$

4.2.5 Numerical Results

The plots in this subsection are given in terms of the rescaled time t' and the dimensionless quantities $\langle p^2 \rangle\, m^2/2\pi B$ and $\kappa\, m/2\pi B$. The rescaled time t' is measured in fm $\times$ GeV, which is a pure number in natural units with $\hbar = 1$ and $c = 1$. This is shown in Eq. (A.1). More information on the choice of units is given in Appendix A.

In Figure 4.1, the numerical results of Eqs. (4.69) to (4.72) are plotted. Equation (4.69) was approximated by the logarithmic function that fits the data for $t' \in [1.5, 2.0]$ fm $\times$ GeV best, namely

$$3.86 + 1.06 \ln t', \tag{4.77}$$

and for Eq. (4.75), the analytical result given by Eq. (4.76) was taken. A comparison between $\Lambda_{UV} = 10\,\text{GeV}$ and $\Lambda_{UV} \to \infty$ is not shown here because the difference is too small to be visible in such a plot. Furthermore, numerical errors, which can be different for various Λ_{UV} have to be taken into account. Therefore, there will be made no distinction between $\Lambda_{UV} = 10\,\text{GeV}$ and $\Lambda_{UV} \to \infty$ in the following plots.

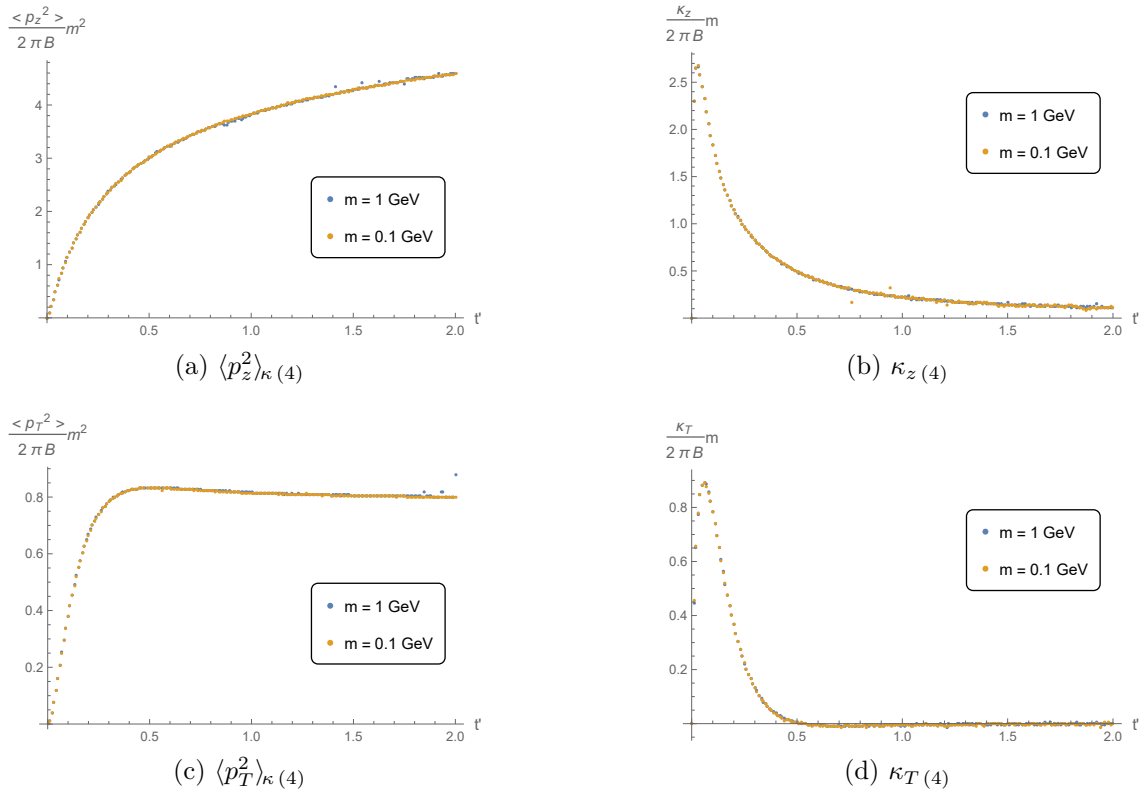

(a) $\langle p_z^2 \rangle_{\kappa\,(4)}$ (b) $\kappa_{z\,(4)}$

(c) $\langle p_T^2 \rangle_{\kappa\,(4)}$ (d) $\kappa_{T\,(4)}$

Figure 4.2: $\langle p_z^2 \rangle_{\kappa\,(4)}$, $\kappa_{z\,(4)}$, $\langle p_T^2 \rangle_{\kappa\,(4)}$ and $\kappa_{T\,(4)}$, comparison between two different values of m

In Figure 4.2, the numerical results of Eqs. (4.69) to (4.72) are compared to those calculated for $m = 0.1\,\text{GeV}$, given by Eqs. (4.55), (4.57), (4.66) and (4.67). The *numerical results* of the latter are rescaled so that they can be compared to the ones of the former, where the rescaling was performed *analytically* in Subsection 4.2.3, before the numerical evaluation. From this figure, one can perceive the numerical error for some calculated points by graphical inspection, but overall, it seems to be small. Note that the comparison shown in Figure 4.2 can also be seen as a comparison of Eqs. (4.55), (4.57), (4.66) and (4.67) for two different values of m, namely $m = 0.1\,\text{GeV}$ and $m = 1\,\text{GeV}$.

In his thesis [12], David Müller simulated a Glasma on a lattice. Figure 4.3 shows the difference between the numerically calculated integrals in this work, Eqs. (4.69) to (4.72), and the momentum broadening extracted from David Müller's simulation for two different values of μ, a parameter of the MV model, which is introduced in Section 2.3. On the lattice, a very diluted Glasma is described by a small μ. In this work, the Glasma is naturally diluted because of the expansion in the particle density ρ, which is made in Chapter 3, and the neglect of all higher orders. Thus, the difference between the two mentioned ways to calculate the momentum broadening in the Glasma is smaller for $\mu = 0.01$ than for $\mu = 0.1$. The other parameters of the lattice simulation were $g = 1$, $m = 0.2\,\text{GeV}$ and $\Lambda_{UV} = 10\,\text{GeV}$. Furthermore, the used symmetry group in the simulation was $SU(2)$, not $SU(3)$. To account for this, the value of B, which is introduced in Eq. (4.48), is chosen accordingly. The

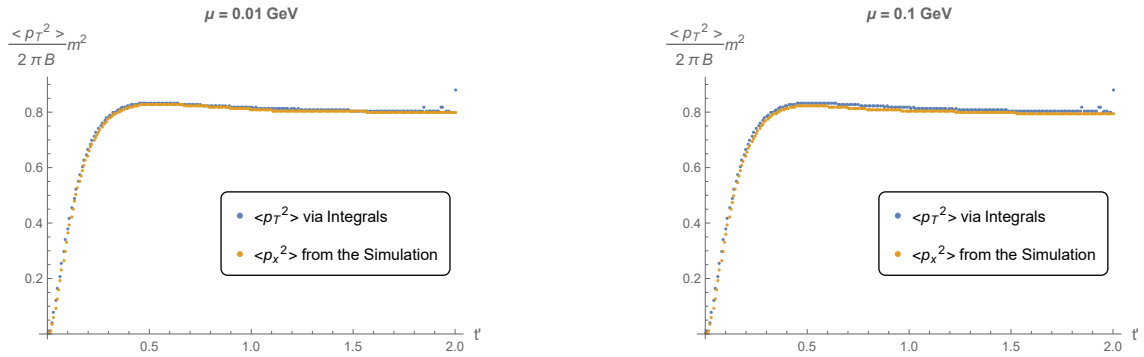

(a) $\langle p_T^2 \rangle_{\kappa\,(4)}$

(b) $\langle p_T^2 \rangle_{\kappa\,(4)}$

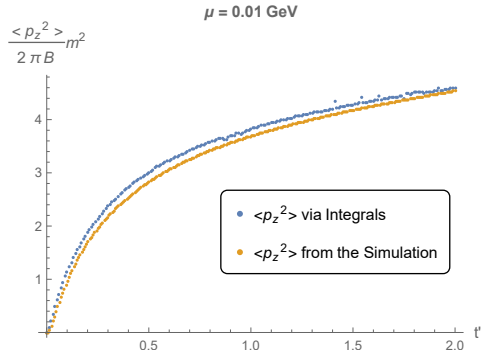

(c) $\langle p_z^2 \rangle_{\kappa\,(4)}$

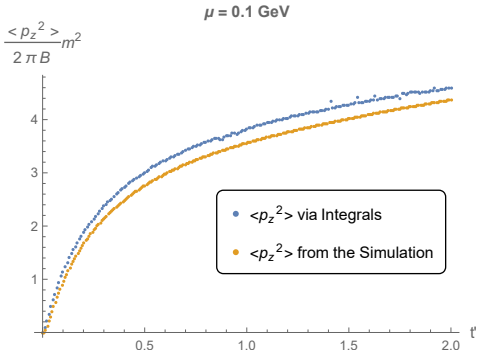

(d) $\langle p_z^2 \rangle_{\kappa\,(4)}$

Figure 4.3: $\langle p_T^2 \rangle_{\kappa\,(4)}$ and $\langle p_z^2 \rangle_{\kappa\,(4)}$, comparison to the Glasma simulation done in [12]

different values of μ change B as well. Note that the relation

$$\langle p_x^2 \rangle_\kappa = \frac{\langle p_T^2 \rangle_\kappa}{2} \tag{4.78}$$

comes into play in Figures 4.3a and 4.3b.

4.3 Test Parton Moving at the Speed of Light: $\langle p^2 \rangle_{\hat{q}}$ and $\hat{q}$

In this section, the trajectory of the test parton is $x_j(t) = t\delta_j^1$, $\dot{x}_j = \delta_j^1$, thus Eqs. (4.30) and (4.32) lead to

$$\begin{aligned} F_{i\,(2)}(t, x_T) &= -\epsilon_{ij}\partial_\tau \partial_j \chi + \delta_i^2 \Delta_T \chi \Big|_{\tau=t} = (-\epsilon_{ij}\partial_t \partial_j + \delta_i^2 \Delta_T)\chi, \quad i = 1, 2 \\ F_{3\,(2)}(t, x_T) &= -\frac{1}{\tau}\Big(\partial_\tau(\tau^2 \epsilon_{(2)}) + \tau^2 \partial_1 \epsilon_{(2)}\Big)\Big|_{\tau=t} = -\frac{1}{t}(\partial_t + \partial_1)(t^2 \epsilon_{(2)}). \end{aligned} \tag{4.79}$$

With the help of Eqs. (3.82) to (3.85), Eq. (4.79) becomes

$$\begin{aligned} F_{i\,(2)}(t, x_T) &= (-\epsilon_{ij}\partial_t \partial_j + \delta_i^2 \Delta_T) \int \mathrm{d}^2 k_T \, \frac{J_0(\omega t)}{\omega^2} e^{i k_T x_T} f_\chi(k_T) \\ &= \int \mathrm{d}^2 k_T \left(\epsilon_{ij} \frac{i k_j}{\omega} J_1(\omega t) - \delta_i^2 J_0(\omega t) \right) e^{i k_1 t} f_\chi(k_T), \end{aligned} \tag{4.80}$$

$$F_{3\,(2)}(t,x_T) = -\frac{1}{t}(\partial_t+\partial_1)\int \mathrm{d}^2k_T\,\frac{t}{\omega}J_1(\omega t)e^{ik_Tx_T}f_\epsilon(k_T)$$
$$= -\int \mathrm{d}^2k_T\left(J_0(\omega t)+\frac{ik_1}{\omega}J_1(\omega t)\right)e^{ik_1t}f_\epsilon(k_T). \tag{4.81}$$

Note that $F_{2\,(2)}(t,x_T)$ in Eq. (4.80) becomes $F_{3\,(2)}(t,x_T)$ in Eq. (4.81) if $f_\chi(k_T)$ is replaced by $f_\epsilon(k_T)$.

4.3.1 Component Transversal to Test Parton and Nuclei: $\langle p_y^2\rangle_{\hat{q}}$ and $\hat{q}_y$

Firstly, $\langle p_y^2\rangle_{\hat{q}}$ will be calculated, $t_0=0$ as usual. Equations (4.27) and (4.80) lead to

$$\langle p_y^2\rangle_{\hat{q}\,(4)}(t) = 2g^2\widetilde{A}\int_0^t \mathrm{d}t'\int_0^t \mathrm{d}t''\int \mathrm{d}^2k_T\int \mathrm{d}^2k_T'\,c(t',k_T)c(t'',k_T')$$
$$\times\, e^{ik_1t'}e^{ik_1't''}\langle \mathrm{Tr}(f_\chi(k_T)f_\chi(k_T'))\rangle, \tag{4.82}$$

with

$$c(t,k_T) = J_0(\omega t)+\frac{ik_1}{\omega}J_1(\omega t). \tag{4.83}$$

With the help of Eqs. (4.48), (4.60) and (4.61), one obtains

$$\langle p_y^2\rangle_{\hat{q}\,(4)}(t) = B\int \mathrm{d}^2k_T g_T(k_T)\int_0^t \mathrm{d}t'\int_0^t \mathrm{d}t''\int \mathrm{d}^2k_T'\,c(t',k_T)c(t'',k_T')$$
$$\times\, e^{ik_1t'}e^{ik_1't''}\delta(k_T+k_T')$$
$$= B\int \mathrm{d}^2k_T g_T(k_T)\int_0^t \mathrm{d}t'\int_0^t \mathrm{d}t''\,c(t',k_T)c(t'',-k_T)e^{ik_1t'}e^{-ik_1t''}. \tag{4.84}$$

The same coordinate changes as before are made, but φ_l and φ_q are kept as integration variables, i.e. the substitution given by Eq. (4.54) is omitted. The result is

$$\frac{\langle p_y^2\rangle_{\hat{q}\,(4)}(t)}{B} = \int_0^{\Lambda_{UV}}\mathrm{d}r_l\int_0^{\Lambda_{UV}}\mathrm{d}r_q\int_0^{2\pi}\mathrm{d}\varphi_l\int_0^{2\pi}\mathrm{d}\varphi_q\,(r_qr_l)^3\left(\frac{\sin(\varphi_q-\varphi_l)}{(r_q^2+m^2)(r_l^2+m^2)}\right)^2$$
$$\times\int_0^t \mathrm{d}t'\int_0^t \mathrm{d}t''\left(\frac{i(r_q\cos\varphi_q+r_l\cos\varphi_l)}{\omega}J_1(\omega t')+J_0(\omega t')\right)$$
$$\times\left(-\frac{i(r_q\cos\varphi_q+r_l\cos\varphi_l)}{\omega}J_1(\omega t'')+J_0(\omega t'')\right)$$
$$\times\, e^{i(r_q\cos\varphi_q+r_l\cos\varphi_l)(t'-t'')}$$
$$= \int_0^{\Lambda_{UV}}\mathrm{d}r_l\int_0^{\Lambda_{UV}}\mathrm{d}r_q\int_0^{2\pi}\mathrm{d}\varphi_l\int_0^{2\pi}\mathrm{d}\varphi_q\,(r_qr_l)^3\left(\frac{\sin(\varphi_q-\varphi_l)}{(r_q^2+m^2)(r_l^2+m^2)}\right)^2$$
$$\times\int_0^t \mathrm{d}t'\int_0^t \mathrm{d}t''\,c(t',k_T(r_q,r_l,\varphi_q,\varphi_l))\Big(c(t'',k_T(r_q,r_l,\varphi_q,\varphi_l))\Big)^*$$
$$\times\, e^{i(r_q\cos\varphi_q+r_l\cos\varphi_l)t'}\Big(e^{i(r_q\cos\varphi_q+r_l\cos\varphi_l)t''}\Big)^*$$
$$= \int_0^{\Lambda_{UV}}\mathrm{d}r_l\int_0^{\Lambda_{UV}}\mathrm{d}r_q\int_0^{2\pi}\mathrm{d}\varphi_l\int_0^{2\pi}\mathrm{d}\varphi_q\,(r_qr_l)^3\left(\frac{\sin(\varphi_q-\varphi_l)}{(r_q^2+m^2)(r_l^2+m^2)}\right)^2$$
$$\times\left|\int_0^t \mathrm{d}t'\,c(t',k_T(r_q,r_l,\varphi_q,\varphi_l))e^{i(r_q\cos\varphi_q+r_l\cos\varphi_l)t'}\right|^2, \tag{4.85}$$

with * denoting the complex conjugate.

The y component of the momentum broadening parameter $\hat{q}$, $\hat{q}_y$, is the time derivative of $\langle p_y^2\rangle_{\hat{q}}$ and reads

$$\frac{\hat{q}_{y\,(4)}(t)}{B} = \int_0^{\Lambda_{UV}} \mathrm{d}r_l \int_0^{\Lambda_{UV}} \mathrm{d}r_q \int_0^{2\pi} \mathrm{d}\varphi_l \int_0^{2\pi} \mathrm{d}\varphi_q \, (r_q r_l)^3 \left(\frac{\sin(\varphi_q - \varphi_l)}{(r_q^2 + m^2)(r_l^2 + m^2)} \right)^2 \times \frac{\mathrm{d}}{\mathrm{d}t} \left| \int_0^t \mathrm{d}t' \, c(t', k_T(r_q, r_l, \varphi_q, \varphi_l)) e^{i(r_q \cos\varphi_q + r_l \cos\varphi_l)t'} \right|^2 . \tag{4.86}$$

4.3.2 Component Longitudinal to Nuclei: $\langle p_z^2\rangle_{\hat{q}}$ and $\hat{q}_z$

Next, $\langle p_z^2\rangle_{\hat{q}}$ is calculated. In analogy to Eq. (4.82), one gets

$$\langle p_z^2\rangle_{\hat{q}\,(4)}(t) = 2g^2 \tilde{A} \int_0^t \mathrm{d}t' \int_0^t \mathrm{d}t'' \int \mathrm{d}^2 k_T \int \mathrm{d}^2 k_T' \, c(t', k_T) c(t'', k_T') \times e^{ik_1 t'} e^{ik_1' t''} \langle \mathrm{Tr}(f_\epsilon(k_T) f_\epsilon(k_T')) \rangle, \tag{4.87}$$

hence

$$\begin{aligned} \frac{\langle p_z^2\rangle_{\hat{q}\,(4)}(t)}{B} &= \int \mathrm{d}^2 k_T g_z(k_T) \int_0^t \mathrm{d}t' \int_0^t \mathrm{d}t'' \int \mathrm{d}^2 k_T' \, c(t', k_T) c(t'', k_T') \\ &\quad \times e^{ik_1 t'} e^{ik_1' t''} \delta(k_T + k_T') \\ &= \int_0^{\Lambda_{UV}} \mathrm{d}r_l \int_0^{\Lambda_{UV}} \mathrm{d}r_q \int_0^{2\pi} \mathrm{d}\varphi_l \int_0^{2\pi} \mathrm{d}\varphi_q \, (r_q r_l)^3 \left(\frac{\cos(\varphi_q - \varphi_l)}{(r_q^2 + m^2)(r_l^2 + m^2)} \right)^2 \\ &\quad \times \left| \int_0^t \mathrm{d}t' \, c(t', k_T(r_q, r_l, \varphi_q, \varphi_l)) e^{i(r_q \cos\varphi_q + r_l \cos\varphi_l)t'} \right|^2 \end{aligned} \tag{4.88}$$

and

$$\frac{\hat{q}_{z\,(4)}(t)}{B} = \int_0^{\Lambda_{UV}} \mathrm{d}r_l \int_0^{\Lambda_{UV}} \mathrm{d}r_q \int_0^{2\pi} \mathrm{d}\varphi_l \int_0^{2\pi} \mathrm{d}\varphi_q \, (r_q r_l)^3 \left(\frac{\cos(\varphi_q - \varphi_l)}{(r_q^2 + m^2)(r_l^2 + m^2)} \right)^2 \times \frac{\mathrm{d}}{\mathrm{d}t} \left| \int_0^t \mathrm{d}t' \, c(t', k_T(r_q, r_l, \varphi_q, \varphi_l)) e^{i(r_q \cos\varphi_q + r_l \cos\varphi_l)t'} \right|^2 . \tag{4.89}$$

The sum $\langle p_\perp^2\rangle_{\hat{q}\,(4)} = \langle p_y^2\rangle_{\hat{q}\,(4)} + \langle p_z^2\rangle_{\hat{q}\,(4)}$ yields

$$\frac{\langle p_\perp^2\rangle_{\hat{q}\,(4)}(t)}{B} = \int_0^{\Lambda_{UV}} \mathrm{d}r_l \int_0^{\Lambda_{UV}} \mathrm{d}r_q \int_0^{2\pi} \mathrm{d}\varphi_l \int_0^{2\pi} \mathrm{d}\varphi_q \, (r_q r_l)^3 \left(\frac{1}{(r_q^2 + m^2)(r_l^2 + m^2)} \right)^2 \times \left| \int_0^t \mathrm{d}t' \, c(t', k_T(r_q, r_l, \varphi_q, \varphi_l)) e^{i(r_q \cos\varphi_q + r_l \cos\varphi_l)t'} \right|^2 \tag{4.90}$$

because of $\cos^2\varphi + \sin^2\varphi = 1$, and the result for the momentum broadening parameter $\hat{q}$ is

$$\frac{\hat{q}_{(4)}(t)}{B} = \int_0^{\Lambda_{UV}} \mathrm{d}r_l \int_0^{\Lambda_{UV}} \mathrm{d}r_q \int_0^{2\pi} \mathrm{d}\varphi_l \int_0^{2\pi} \mathrm{d}\varphi_q \, (r_q r_l)^3 \left(\frac{1}{(r_q^2 + m^2)(r_l^2 + m^2)} \right)^2 \times \frac{\mathrm{d}}{\mathrm{d}t} \left| \int_0^t \mathrm{d}t' \, c(t', k_T(r_q, r_l, \varphi_q, \varphi_l)) e^{i(r_q \cos\varphi_q + r_l \cos\varphi_l)t'} \right|^2 . \tag{4.91}$$

4.3.3 Component Longitudinal to Test Parton: $\langle p_x^2 \rangle_{\hat{q}}$

Lastly, $\langle p_x^2 \rangle_{\hat{q}}$ is calculated. It does not contribute to $\hat{q}$ because the latter is defined as the time derivative of $\langle p_\perp^2 \rangle_{\hat{q}}$, i.e. perpendicular to the trajectory of the test parton, but due to the similarity to the other ones, the x component is not laborious to calculate and shall be given here. In analogy to Eqs. (4.82) and (4.87), one obtains

$$\begin{aligned}\langle p_x^2 \rangle_{\hat{q}\,(4)}(t) = 2g^2 \widetilde{A} \int_0^t \mathrm{d}t' \int_0^t \mathrm{d}t'' \int \mathrm{d}^2 k_T \int \mathrm{d}^2 k_T' \, \frac{i^2 k_2 k_2'}{\omega \omega'} J_1(\omega t') J_1(\omega' t'') \\ \times e^{ik_1 t'} e^{ik_1' t''} \langle \mathrm{Tr}(f_\chi(k_T) f_\chi(k_T')) \rangle,\end{aligned} \tag{4.92}$$

therefore

$$\begin{aligned}\frac{\langle p_x^2 \rangle_{\hat{q}\,(4)}(t)}{B} &= \int \mathrm{d}^2 k_T g_T(k_T) \int_0^t \mathrm{d}t' \int_0^t \mathrm{d}t'' \int \mathrm{d}^2 k_T' \, \frac{i^2 k_2 k_2'}{\omega \omega'} J_1(\omega t') J_1(\omega' t'') \\ &\quad \times e^{ik_1 t'} e^{ik_1' t''} \delta(k_T + k_T') \\ &= \int_0^{\Lambda_{UV}} \mathrm{d}r_l \int_0^{\Lambda_{UV}} \mathrm{d}r_q \int_0^{2\pi} \mathrm{d}\varphi_l \int_0^{2\pi} \mathrm{d}\varphi_q \, (r_q r_l)^3 \left(\frac{\sin(\varphi_q - \varphi_l)}{(r_q^2 + m^2)(r_l^2 + m^2)} \right)^2 \\ &\quad \times \frac{(r_q \sin\varphi_q + r_l \sin\varphi_l)^2}{\omega^2} \left| \int_0^t \mathrm{d}t' \, J_1(\omega t') e^{i(r_q \cos\varphi_q + r_l \cos\varphi_l)t'} \right|^2 .\end{aligned} \tag{4.93}$$

4.3.4 Dependence on Ultraviolet Cut-Off and Infrared Regulator

The dependence of $\langle p_i^2 \rangle_{\hat{q}\,(4)}$ and $\hat{q}_{i\,(4)}$ on Λ_{UV} and m can be examined analogously to the dependence of the respective κ quantities, $\langle p_i^2 \rangle_{\kappa\,(4)}$ and $\kappa_{i\,(4)}$, in Subsection 4.2.3. The integrand of Eq. (4.85) can be made independent of m by substituting $r_{q,l}' = r_{q,l}/m$

$$\begin{aligned}\frac{\langle p_y^2 \rangle_{\hat{q}\,(4)}(t)}{B} &= \int_0^{\Lambda_{UV}} \mathrm{d}r_l \int_0^{\Lambda_{UV}} \mathrm{d}r_q \int_0^{2\pi} \mathrm{d}\varphi_l \int_0^{2\pi} \mathrm{d}\varphi_q \, (r_q r_l)^3 \left(\frac{\sin(\varphi_q - \varphi_l)}{(r_q^2 + m^2)(r_l^2 + m^2)} \right)^2 \\ &\quad \times \left| \int_0^t \mathrm{d}t' \, c(t', k_T(r_q, r_l, \varphi_q, \varphi_l)) e^{i(r_q \cos\varphi_q + r_l \cos\varphi_l)t'} \right|^2 \\ &= \int_0^{\frac{\Lambda_{UV}}{m}} m \mathrm{d}r_l' \int_0^{\frac{\Lambda_{UV}}{m}} m \mathrm{d}r_q' \int_0^{2\pi} \mathrm{d}\varphi_l \int_0^{2\pi} \mathrm{d}\varphi_q \, m^6 (r_q' r_l')^3 \left(\frac{\sin(\varphi_q - \varphi_l)}{m^4 (r_q'^2 + 1)(r_l'^2 + 1)} \right)^2 \\ &\quad \times \left| \int_0^t \mathrm{d}t' \, c(t', k_T(m r_q', m r_l', \varphi_q, \varphi_l)) e^{im(r_q' \cos\varphi_q + r_l' \cos\varphi_l)t'} \right|^2 \\ &= \int_0^{\frac{\Lambda_{UV}}{m}} \mathrm{d}r_l' \int_0^{\frac{\Lambda_{UV}}{m}} \mathrm{d}r_q' \int_0^{2\pi} \mathrm{d}\varphi_l \int_0^{2\pi} \mathrm{d}\varphi_q \, (r_q' r_l')^3 \left(\frac{\sin(\varphi_q - \varphi_l)}{(r_q'^2 + 1)(r_l'^2 + 1)} \right)^2 \\ &\quad \times \left| \int_0^t \mathrm{d}t' \, c(mt', k_T(r_q', r_l', \varphi_q, \varphi_l)) e^{i(r_q' \cos\varphi_q + r_l' \cos\varphi_l)mt'} \right|^2 \\ &= \int_0^{\frac{\Lambda_{UV}}{m}} \mathrm{d}r_l' \int_0^{\frac{\Lambda_{UV}}{m}} \mathrm{d}r_q' \int_0^{2\pi} \mathrm{d}\varphi_l \int_0^{2\pi} \mathrm{d}\varphi_q \, (r_q' r_l')^3 \left(\frac{\sin(\varphi_q - \varphi_l)}{(r_q'^2 + 1)(r_l'^2 + 1)} \right)^2 \\ &\quad \times \frac{1}{m^2} \left| \int_0^{\widehat{t}} \mathrm{d}\widehat{t}' \, c(\widehat{t}', k_T(r_q', r_l', \varphi_q, \varphi_l)) e^{i(r_q' \cos\varphi_q + r_l' \cos\varphi_l)\widehat{t}'} \right|^2 .\end{aligned} \tag{4.94}$$

In the last step, the substitution $\widehat{t} = mt$ was made. If one takes the limit $\Lambda_{UV} \to \infty$ and uses the rescaled time, which is now called $\widehat{t}$ because t' is reserved for the

integration variable, $\langle p_y^2\rangle_{\hat{q}\,(4)} m^2$ is independent of both the ultraviolet cut-off and the infrared regulator. (In Subsection 4.3.5, the rescaled time will be called t' again to keep it consistent with Subsection 4.2.5.) The other quantities corresponding to the momentum broadening can be treated analogously. After renaming the integration variables, one obtains

$$\frac{\langle p_y^2\rangle_{\hat{q}\,(4)}(t)}{B} m^2 = \int_0^\infty \mathrm{d}r_l \int_0^\infty \mathrm{d}r_q \int_0^{2\pi} \mathrm{d}\varphi_l \int_0^{2\pi} \mathrm{d}\varphi_q \, (r_q r_l)^3 \left(\frac{\sin(\varphi_q - \varphi_l)}{(r_q^2+1)(r_l^2+1)} \right)^2 \times \left| \int_0^{\widehat{t}} \mathrm{d}t' \, c(t', k_T(r_q, r_l, \varphi_q, \varphi_l)) e^{i(r_q \cos\varphi_q + r_l \cos\varphi_l)t'} \right|^2 , \tag{4.95}$$

$$\frac{\hat{q}_{y\,(4)}(t)}{B} m = \int_0^\infty \mathrm{d}r_l \int_0^\infty \mathrm{d}r_q \int_0^{2\pi} \mathrm{d}\varphi_l \int_0^{2\pi} \mathrm{d}\varphi_q \, (r_q r_l)^3 \left(\frac{\sin(\varphi_q - \varphi_l)}{(r_q^2+1)(r_l^2+1)} \right)^2 \times \frac{\mathrm{d}}{\mathrm{d}\widehat{t}} \left| \int_0^{\widehat{t}} \mathrm{d}t' \, c(t', k_T(r_q, r_l, \varphi_q, \varphi_l)) e^{i(r_q \cos\varphi_q + r_l \cos\varphi_l)t'} \right|^2 , \tag{4.96}$$

$$\frac{\langle p_z^2\rangle_{\hat{q}\,(4)}(t)}{B} m^2 = \int_0^\infty \mathrm{d}r_l \int_0^\infty \mathrm{d}r_q \int_0^{2\pi} \mathrm{d}\varphi_l \int_0^{2\pi} \mathrm{d}\varphi_q \, (r_q r_l)^3 \left(\frac{\cos(\varphi_q - \varphi_l)}{(r_q^2+1)(r_l^2+1)} \right)^2 \times \left| \int_0^{\widehat{t}} \mathrm{d}t' \, c(t', k_T(r_q, r_l, \varphi_q, \varphi_l)) e^{i(r_q \cos\varphi_q + r_l \cos\varphi_l)t'} \right|^2 , \tag{4.97}$$

$$\frac{\hat{q}_{z\,(4)}(t)}{B} m = \int_0^\infty \mathrm{d}r_l \int_0^\infty \mathrm{d}r_q \int_0^{2\pi} \mathrm{d}\varphi_l \int_0^{2\pi} \mathrm{d}\varphi_q \, (r_q r_l)^3 \left(\frac{\cos(\varphi_q - \varphi_l)}{(r_q^2+1)(r_l^2+1)} \right)^2 \times \frac{\mathrm{d}}{\mathrm{d}\widehat{t}} \left| \int_0^{\widehat{t}} \mathrm{d}t' \, c(t', k_T(r_q, r_l, \varphi_q, \varphi_l)) e^{i(r_q \cos\varphi_q + r_l \cos\varphi_l)t'} \right|^2 , \tag{4.98}$$

$$\frac{\langle p_\perp^2\rangle_{\hat{q}\,(4)}(t)}{B} m^2 = \int_0^\infty \mathrm{d}r_l \int_0^\infty \mathrm{d}r_q \int_0^{2\pi} \mathrm{d}\varphi_l \int_0^{2\pi} \mathrm{d}\varphi_q \, (r_q r_l)^3 \left(\frac{1}{(r_q^2+1)(r_l^2+1)} \right)^2 \times \left| \int_0^{\widehat{t}} \mathrm{d}t' \, c(t', k_T(r_q, r_l, \varphi_q, \varphi_l)) e^{i(r_q \cos\varphi_q + r_l \cos\varphi_l)t'} \right|^2 , \tag{4.99}$$

$$\frac{\hat{q}_{(4)}(t)}{B} m = \int_0^\infty \mathrm{d}r_l \int_0^\infty \mathrm{d}r_q \int_0^{2\pi} \mathrm{d}\varphi_l \int_0^{2\pi} \mathrm{d}\varphi_q \, (r_q r_l)^3 \left(\frac{1}{(r_q^2+1)(r_l^2+1)} \right)^2 \times \frac{\mathrm{d}}{\mathrm{d}\widehat{t}} \left| \int_0^{\widehat{t}} \mathrm{d}t' \, c(t', k_T(r_q, r_l, \varphi_q, \varphi_l)) e^{i(r_q \cos\varphi_q + r_l \cos\varphi_l)t'} \right|^2 , \tag{4.100}$$

$$\frac{\langle p_x^2\rangle_{\hat{q}\,(4)}(t)}{B} m^2 = \int_0^\infty \mathrm{d}r_l \int_0^\infty \mathrm{d}r_q \int_0^{2\pi} \mathrm{d}\varphi_l \int_0^{2\pi} \mathrm{d}\varphi_q \, (r_q r_l)^3 \left(\frac{\sin(\varphi_q - \varphi_l)}{(r_q^2+1)(r_l^2+1)} \right)^2 \times \frac{(r_q \sin\varphi_q + r_l \sin\varphi_l)^2}{\omega^2} \left| \int_0^{\widehat{t}} \mathrm{d}t' \, J_1(\omega t') e^{i(r_q \cos\varphi_q + r_l \cos\varphi_l)t'} \right|^2 . \tag{4.101}$$

4.3.5 Numerical Results

The plots in this subsection are given in terms of the rescaled time t' and the dimensionless quantity $\langle p^2\rangle\, m^2/2\pi B$. As explained in Subsection 4.2.5, the rescaled time t' is measured in fm $\times$ GeV, which is a pure number in natural units with $\hbar = 1$ and $c = 1$.

The numerical results of Eqs. (4.85), (4.88), (4.90) and (4.93) are plotted in Figure 4.4 for $m = 0.2\,\mathrm{GeV}$. The y component, which describes the direction that is transversal to not only the trajectory of the test parton, but also to the axis defined by the colliding nuclei, is the only one with a maximum in the analysed time interval. This behaviour is analogous to $\langle p^2 \rangle_{\kappa\,(4)}$ in Figure 4.1. There, it was also the transversal component that had a maximum. However, the whole transversal plane showed the same behaviour because there was no second special direction, given that the test parton was at rest. Figure 4.4d shows $\langle p_\perp^2 \rangle_{\hat{q}\,(4)}$ calculated in two different ways, once by calculating it as per Eq. (4.90) and once by adding up the results for $\langle p_y^2 \rangle_{\hat{q}\,(4)}$ and $\langle p_z^2 \rangle_{\hat{q}\,(4)}$. Neither way leads to a smooth plot for large t'. The plot for the z component, Figure 4.4b, looks similar to Figure 4.4d for large t'. This behaviour seems to stem from numerical errors during the integration process.

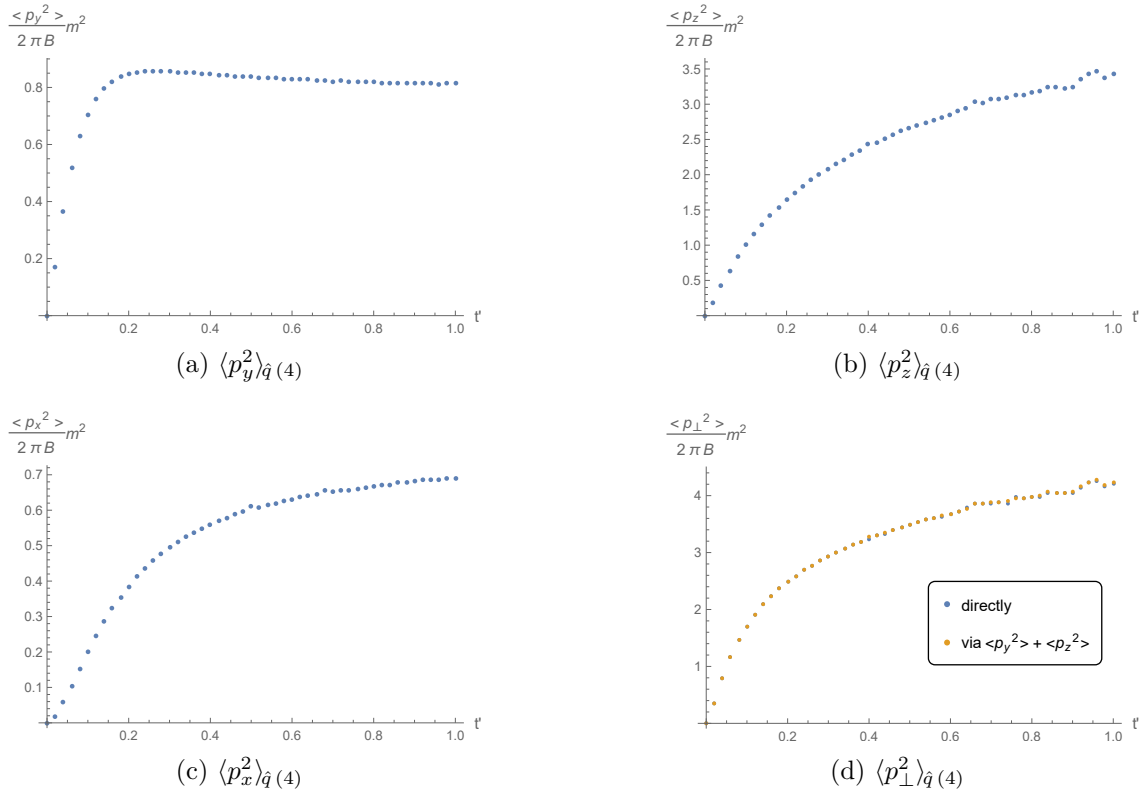

(a) $\langle p_y^2 \rangle_{\hat{q}\,(4)}$ (b) $\langle p_z^2 \rangle_{\hat{q}\,(4)}$

(c) $\langle p_x^2 \rangle_{\hat{q}\,(4)}$ (d) $\langle p_\perp^2 \rangle_{\hat{q}\,(4)}$

Figure 4.4: $\langle p_y^2 \rangle_{\hat{q}\,(4)}$, $\langle p_z^2 \rangle_{\hat{q}\,(4)}$, $\langle p_x^2 \rangle_{\hat{q}\,(4)}$ and $\langle p_\perp^2 \rangle_{\hat{q}\,(4)}$, $m = 0.2\,\mathrm{GeV}$

Figure 4.5 substantiates the idea that the z component and the $\perp$ component of $\langle p^2 \rangle_{\hat{q}\,(4)}$ should not be trusted for large t. It shows a comparison between two different values for m, namely $m = 0.1\,\mathrm{GeV}$ and $m = 0.2\,\mathrm{GeV}$. If one wants to rescale data for $m = 0.1\,\mathrm{GeV}$, one needs data for a twice as large $t = t'/m$ than to rescale data for $m = 0.2\,\mathrm{GeV}$, i.e. data for $t \in [0, 10]\,\mathrm{fm}$, as opposed to $t \in [0, 5]\,\mathrm{fm}$ in the present case. Figure 4.5b and Figure 4.5d show a larger numerical error for the smaller m at $t' > 0.5\,\mathrm{fm} \times \mathrm{GeV}$ because the calculation is less precise for larger t.

Figure 4.6 shows the difference between the momentum broadening of a test parton in the Glasma simulated on a lattice for $m = 0.2\,\mathrm{GeV}$ and the numerically calculated

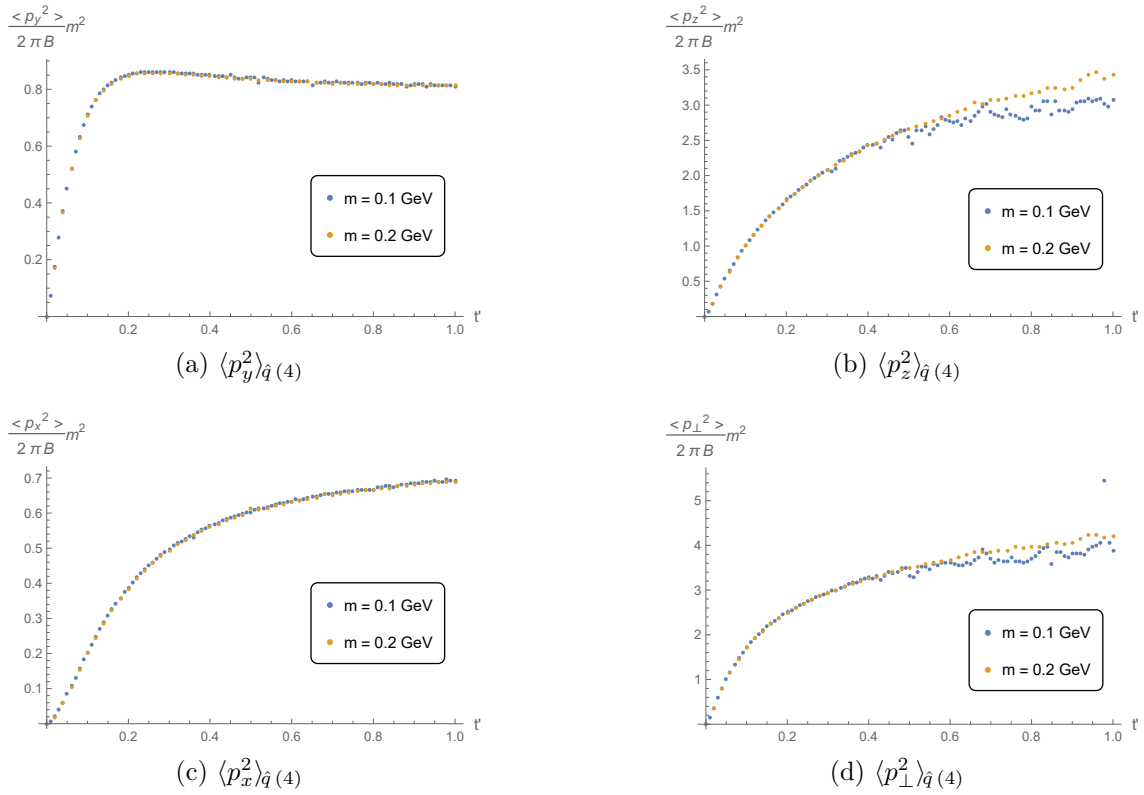

(a) $\langle p_y^2 \rangle_{\hat{q}\,(4)}$ (b) $\langle p_z^2 \rangle_{\hat{q}\,(4)}$

(c) $\langle p_x^2 \rangle_{\hat{q}\,(4)}$ (d) $\langle p_\perp^2 \rangle_{\hat{q}\,(4)}$

Figure 4.5: $\langle p_y^2 \rangle_{\hat{q}\,(4)}$, $\langle p_z^2 \rangle_{\hat{q}\,(4)}$, $\langle p_x^2 \rangle_{\hat{q}\,(4)}$ and $\langle p_\perp^2 \rangle_{\hat{q}\,(4)}$, comparison between different values of m

integrals for two different values of μ. The simulation of the Glasma was done in [12], as explained in Subsection 4.2.5. This figure shows a good agreement of these two distinct ways of calculating the momentum broadening parameters in a highly diluted Glasma, especially for the x and z component. The difference is again slightly smaller for smaller μ.

4.4 Correlators

The quantity $\langle p^2 \rangle$ can be calculated in two ways. One way is to perform the time integration before the momentum integration, as is done in the previous sections, for κ analytically, for $\hat{q}$ numerically. The other way is to perform the momentum integration numerically before the time integration. The quantities obtained in this intermediate step are the correlators of the fields E and B. They are discussed in the following.

4.4.1 Correlators Corresponding to κ

The starting point is Eq. (4.27)

$$\begin{aligned}\langle p^i p^i \rangle_{(4)}(t) &= 2g^2 \widetilde{A} \int_{t_0}^{t} \mathrm{d}t' \int_{t_0}^{t} \mathrm{d}t'' \, \langle \mathrm{Tr}(F^i_{(2)}(x^j(t'), t') F^i_{(2)}(x^j(t''), t'')) \rangle \\ &= 2g^2 \widetilde{A} \int_{0}^{t} \mathrm{d}t' \int_{0}^{t} \mathrm{d}t'' \, \langle \mathrm{Tr}(E^i_{(2)}(t', x_0) E^i_{(2)}(t'', x_0)) \rangle. \end{aligned} \tag{4.102}$$

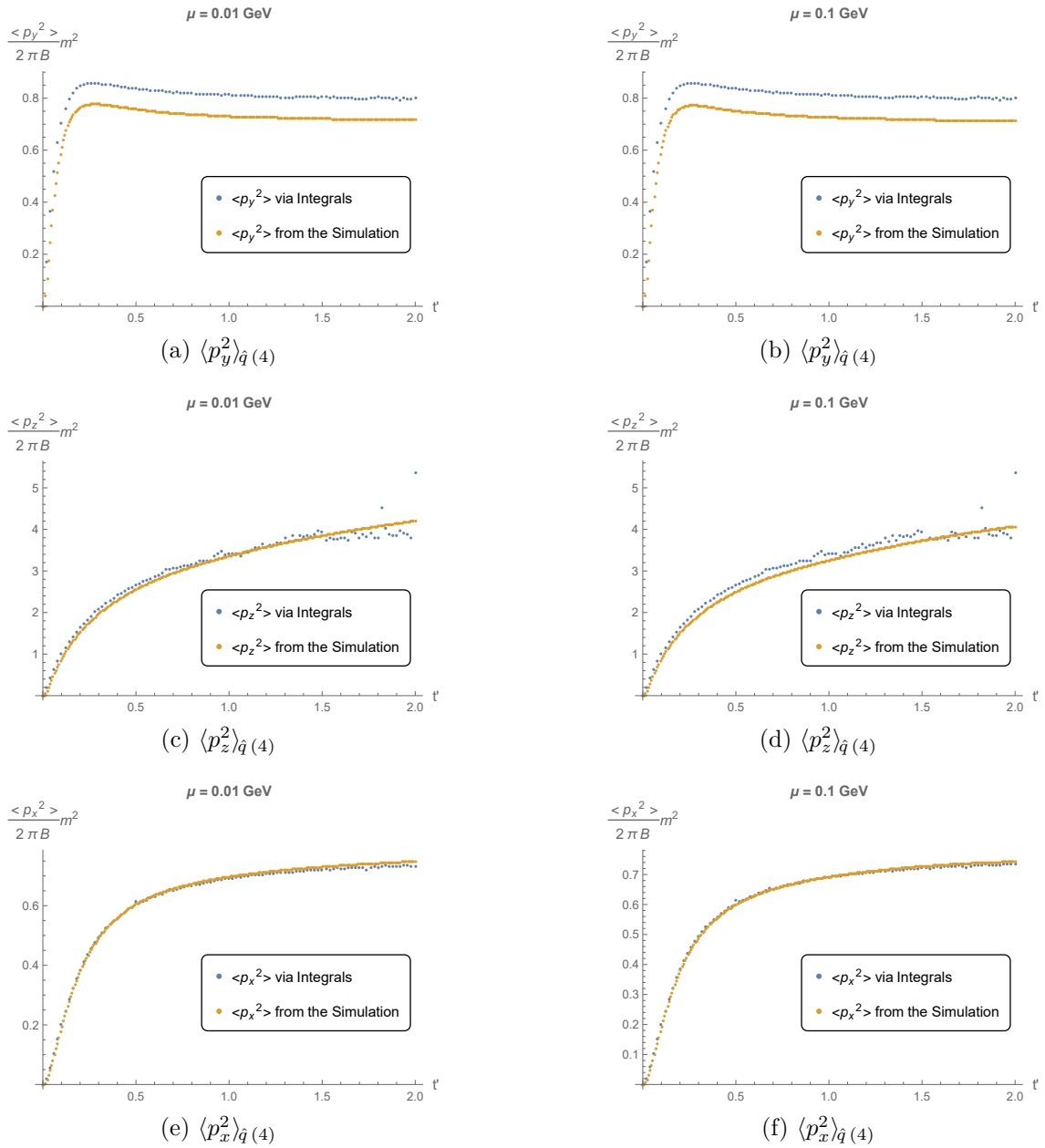

(a) $\langle p_y^2 \rangle_{\hat{q}\,(4)}$ (b) $\langle p_y^2 \rangle_{\hat{q}\,(4)}$

(c) $\langle p_z^2 \rangle_{\hat{q}\,(4)}$ (d) $\langle p_z^2 \rangle_{\hat{q}\,(4)}$

(e) $\langle p_x^2 \rangle_{\hat{q}\,(4)}$ (f) $\langle p_x^2 \rangle_{\hat{q}\,(4)}$

Figure 4.6: $\langle p_y^2 \rangle_{\hat{q}\,(4)}$, $\langle p_z^2 \rangle_{\hat{q}\,(4)}$ and $\langle p_x^2 \rangle_{\hat{q}\,(4)}$, comparison to the Glasma simulation done in [12]

In the last step,

$$\dot{x}^i = 0 \tag{4.103}$$

and therefore

$$F_i = E_i + \epsilon_i^{jk} \dot{x}_j B_k = E_i \tag{4.104}$$

were used.

The calculation works completely analogously to the one in Section 4.2, but this time, the t integrations in Eqs. (4.49) and (4.62) are not performed. The result is, in analogy to Eq. (4.55),

$$\begin{aligned}\frac{\langle p_z^2 \rangle_{\kappa\,(4)}(t)}{2\pi B} = \int_0^{\Lambda_{UV}} \mathrm{d}r_l \int_0^{\Lambda_{UV}} \mathrm{d}r_q \int_0^{2\pi} \mathrm{d}\varphi\, (r_q r_l)^3 \left(\frac{\cos\varphi}{(r_q^2+m^2)(r_l^2+m^2)} \right)^2 \\ \times \int_0^t \mathrm{d}t' \int_0^t \mathrm{d}t'' J_0(\omega t') J_0(\omega t'').\end{aligned} \tag{4.105}$$

From Eqs. (4.102) and (4.105) one can deduce

$$\begin{aligned}&\mathrm{Tr}\langle E_{z\,(2)}(t') E_{z\,(2)}(t'')\rangle \\ &= \frac{\pi B}{g^2 \widetilde{A}} \int_0^{\Lambda_{UV}} \mathrm{d}r_l \int_0^{\Lambda_{UV}} \mathrm{d}r_q \int_0^{2\pi} \mathrm{d}\varphi\, (r_q r_l)^3 \left(\frac{\cos\varphi}{(r_q^2+m^2)(r_l^2+m^2)} \right)^2 J_0(\omega t') J_0(\omega t'').\end{aligned} \tag{4.106}$$

The argument x_0 is dropped because these correlators do not depend on it.

Analogously one obtains

$$\begin{aligned}&\mathrm{Tr}\langle E_{T\,(2)}(t') E_{T\,(2)}(t'')\rangle \\ &= \frac{\pi B}{g^2 \widetilde{A}} \int_0^{\Lambda_{UV}} \mathrm{d}r_l \int_0^{\Lambda_{UV}} \mathrm{d}r_q \int_0^{2\pi} \mathrm{d}\varphi\, (r_q r_l)^3 \left(\frac{\sin\varphi}{(r_q^2+m^2)(r_l^2+m^2)} \right)^2 J_1(\omega t') J_1(\omega t'')\end{aligned} \tag{4.107}$$

and the x and y component of the correlators are

$$\mathrm{Tr}\langle E_{x\,(2)}(t') E_{x\,(2)}(t'')\rangle = \mathrm{Tr}\langle E_{y\,(2)}(t') E_{y\,(2)}(t'')\rangle = \frac{1}{2}\,\mathrm{Tr}\langle E_{T\,(2)}(t') E_{T\,(2)}(t'')\rangle. \tag{4.108}$$

4.4.2 Correlators Corresponding to $\hat{q}$

The starting point is again Eq. (4.27)

$$\begin{aligned}\langle p^i p^i \rangle_{(4)}(t) &= 2g^2 \widetilde{A} \int_{t_0}^t \mathrm{d}t' \int_{t_0}^t \mathrm{d}t'' \,\langle \mathrm{Tr}(F^i_{(2)}(x^j(t'),t') F^i_{(2)}(x^j(t''),t''))\rangle \\ &= 2g^2 \widetilde{A} \int_0^t \mathrm{d}t' \int_0^t \mathrm{d}t'' \,\langle \mathrm{Tr}(F^i_{(2)}(t', x_T(t')) F^i_{(2)}(t'', x_T(t'')))\rangle,\end{aligned} \tag{4.109}$$

with

$$x_T(t) = \begin{pmatrix} t \\ 0 \end{pmatrix}. \tag{4.110}$$

The force is in terms of E and B

$$F_{y\,(2)} = E_{y\,(2)} + \epsilon_2^{jk}\dot{x}B_{k\,(2)} = E_{y\,(2)} - B_{z\,(2)} \tag{4.111}$$

and becomes for $\eta = 0$

$$\begin{aligned} E_{y\,(2)} &= \ F_{\tau 2\,(2)} \ = \partial_\tau \partial_1 \chi, \\ B_{z\,(2)} &= -F_{12\,(2)} = -\Delta_T \chi, \end{aligned} \tag{4.112}$$

as can be seen with the help of Eqs. (4.30) and (4.32).

From Eq. (4.80), it can be deduced that

$$\begin{aligned} E_{y\,(2)}(t', x_T(t')) &= -\int \mathrm{d}^2 k_T \, \frac{ik_1}{\omega} J_1(\omega t') e^{ik_1 t'} f_\chi(k_T), \\ B_{z\,(2)}(t', x_T(t')) &= \int \mathrm{d}^2 k_T \, J_0(\omega t') e^{ik_1 t'} f_\chi(k_T). \end{aligned} \tag{4.113}$$

Equation (4.111) leads to

$$\mathrm{Tr}\langle F_{y\,(2)} F_{y\,(2)}\rangle = \mathrm{Tr}\langle E_{y\,(2)} E_{y\,(2)}\rangle + \mathrm{Tr}\langle B_{z\,(2)} B_{z\,(2)}\rangle - \mathrm{Tr}\langle E_{y\,(2)} B_{z\,(2)}\rangle - \mathrm{Tr}\langle B_{z\,(2)} E_{y\,(2)}\rangle, \tag{4.114}$$

with

$$\begin{aligned} &\mathrm{Tr}\langle E_{y\,(2)}(t', x_T(t')) E_{y\,(2)}(t'', x_T(t''))\rangle \\ &= \int \mathrm{d}^2 k_T \int \mathrm{d}^2 k'_T \, \frac{i^2 k_1 k'_1}{\omega \omega'} J_1(\omega t') J_1(\omega' t'') e^{ik_1 t'} e^{ik'_1 t''} \, \mathrm{Tr}\langle f_\chi(k_T) f_\chi(k'_T)\rangle \\ &= \frac{B}{2g^2 \widetilde{A}} \int_0^{\Lambda_{UV}} \mathrm{d}r_l \int_0^{\Lambda_{UV}} \mathrm{d}r_q \int_0^{2\pi} \mathrm{d}\varphi_l \int_0^{2\pi} \mathrm{d}\varphi_q \, (r_q r_l)^3 \left(\frac{\sin(\varphi_q - \varphi_l)}{(r_q^2 + m^2)(r_l^2 + m^2)} \right)^2 \frac{(k_1)^2}{\omega^2} \\ &\quad \times J_1(\omega t') J_1(\omega t'') e^{ik_1 t'} e^{-ik_1 t''}, \end{aligned} \tag{4.115}$$

$$\begin{aligned} &\mathrm{Tr}\langle B_{z\,(2)}(t', x_T(t')) B_{z\,(2)}(t'', x_T(t''))\rangle \\ &= \int \mathrm{d}^2 k_T \int \mathrm{d}^2 k'_T \, J_0(\omega t') J_0(\omega' t'') e^{ik_1 t'} e^{ik'_1 t''} \, \mathrm{Tr}\langle f_\chi(k_T) f_\chi(k'_T)\rangle \\ &= \frac{B}{2g^2 \widetilde{A}} \int_0^{\Lambda_{UV}} \mathrm{d}r_l \int_0^{\Lambda_{UV}} \mathrm{d}r_q \int_0^{2\pi} \mathrm{d}\varphi_l \int_0^{2\pi} \mathrm{d}\varphi_q \, (r_q r_l)^3 \left(\frac{\sin(\varphi_q - \varphi_l)}{(r_q^2 + m^2)(r_l^2 + m^2)} \right)^2 \\ &\quad \times J_0(\omega t') J_0(\omega t'') e^{ik_1 t'} e^{-ik_1 t''}, \end{aligned} \tag{4.116}$$

$$\begin{aligned} &- \mathrm{Tr}\langle E_{y\,(2)}(t', x_T(t')) B_{z\,(2)}(t'', x_T(t''))\rangle \\ &= \int \mathrm{d}^2 k_T \int \mathrm{d}^2 k'_T \, \frac{ik_1}{\omega} J_1(\omega t') J_0(\omega' t'') e^{ik_1 t'} e^{ik'_1 t''} \, \mathrm{Tr}\langle f_\chi(k_T) f_\chi(k'_T)\rangle \\ &= \frac{B}{2g^2 \widetilde{A}} \int_0^{\Lambda_{UV}} \mathrm{d}r_l \int_0^{\Lambda_{UV}} \mathrm{d}r_q \int_0^{2\pi} \mathrm{d}\varphi_l \int_0^{2\pi} \mathrm{d}\varphi_q \, (r_q r_l)^3 \left(\frac{\sin(\varphi_q - \varphi_l)}{(r_q^2 + m^2)(r_l^2 + m^2)} \right)^2 \frac{ik_1}{\omega} \\ &\quad \times J_1(\omega t') J_0(\omega t'') e^{ik_1 t'} e^{-ik_1 t''}, \end{aligned} \tag{4.117}$$

$$
\begin{aligned}
&- \mathrm{Tr}\langle B_{z\,(2)}(t', x_T(t'))E_{y\,(2)}(t'', x_T(t''))\rangle \\
&= \int \mathrm{d}^2k_T \int \mathrm{d}^2k'_T \, \frac{ik'_1}{\omega'} J_0(\omega t')J_1(\omega' t'')e^{ik_1 t'}e^{ik'_1 t''}\,\mathrm{Tr}\langle f_\chi(k_T)f_\chi(k'_T)\rangle \\
&= -\frac{B}{2g^2\widetilde{A}} \int_0^{\Lambda_{UV}} \mathrm{d}r_l \int_0^{\Lambda_{UV}} \mathrm{d}r_q \int_0^{2\pi} \mathrm{d}\varphi_l \int_0^{2\pi} \mathrm{d}\varphi_q \, (r_q r_l)^3 \left(\frac{\sin(\varphi_q - \varphi_l)}{(r_q^2+m^2)(r_l^2+m^2)} \right)^2 \frac{ik_1}{\omega} \\
&\quad \times J_0(\omega t')J_1(\omega t'')e^{ik_1 t'}e^{-ik_1 t''}
\end{aligned} \tag{4.118}
$$

and

$$
k_1 = r_q \cos\varphi_q + r_l \cos\varphi_l. \tag{4.119}
$$

The z component of the force can be written in terms of E and B as follows

$$
F_{z\,(2)} = E_{z\,(2)} + \epsilon_3^{jk} \dot{x} B_{k\,(2)} = E_{z\,(2)} + B_{y\,(2)}. \tag{4.120}
$$

For $\eta = 0$, E and B can be written as

$$
\begin{aligned}
E_{z\,(2)} &= \frac{1}{t} F_{t\eta\,(2)} = -\frac{1}{t}\partial_t(t^2 \epsilon^\eta_{(2)}), \\
B_{y\,(2)} &= -\frac{1}{t} F_{\eta 1\,(2)} = -\frac{1}{t}\partial_i(t^2 \epsilon^\eta_{(2)}).
\end{aligned} \tag{4.121}
$$

One can make use of Eqs. (4.30) and (4.32) to verify this. Note that $\tau = t$ for $\eta = 0$.

From Eq. (4.81), one can deduce

$$
\begin{aligned}
E_{z\,(2)}(t', x_T(t')) &= -\int \mathrm{d}^2k_T \, J_0(\omega t')e^{ik_1 t'} f_\epsilon(k_T), \\
B_{y\,(2)}(t', x_T(t')) &= -\int \mathrm{d}^2k_T \, \frac{ik_1}{\omega} J_1(\omega t')e^{ik_1 t'} f_\epsilon(k_T).
\end{aligned} \tag{4.122}
$$

Equation (4.120) leads to

$$
\mathrm{Tr}\langle F_{z\,(2)}F_{z\,(2)}\rangle = \mathrm{Tr}\langle E_{z\,(2)}E_{z\,(2)}\rangle + \mathrm{Tr}\langle B_{y\,(2)}B_{y\,(2)}\rangle + \mathrm{Tr}\langle E_{z\,(2)}B_{y\,(2)}\rangle + \mathrm{Tr}\langle B_{y\,(2)}E_{z\,(2)}\rangle, \tag{4.123}
$$

with

$$
\begin{aligned}
&\mathrm{Tr}\langle E_{z\,(2)}(t', x_T(t'))E_{z\,(2)}(t'', x_T(t''))\rangle \\
&= \int \mathrm{d}^2k_T \int \mathrm{d}^2k'_T \, J_0(\omega t')J_0(\omega' t'')e^{ik_1 t'}e^{ik'_1 t''}\,\mathrm{Tr}\langle f_\epsilon(k_T)f_\epsilon(k'_T)\rangle \\
&= \frac{B}{2g^2\widetilde{A}} \int_0^{\Lambda_{UV}} \mathrm{d}r_l \int_0^{\Lambda_{UV}} \mathrm{d}r_q \int_0^{2\pi} \mathrm{d}\varphi_l \int_0^{2\pi} \mathrm{d}\varphi_q \, (r_q r_l)^3 \left(\frac{\cos(\varphi_q - \varphi_l)}{(r_q^2+m^2)(r_l^2+m^2)} \right)^2 \\
&\quad \times J_0(\omega t')J_0(\omega t'')e^{ik_1 t'}e^{-ik_1 t''},
\end{aligned} \tag{4.124}
$$

$$
\begin{aligned}
&\mathrm{Tr}\langle B_{y\,(2)}(t', x_T(t'))B_{y\,(2)}(t'', x_T(t''))\rangle \\
&= \int \mathrm{d}^2k_T \int \mathrm{d}^2k'_T \, \frac{i^2 k_1 k'_1}{\omega\omega'} J_1(\omega t')J_1(\omega' t'')e^{ik_1 t'}e^{ik'_1 t''}\,\mathrm{Tr}\langle f_\epsilon(k_T)f_\epsilon(k'_T)\rangle \\
&= \frac{B}{2g^2\widetilde{A}} \int_0^{\Lambda_{UV}} \mathrm{d}r_l \int_0^{\Lambda_{UV}} \mathrm{d}r_q \int_0^{2\pi} \mathrm{d}\varphi_l \int_0^{2\pi} \mathrm{d}\varphi_q \, (r_q r_l)^3 \left(\frac{\cos(\varphi_q - \varphi_l)}{(r_q^2+m^2)(r_l^2+m^2)} \right)^2 \frac{(k_1)^2}{\omega^2} \\
&\quad \times J_1(\omega t')J_1(\omega t'')e^{ik_1 t'}e^{-ik_1 t''},
\end{aligned} \tag{4.125}
$$

$$
\begin{aligned}
&\mathrm{Tr}\langle E_{z\,(2)}(t', x_T(t'))B_{y\,(2)}(t'', x_T(t''))\rangle \\
&= \int \mathrm{d}^2k_T \int \mathrm{d}^2k'_T \, \frac{ik'_1}{\omega'} J_0(\omega t') J_1(\omega' t'') e^{ik_1 t'} e^{ik'_1 t''} \, \mathrm{Tr}\langle f_\epsilon(k_T) f_\epsilon(k'_T)\rangle \\
&= -\frac{B}{2g^2\widetilde{A}} \int_0^{\Lambda_{UV}} \mathrm{d}r_l \int_0^{\Lambda_{UV}} \mathrm{d}r_q \int_0^{2\pi} \mathrm{d}\varphi_l \int_0^{2\pi} \mathrm{d}\varphi_q \, (r_q r_l)^3 \left(\frac{\cos(\varphi_q - \varphi_l)}{(r_q^2 + m^2)(r_l^2 + m^2)} \right)^2 \frac{ik_1}{\omega} \\
&\quad \times J_0(\omega t') J_1(\omega t'') e^{ik_1 t'} e^{-ik_1 t''},
\end{aligned} \tag{4.126}
$$

$$
\begin{aligned}
&\mathrm{Tr}\langle B_{y\,(2)}(t', x_T(t'))E_{z\,(2)}(t'', x_T(t''))\rangle \\
&= \int \mathrm{d}^2k_T \int \mathrm{d}^2k'_T \, \frac{ik_1}{\omega} J_1(\omega t') J_0(\omega' t'') e^{ik_1 t'} e^{ik'_1 t''} \, \mathrm{Tr}\langle f_\epsilon(k_T) f_\epsilon(k'_T)\rangle \\
&= \frac{B}{2g^2\widetilde{A}} \int_0^{\Lambda_{UV}} \mathrm{d}r_l \int_0^{\Lambda_{UV}} \mathrm{d}r_q \int_0^{2\pi} \mathrm{d}\varphi_l \int_0^{2\pi} \mathrm{d}\varphi_q \, (r_q r_l)^3 \left(\frac{\cos(\varphi_q - \varphi_l)}{(r_q^2 + m^2)(r_l^2 + m^2)} \right)^2 \frac{ik_1}{\omega} \\
&\quad \times J_1(\omega t') J_0(\omega t'') e^{ik_1 t'} e^{-ik_1 t''}.
\end{aligned} \tag{4.127}
$$

The force component that is yet to be discussed is the x component

$$
F_{x\,(2)} = E_{x\,(2)} + \epsilon_1^{jk} \dot{x} B_{k\,(2)} = E_{x\,(2)}. \tag{4.128}
$$

Setting $\eta = 0$ leads to

$$
E_{x\,(2)} = F_{\tau 1\,(2)} = -\partial_\tau \partial_2 \chi, \tag{4.129}
$$

see Eqs. (4.30) and (4.32), with

$$
E_{x\,(2)}(t', x_T(t')) = \int \mathrm{d}^2k_T \, \frac{ik_2}{\omega} J_1(\omega t') e^{ik_1 t'} f_\chi(k_T). \tag{4.130}
$$

The correlator reads

$$
\begin{aligned}
&\mathrm{Tr}\langle E_{x\,(2)}(t', x_T(t'))E_{x\,(2)}(t'', x_T(t''))\rangle \\
&= \int \mathrm{d}^2k_T \int \mathrm{d}^2k'_T \, \frac{i^2 k_2 k'_2}{\omega\omega'} J_1(\omega t') J_1(\omega' t'') e^{ik_1 t'} e^{ik'_1 t''} \, \mathrm{Tr}\langle f_\chi(k_T) f_\chi(k'_T)\rangle \\
&= \frac{B}{2g^2\widetilde{A}} \int_0^{\Lambda_{UV}} \mathrm{d}r_l \int_0^{\Lambda_{UV}} \mathrm{d}r_q \int_0^{2\pi} \mathrm{d}\varphi_l \int_0^{2\pi} \mathrm{d}\varphi_q \, (r_q r_l)^3 \left(\frac{\sin(\varphi_q - \varphi_l)}{(r_q^2 + m^2)(r_l^2 + m^2)} \right)^2 \frac{(k_2)^2}{\omega^2} \\
&\quad \times J_1(\omega t') J_1(\omega t'') e^{ik_1 t'} e^{-ik_1 t''},
\end{aligned} \tag{4.131}
$$

with

$$
k_2 = r_q \sin\varphi_q + r_l \sin\varphi_l. \tag{4.132}
$$

4.4.3 Numerical Results

The axes of the three dimensional plots in this subsection are

$$
\begin{aligned}
\bar{t} &= \frac{t' + t''}{2}, \\
\Delta t &= t' - t''
\end{aligned} \tag{4.133}
$$

in the region $0 < t', t'' < t$ and the dimensionless quantity $g^2\widetilde{A}/\pi B \times \mathrm{Tr}\langle FF\rangle$, $\mathrm{Tr}\langle FF\rangle$ denoting some correlator. In this region, the correlators are needed for the integrand in Eq. (4.102). The two dimensional plots in this subsection are given in terms of the rescaled time t' and the dimensionless quantity $\langle p^2\rangle\, m^2/2\pi B$.

Figure 4.7 displays the correlators corresponding to κ, which are given by Eqs. (4.106) and (4.107). Figure 4.7b only shows the negative values of $\langle E_T(t')E_T(t'')\rangle$. These negative values explain the decrease of $\langle p_T^2\rangle_{\kappa\,(4)}$ in Figure 4.1c after a finite time. $\langle E_z(t')E_z(t'')\rangle$ is non-negative everywhere and $\langle p_z^2\rangle_{\kappa\,(4)}$ in Figure 4.1a grows indefinitely.

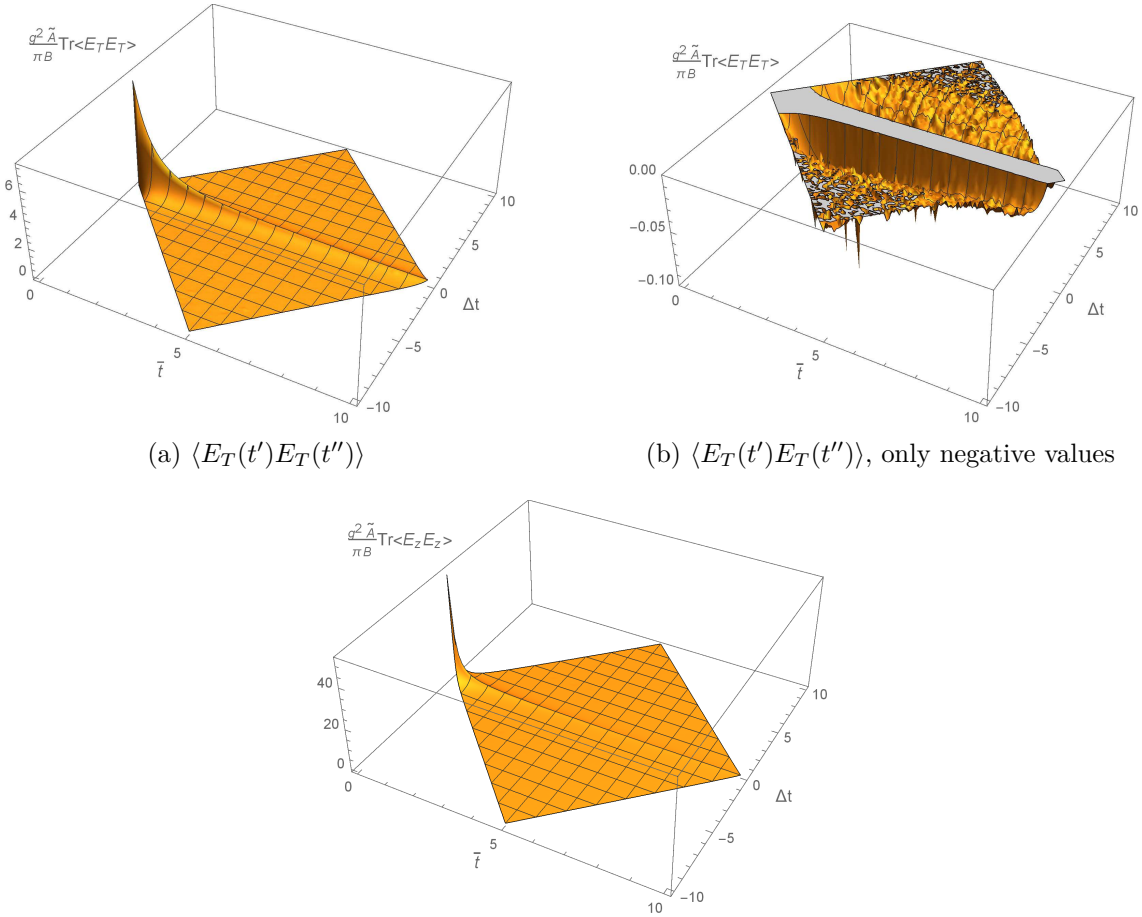

(a) $\langle E_T(t')E_T(t'')\rangle$

(b) $\langle E_T(t')E_T(t'')\rangle$, only negative values

(c) $\langle E_z(t')E_z(t'')\rangle$

Figure 4.7: $\langle E_T(t')E_T(t'')\rangle$ and $\langle E_z(t')E_z(t'')\rangle$, $m = 0.1\,\mathrm{GeV}$

If one integrates the κ correlators with respect to t' and t'', one obtains per definition the respective $\langle p^2\rangle_{\kappa\,(4)}$. The results for the correlators in Figure 4.7 were numerical for a finite number of t', t'', hence the t' and t'' integrations have to be replaced by some integration rule for discrete data points. Figure 4.8 compares the trapezoidal rule applied to the numerical results for the correlators to directly calculating $\langle p^2\rangle_{\kappa\,(4)}$ by numerically solving the three integrals in Eqs. (4.55) and (4.66). These two ways lead to similar results, which allows for the conclusion that numerical errors in the calculation are not too significant.

Figure 4.9 shows the real part of the correlators corresponding to $\hat{q}_y$. Figure 4.9b sets the focus on the negative values and explains why $\langle p_y^2\rangle_{\hat{q}\,(4)}$ in Figure 4.6 decreases after a finite time. Figure 4.9c displays the imaginary part. Due to the fact that the latter should vanish, it can be taken as a measure of the accuracy of the results presented here.

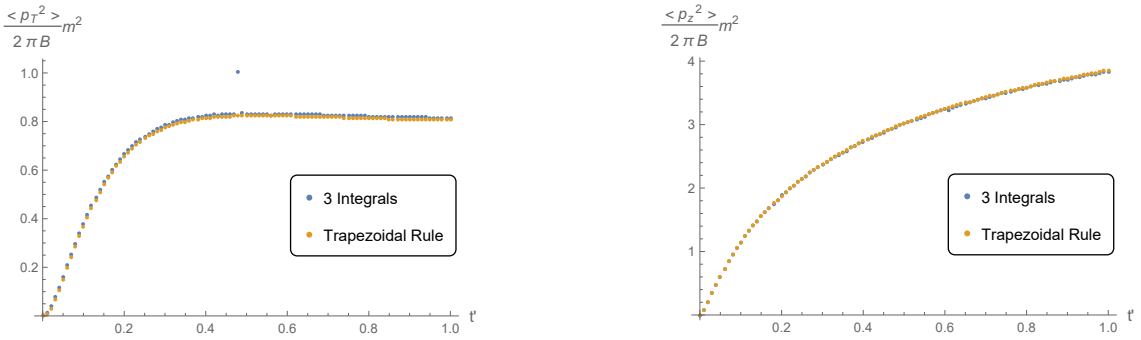

(a) $\langle p_T^2 \rangle_{\kappa\,(4)}$ (b) $\langle p_z^2 \rangle_{\kappa\,(4)}$

Figure 4.8: $\langle p_T^2 \rangle_{\kappa\,(4)}$ and $\langle p_z^2 \rangle_{\kappa\,(4)}$, $m = 0.1\,\mathrm{GeV}$, comparison between directly calculating $\langle p^2 \rangle$ and computing the correlators first

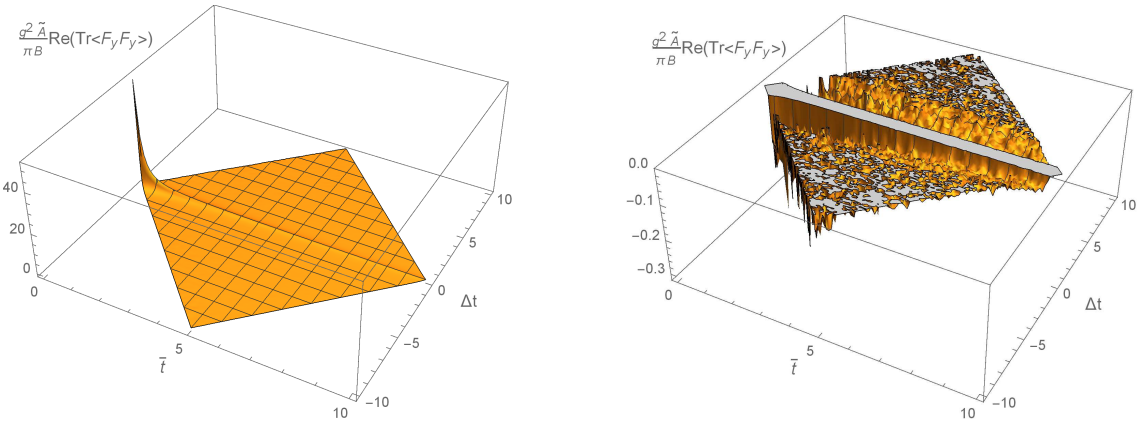

(a) $\Re\langle F_y(t')F_y(t'')\rangle$ (b) $\Re\langle F_y(t')F_y(t'')\rangle$, only negative values

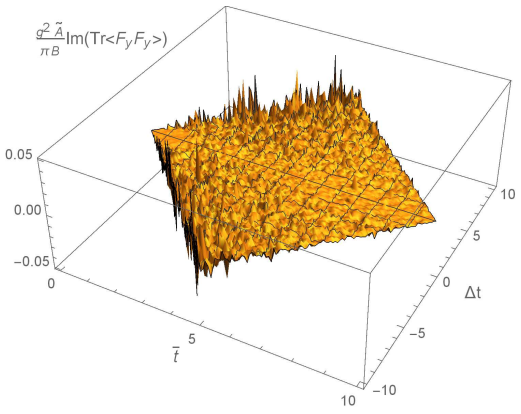

(c) $\Im\langle F_y(t')F_y(t'')\rangle$

Figure 4.9: $\langle F_y(t')F_y(t'')\rangle$, $m = 0.1\,\mathrm{GeV}$

To convince oneself that the imaginary part should indeed vanish, one can take the correlator in Eq. (4.115). In the intermediate step, one has

$$\begin{aligned}&\mathrm{Tr}\langle E_{y\,(2)}(t', x_T(t'))E_{y\,(2)}(t'', x_T(t''))\rangle \\ &= -\int \mathrm{d}^2k_T \int \mathrm{d}^2k'_T \,\frac{k_1 k'_1}{\omega\omega'} J_1(\omega t')J_1(\omega' t'')e^{ik_1 t'}e^{ik'_1 t''}\,\mathrm{Tr}\langle f_\chi(k_T)f_\chi(k'_T)\rangle. \end{aligned} \tag{4.134}$$

Before proving that this quantity is real, one can inspect Eq. (4.60) and see that the quantity $\mathrm{Tr}\langle f_\chi(k_T)f_\chi(k'_T)\rangle$ is real and that

$$\begin{aligned}&\mathrm{Tr}\langle f_\chi(-k_T)f_\chi(-k'_T)\rangle = \frac{12g^6\mu^4}{(2\pi)^4}\delta(-(k_T+k'_T)) \\ &\times\int \mathrm{d}^2l_T \,\frac{(k_T+l_T)^2 l_T^2 - (k_i+l_i)l_i(k_j+l_j)l_j}{((k_T+l_T)^2+m^2)^2(l_T^2+m^2)^2}\theta(\Lambda_{UV}-|k_T+l_T|)\theta(\Lambda_{UV}-|l_T|) \\ &= \frac{12g^6\mu^4}{(2\pi)^4}\delta((k_T+k'_T)) \\ &\times\int \mathrm{d}^2l_T \,\frac{(k_T-l_T)^2 l_T^2 - (k_i-l_i)l_i(k_j-l_j)l_j}{((k_T-l_T)^2+m^2)^2(l_T^2+m^2)^2}\theta(\Lambda_{UV}-|k_T-l_T|)\theta(\Lambda_{UV}-|l_T|) \\ &= \mathrm{Tr}\langle f_\chi(k_T)f_\chi(k'_T)\rangle. \end{aligned} \tag{4.135}$$

Here, the fact that the δ function is even and the substitution $l_T \to -l_T$ were used. The complex conjugate of Eq. (4.134) is

$$\begin{aligned}&\mathrm{Tr}\langle E_{y\,(2)}(t', x_T(t'))E_{y\,(2)}(t'', x_T(t''))\rangle^* \\ &= \left(-\int \mathrm{d}^2k_T \int \mathrm{d}^2k'_T \,\frac{k_1 k'_1}{\omega\omega'} J_1(\omega t')J_1(\omega' t'')e^{ik_1 t'}e^{ik'_1 t''}\,\mathrm{Tr}\langle f_\chi(k_T)f_\chi(k'_T)\rangle\right)^* \\ &= -\int \mathrm{d}^2k_T \int \mathrm{d}^2k'_T \,\frac{k_1 k'_1}{\omega\omega'} J_1(\omega t')J_1(\omega' t'')e^{-ik_1 t'}e^{-ik'_1 t''}\,\mathrm{Tr}\langle f_\chi(k_T)f_\chi(k'_T)\rangle \\ &= -\int \mathrm{d}^2k_T \int \mathrm{d}^2k'_T \,\frac{k_1 k'_1}{\omega\omega'} J_1(\omega t')J_1(\omega' t'')e^{ik_1 t'}e^{ik'_1 t''}\,\mathrm{Tr}\langle f_\chi(-k_T)f_\chi(-k'_T)\rangle \\ &= -\int \mathrm{d}^2k_T \int \mathrm{d}^2k'_T \,\frac{k_1 k'_1}{\omega\omega'} J_1(\omega t')J_1(\omega' t'')e^{ik_1 t'}e^{ik'_1 t''}\,\mathrm{Tr}\langle f_\chi(k_T)f_\chi(k'_T)\rangle \\ &= \mathrm{Tr}\langle E_{y\,(2)}(t', x_T(t'))E_{y\,(2)}(t'', x_T(t''))\rangle, \end{aligned} \tag{4.136}$$

which means that this correlator is indeed real. The substitutions $k_T \to -k_T$ and $k'_T \to -k'_T$ were used. The proofs for the other correlators work analogously.

The real part of the correlators corresponding to $\hat{q}_z$ and $\langle p_x^2\rangle_{\hat{q}}$ are presented in Figure 4.10. There are no negative values deviating from 0 big enough that they could not be numerical errors, and $\langle p_z^2\rangle_{\hat{q}\,(4)}$ and $\langle p_x^2\rangle_{\hat{q}\,(4)}$ in Figure 4.6 grow indefinitely.

One can integrate the $\hat{q}$ correlators with respect to t' and t'' to obtain the respective $\langle p^2\rangle_{\hat{q}\,(4)}$. Their results are compared to the numerical solution of five integrals, which are given by Eqs. (4.85), (4.88) and (4.93) in Figure 4.11. In Figure 4.11a, the result obtained with the help of the trapezoidal rule deviates from the numerical solution given by Eq. (4.85). Due to the fact that the latter shows a decline of $\langle p_y^2\rangle_{\hat{q}\,(4)}$, in analogy to the result on the lattice, which is presented in Figure 4.6, the error of

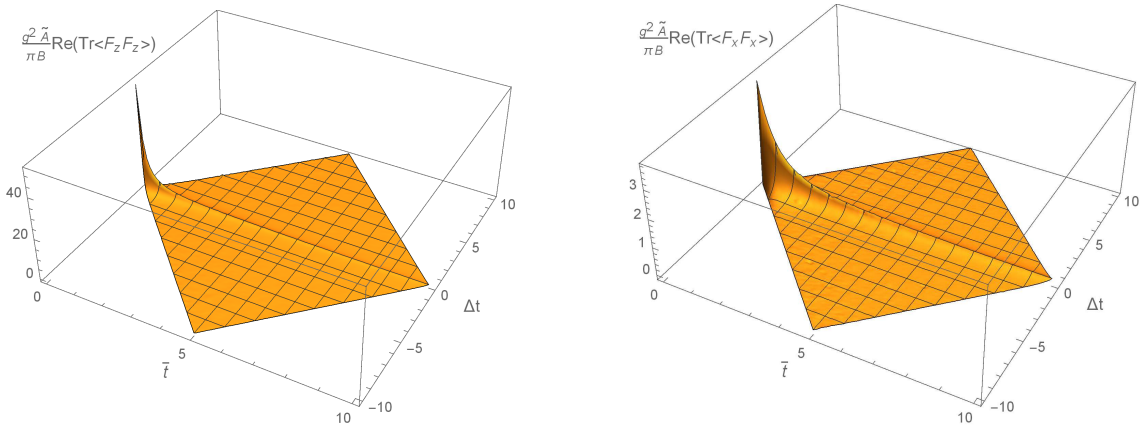

(a) $\Re\langle F_z(t')F_z(t'')\rangle$ (b) $\Re\langle F_x(t')F_x(t'')\rangle$

Figure 4.10: $\Re\langle F_z(t')F_z(t'')\rangle$ and $\Re\langle F_x(t')F_x(t'')\rangle$, $m = 0.1\,\mathrm{GeV}$

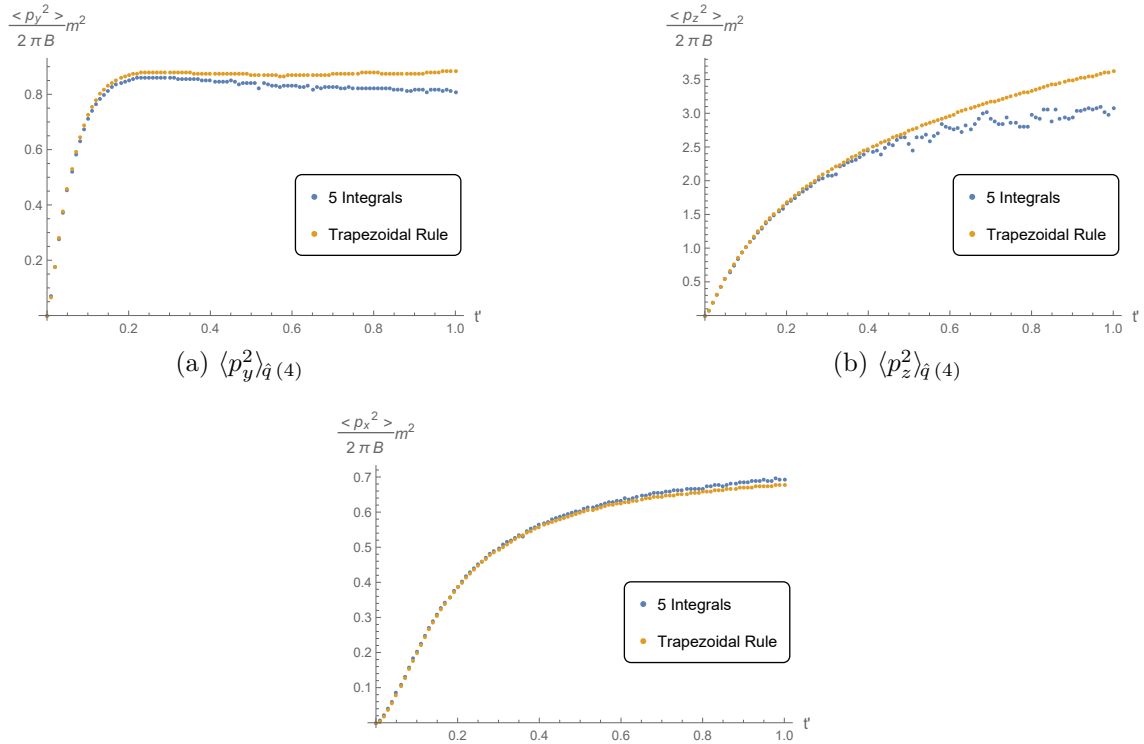

(a) $\langle p_y^2\rangle_{\hat{q}\,(4)}$ (b) $\langle p_z^2\rangle_{\hat{q}\,(4)}$

(c) $\langle p_x^2\rangle_{\hat{q}\,(4)}$

Figure 4.11: $\langle p_y^2\rangle_{\hat{q}\,(4)}$, $\langle p_z^2\rangle_{\hat{q}\,(4)}$ and $\langle p_x^2\rangle_{\hat{q}\,(4)}$, $m = 0.1\,\mathrm{GeV}$, comparison between directly calculating $\langle p^2\rangle$ and computing the correlators first

the calculation via the correlators and the trapezoidal rule seems to become too large. Similarly, the calculation method that uses the trapezoidal rule yields too large values for $\langle p_z^2 \rangle_{\hat{q}\,(4)}$ for large t, as can be seen in a comparison of Figures 4.11b and 4.6. The erratic behaviour of the numerical solution of Eq. (4.88) for large t stems from numerical errors. The difference between the two calculation methods for $\langle p_x^2 \rangle_{\hat{q}\,(4)}$ is small, as is shown in Figure 4.11c.

Conclusion and Outlook

The main part of this master's thesis is the calculation of the momentum broadening of a test parton in the Glasma. A prerequisite for this task is the description of the Glasma, for which the model of choice is the Colour Glass Condensate. In the framework of the Colour Glass Condensate, one nucleus moving at the speed of light is discussed. Then, two nuclei moving at the speed of light towards each other are analysed. Before the collision, they do not influence each other because they are causally separated and can be described by the superposition of two single nucleus solutions. After the collision, in other words, in the forward light cone of the collision, the Glasma is created. There, non-linear effects occur due to self interaction, and the solution can no longer be obtained by superposition of the single nucleus solutions. The Yang-Mills equations, which are the equations of motion of the Glasma, are derived in Milne coordinates, and the initial conditions of the Glasma are stated.

To find a solution of the Glasma, the Yang-Mills equations and the corresponding initial conditions are analytically expanded. The expansion parameter is the particle density ρ of the colliding nuclei in the light cone gauge. It is shown that the lowest non-vanishing order of the vector potential A_μ that describes the Glasma is two, and its solution is given. Then, it is analysed if this solution is different if one chooses the expansion parameter in another gauge, e.g. the covariant gauge. It turns out that the solution remains the same not only for the particle density in the covariant gauge, but for a more general particle density $\widehat{\rho}$, as explained in Subsection 3.4.2.

Equipped with a solution of second order of the vector potential that describes the Glasma, a formula for the momentum broadening parameters κ and $\hat{q}$ is derived, more precisely a formula for $\langle p^2 \rangle$. It depends on the trajectory of the test parton. κ and $\hat{q}$ are then obtained by taking the time derivative of $\langle p^2 \rangle$; the former corresponds to a resting test parton, the latter to a test parton moving at the speed of light perpendicular to the direction, in which the colliding nuclei that created the Glasma travelled. The MV model is slightly altered by introducing an ultraviolet cut-off and an infrared regulator. It is used to calculate the ensemble averages $\langle \ldots \rangle$ that occur during the derivation of the formula for $\langle p^2 \rangle$.

Due to the lowest non-vanishing order of the vector potential A_μ being two, the lowest non-vanishing order of $\langle p^2 \rangle$ is four. At this order each of the components of $\langle p^2 \rangle$ is discussed for both of the aforementioned trajectories of the test parton. The corresponding formulas contain multidimensional integrals, which are evaluated numerically using Mathematica. The numerical results are compared to $\langle p^2 \rangle$ extracted

from a lattice simulation of the Glasma, which was done in [12]. The results of these two different approaches are in good agreement.

If one performs only the momentum integrals describing $\langle p^2 \rangle$, but not the time integrals, one obtains correlators of the electric and magnetic fields. These correlators are calculated and plotted. As a check of validity, the time integration of the correlators is performed with the help of the trapezoidal rule and the results are compared to the ones of $\langle p^2 \rangle$ calculated directly. The good agreement of these results suggests that the numerical errors are small.

As an outlook, let me propose some ideas and possible extensions. The description of the Glasma in this work limits it to be rapidity invariant because the MV model, which is presented in Section 2.3, describes a nucleus as an infinitely thin colour sheet moving at the speed of light. Ultimately, one wants to incorporate rapidity dependencies to better approximate a realistic Glasma, thus each nucleus needs some finite longitudinal structure. That means that the nucleus moving in x^+ direction would no longer be infinitely thin in x^- direction. Due to the finite extent of $\rho_a(x^-, x_T)$ in x^- direction, there would no longer be a boundary condition that is confined to the x^+ axis, like in Eq. (2.40), and a different approach than the one in this work has to be chosen to calculate the vector field and the forces in the Glasma.

The momentum broadening was calculated to the lowest non-vanishing order in the particle density ρ. An obvious extension would be the calculation of the next order. Maybe it can explain why $\langle p_y^2 \rangle_{\hat{q}\,(4)}$ in Figure 4.6 fits the simulation on the lattice worse than the x and z component. Note that a fifth order solution of the momentum broadening requires a third order solution of the vector potential.

The high dilution of the Glasma, which justifies the focus on the lowest vanishing order of the momentum broadening, does not resemble a realistic Glasma. In the future, it is therefore of interest to set the focus on the lattice simulation of the Glasma, which has been done with $SU(2)$ as gauge group, and redo it for $SU(3)$. There, a denser Glasma can be analysed as well. The results can be compared to the ones given in this master's thesis because the gauge group only affects the prefactor B defined in Eq. (4.48), not the occurring integrals.

Appendix A

Notations and Conventions

In this work, natural units $c = 1$ and $\hbar = 1$ are chosen. Furthermore, energies are measured in GeV. The unit of time is fm and the unit of momentum is GeV. The ultraviolet cut-off Λ_{UV} and the infrared regulator m are measured in GeV as well. The unit of the rescaled time $t' = mt$ is fm $\times$ GeV, which is a pure number in natural units with $\hbar = 1$ and $c = 1$. This can be checked by verifying the relation

$$1\,\text{GeV} \times 1\,\text{fm} \approx 5.08\,\hbar c. \tag{A.1}$$

The average momentum squared $\langle p^2 \rangle$ is given in GeV^2, the momentum broadening parameters κ and $\hat{q}$ in GeV^3, the unit of μ is GeV and the one of B due to Eq. (4.48) GeV^4. The quantities $\langle p^2 \rangle\, m^2/B$, $\kappa\, m/B$ and $\hat{q}\, m/B$ are thus dimensionless.

The metric that is used in this master's thesis reads

$$\eta_{\mu\nu} = \text{diag}(1, -1, -1, -1)_{\mu\nu} \tag{A.2}$$

in (t, x, y, z) coordinates.

The Laplace operator in the transverse plane Δ_T is defined as

$$\partial_i \partial^i = -\Delta_T, \qquad i = 1, 2. \tag{A.3}$$

The covariant derivative D_μ acting on a vector field B_ν yields

$$D_\mu B_\nu = \partial_\mu B_\nu + ig[A_\mu, B_\nu], \tag{A.4}$$

and the field strength tensor $F_{\mu\nu}$ is given by

$$F_{\mu\nu} = \partial_\mu A_\nu - \partial_\nu A_\mu + ig[A_\mu, A_\nu]. \tag{A.5}$$

The partial Fourier transform in the transverse plane is defined as

$$\widetilde{\alpha}(\tau, k_T) = \int \mathrm{d}^2 x_T\, \alpha(\tau, x_T) e^{-ik_T x_T}, \tag{A.6}$$

with

$$k_T x_T = \sum_{i=1}^{2} k_i x_i, \tag{A.7}$$

and the inverse Fourier transform is given by

$$\alpha(\tau, x_T) = \frac{1}{(2\pi)^2} \int \mathrm{d}^2 k_T \, \tilde{\alpha}(\tau, k_T) e^{i k_T x_T}. \tag{A.8}$$

That fixes the normalisation factor in the Convolution Theorem

$$f \cdot g = \frac{1}{(2\pi)^2} \mathcal{F}^{-1}(\mathcal{F}(f) * \mathcal{F}(g)). \tag{A.9}$$

$\mathcal{F}$ and $\mathcal{F}^{-1}$ denote the Fourier transform and its inverse, respectively, and $*$ marks the convolution

$$(f * g)(x_T) = \int \mathrm{d}^2 y_T \, f(x_T - y_T) g(y_T). \tag{A.10}$$

The Fierz identity for $SU(N_c)$ can be written in the following form [13]

$$\mathrm{Tr}(t_a A)\,\mathrm{Tr}(t_a B) = \frac{1}{2}\Big(\mathrm{Tr}(AB) - \frac{1}{N_c}\,\mathrm{Tr}(A)\,\mathrm{Tr}(B)\Big). \tag{A.11}$$

An integral of the form $\int \mathrm{d}^2 k_T e^{i k_T x_T}$ is to be understood as $\iint_{\mathbb{R}^2} \mathrm{d}k_x \mathrm{d}k_y e^{i(k_x x + k_y y)}$.

The epsilon tensor with all lower case indices in ascending order is defined to be equal to one in three dimensions as well as in the two dimensional case

$$\begin{aligned} \epsilon_{123} &= 1, \\ \epsilon_{12} &= 1. \end{aligned} \tag{A.12}$$

Appendix B

Coordinate Systems

In addition to Cartesian coordinates, two other coordinate systems are used, light cone coordinates and Milne coordinates. They are discussed in the following.

B.1 Light Cone Coordinates

Light cone coordinates are defined by

$$\begin{aligned} x^+ &= \frac{1}{\sqrt{2}}(t+z), \\ x^- &= \frac{1}{\sqrt{2}}(t-z), \\ x_T &= \begin{pmatrix} x \\ y \end{pmatrix}. \end{aligned} \tag{B.1}$$

The line element is

$$\mathrm{d}s^2 = \eta_{\mu\nu}\mathrm{d}x^\mu \mathrm{d}x^\nu = 2\mathrm{d}x^+\mathrm{d}x^- - \mathrm{d}x^2 - \mathrm{d}y^2, \tag{B.2}$$

with the metric

$$\eta_{\mu\nu} = \begin{pmatrix} 0 & 1 & 0 & 0 \\ 1 & 0 & 0 & 0 \\ 0 & 0 & -1 & 0 \\ 0 & 0 & 0 & -1 \end{pmatrix}_{\mu\nu}. \tag{B.3}$$

The volume form reads

$$\mathrm{d}^4x = \mathrm{d}x^+\mathrm{d}x^-\mathrm{d}^2x_T. \tag{B.4}$$

B.2 Milne Coordinates

The definition of Milne coordinates, to which are also referred as (τ, η) or (τ, η, x_T) coordinates, is given by

$$\begin{aligned} \tau &= \sqrt{2x^+x^-} \quad = \frac{1}{\sqrt{2}}(t^2 - z^2), \\ \eta &= \frac{1}{2}\ln\left(\frac{x^+}{x^-}\right) = \frac{1}{2}\ln\left(\frac{t+z}{t-z}\right), \\ x_T &= \begin{pmatrix} x \\ y \end{pmatrix}. \end{aligned} \tag{B.5}$$

The range of the proper time τ and the spacetime rapidity η is

$$\begin{aligned} &\tau \in (0, \infty), \\ &\eta \in (-\infty, \infty). \end{aligned} \tag{B.6}$$

The line element written in these coordinates reads

$$\mathrm{d}s^2 = g_{\mu\nu}\mathrm{d}x^\mu \mathrm{d}x^\nu = \mathrm{d}\tau^2 - \mathrm{d}x^2 - \mathrm{d}y^2 - \tau^2 \mathrm{d}\eta^2, \tag{B.7}$$

with the metric

$$g_{\mu\nu} = \begin{pmatrix} 1 & 0 & 0 & 0 \\ 0 & -1 & 0 & 0 \\ 0 & 0 & -1 & 0 \\ 0 & 0 & 0 & -\tau^2 \end{pmatrix}_{\mu\nu}, \tag{B.8}$$

and the volume form is

$$\mathrm{d}^4 x = \tau \mathrm{d}\tau \, \mathrm{d}^2 x_T \, \mathrm{d}\eta. \tag{B.9}$$

The electromagnetic fields in (t, x, y, z) coordinates and the field strength tensor in (τ, η, x_T) coordinates are connected by

$$\begin{aligned} E_i &= F_{\tau i} \cosh\eta - \frac{1}{\tau} F_{\eta i} \sinh\eta, \quad i = 1, 2 \\ E_3 &= \frac{1}{\tau} F_{\tau\eta}, \\ B_i &= \epsilon_{ij} \Big(F_{j\tau} \sinh\eta + \frac{1}{\tau} F_{\eta j} \cosh\eta \Big), \quad i, j = 1, 2 \\ B_3 &= -F_{12}. \end{aligned} \tag{B.10}$$

B.2.1 Yang-Mills Equations in Milne Coordinates

A similar calculation to the one presented in this subsection can be found in [12]. The Yang-Mills action reads

$$S = -\frac{1}{2} \int \mathrm{d}^4 x \ \mathrm{Tr}(F_{\mu\nu} F^{\mu\nu}). \tag{B.11}$$

The term $F_{\mu\nu}F^{\mu\nu}$ can be written in (τ, η) coordinates

$$\begin{aligned} F_{\mu\nu}F^{\mu\nu} &= 2F_{\tau\eta}F^{\tau\eta} + 2F_{\tau i}F^{\tau i} + 2F_{\eta i}F^{\eta i} + F_{ij}F^{ij} \\ &= 2F_{\tau\eta}F_{\tau\eta}g^{\tau\tau}g^{\eta\eta} + 2F_{\tau i}F_{\tau j}g^{\tau\tau}g^{ij} + 2F_{\eta i}F_{\eta j}g^{\eta\eta}g^{ij} + F_{ij}F_{kl}g^{ik}g^{jl} \\ &= -\frac{2}{\tau^2}(F_{\tau\eta})^2 - 2(F_{\tau i})^2 + \frac{2}{\tau^2}(F_{\eta i})^2 + (F_{ij})^2 \end{aligned} \tag{B.12}$$

and inserted into Eq. (B.11)

$$S = \int \mathrm{d}\tau \, \mathrm{d}^2 x_T \, \mathrm{d}\eta \ \mathrm{Tr}\Big(\frac{1}{\tau}(F_{\tau\eta})^2 + \tau (F_{\tau i})^2 - \frac{1}{\tau}(F_{\eta i})^2 - \frac{\tau}{2}(F_{ij})^2 \Big), \tag{B.13}$$

where Eq. (B.9) has already been used.

The action, which is given by Eq. (B.13), will now be varied with respect to A_τ to obtain the first equation of motion

$$\delta_\tau S \equiv \delta_{A_\tau} S = 2 \int \mathrm{d}\tau \, \mathrm{d}^2 x_T \, \mathrm{d}\eta \; \mathrm{Tr}\Big(\frac{1}{\tau} F_{\tau\eta} \delta_\tau F_{\tau\eta} + \tau F_{\tau i} \delta_\tau F_{\tau i} \Big). \tag{B.14}$$

The variations of the two separate terms are

$$\begin{aligned} \delta_\tau F_{\tau\eta} &= -\partial_\eta \delta A_\tau + ig \delta_\tau [A_\tau, A_\eta] \\ &= -\partial_\eta \delta A_\tau + ig [\delta A_\tau, A_\eta], \\ \delta_\tau F_{\tau i} &= -\partial_i \delta A_\tau + ig [\delta A_\tau, A_i], \end{aligned} \tag{B.15}$$

and the variation of the action becomes

$$\begin{aligned} \delta_\tau S &= 2 \int \mathrm{d}\tau \, \mathrm{d}^2 x_T \, \mathrm{d}\eta \; \mathrm{Tr}\Big(\frac{1}{\tau} F_{\tau\eta} (-\partial_\eta \delta A_\tau + ig [\delta A_\tau, A_\eta]) \\ &\quad + \tau F_{\tau i} (-\partial_i \delta A_\tau + ig [\delta A_\tau, A_i]) \Big) \\ &= 2 \int \mathrm{d}\tau \, \mathrm{d}^2 x_T \, \mathrm{d}\eta \; \mathrm{Tr}\Big(\frac{1}{\tau} (\partial_\eta F_{\tau\eta} \delta A_\tau + F_{\tau\eta} ig [\delta A_\tau, A_\eta]) \\ &\quad + \tau (\partial_i F_{\tau i} \delta A_\tau + ig F_{\tau i} [\delta A_\tau, A_i]) \Big) \\ &= 2 \int \mathrm{d}\tau \, \mathrm{d}^2 x_T \, \mathrm{d}\eta \; \mathrm{Tr}\Big(\frac{1}{\tau} (\partial_\eta F_{\tau\eta} + ig [A_\eta, F_{\tau\eta}]) \delta A_\tau + \tau (\partial_i F_{\tau i} + ig [A_i, F_{\tau i}]) \delta A_\tau \Big) \\ &= 2 \int \mathrm{d}\tau \, \mathrm{d}^2 x_T \, \mathrm{d}\eta \; \mathrm{Tr}\Big(\frac{1}{\tau} D_\eta F_{\tau\eta} + \tau D_i F_{\tau i} \Big) \delta A_\tau. \end{aligned} \tag{B.16}$$

In the first step, integration by parts was used, in the second step, the cyclicity of the trace was exploited. Demanding that the variation of the action vanishes for all possible variations leads to

$$\frac{1}{\tau} D_\eta F_{\tau\eta} + \tau D_i F_{\tau i} = 0. \tag{B.17}$$

Before the variation with respect to the other coordinates is done, the Fock-Schwinger gauge can be employed because A_τ is a constant factor in these variations and would be set to zero afterwards anyway. The terms multiplied by it can therefore be neglected from the beginning of the calculation. Also, the assumption of boost invariance $\partial_\eta A^\mu = 0$ is exploited. After setting $A_\tau = 0$, the action takes the form

$$S = \int \mathrm{d}\tau \, \mathrm{d}^2 x_T \, \mathrm{d}\eta \; \mathrm{Tr}\Big(\frac{1}{\tau} (\partial_\tau A_\eta)^2 + \tau (\partial_\tau A_i)^2 - \frac{1}{\tau} (D_i A_\eta)^2 - \frac{\tau}{2} (F_{ij})^2 \Big). \tag{B.18}$$

Varying Eq. (B.18) with respect to A_η yields

$$\begin{aligned} \delta_\eta S \equiv \delta_{A_\eta} S &= 2 \int \mathrm{d}\tau \, \mathrm{d}^2 x_T \, \mathrm{d}\eta \; \mathrm{Tr}\Big(\frac{1}{\tau} \partial_\tau A_\eta \partial_\tau \delta A_\eta - \frac{1}{\tau} D_i A_\eta D_i \delta A_\eta \Big) \\ &= 2 \int \mathrm{d}\tau \, \mathrm{d}^2 x_T \, \mathrm{d}\eta \; \mathrm{Tr}\Big(-\partial_\tau \Big(\frac{1}{\tau} \partial_\tau A_\eta \Big) + \frac{1}{\tau} D_i^2 A_\eta \Big) \delta A_\eta. \end{aligned} \tag{B.19}$$

From this variation, the following equation of motion can be deduced

$$\partial_\tau \Big(\frac{1}{\tau} \partial_\tau A_\eta \Big) + \frac{1}{\tau} D_i D^i A_\eta = 0. \tag{B.20}$$

The variation that is yet to be performed is the one of Eq. (B.18) with respect to A_k

$$\delta_k S \equiv \delta_{A_k} S = 2 \int \mathrm{d}\tau \, \mathrm{d}^2 x_T \, \mathrm{d}\eta \, \mathrm{Tr}\Big(\tau \partial_\tau A_i \partial_\tau \delta_k A_i - \frac{1}{\tau} D_i A_\eta \delta_k D_i A_\eta - \frac{\tau}{2} F_{ij} \delta_k F_{ij} \Big). \tag{B.21}$$

The variations of the three separate terms give

$$\begin{aligned} \delta_k A_j &= \delta_{kj} \delta A_k \\ \delta_k D_i A_\eta &= ig \delta_{ki} [\delta A_k, A_\eta] \\ F_{ij} \delta_k F_{ij} &= F_{ij} (\delta_{kj} \partial_i \delta A_k - \delta_{ki} \partial_j \delta A_k + ig(\delta_{ki}[\delta A_k, A_j] + \delta_{kj}[A_i, \delta A_k])) \\ &= F_{ik} (\partial_i \delta A_k - ig[\delta A_k, A_i]) + F_{kj}(-\partial_j \delta A_k + ig[\delta A_k, A_j]) \\ &= 2F_{kj}(-\partial_j \delta A_k + ig[\delta A_k, A_j]). \end{aligned} \tag{B.22}$$

Using integration by parts and the cyclicity of the trace, the last term can be rewritten as

$$\int \mathrm{d}\tau \, \mathrm{d}^2 x_T \, \mathrm{d}\eta \, \mathrm{Tr}(2F_{kj}(-\partial_j \delta A_k + ig[\delta A_k, A_j])) = \int \mathrm{d}\tau \, \mathrm{d}^2 x_T \, \mathrm{d}\eta \, \mathrm{Tr}(2 D_j F_{kj} \delta_{A_k}). \tag{B.23}$$

Plugging the relations given in Eqs. (B.22) and (B.23) into Eq. (B.21) yields

$$\begin{aligned} \delta_k S &= -2 \int \mathrm{d}\tau \, \mathrm{d}^2 x_T \, \mathrm{d}\eta \, \mathrm{Tr}\Big(\partial_\tau (\tau \partial_\tau A_k) \delta A_k + \frac{ig}{\tau} D_k A_\eta [\delta A_k, A_\eta] + \tau D_j F_{kj} \delta A_k \Big) \\ &= -2 \int \mathrm{d}\tau \, \mathrm{d}^2 x_T \, \mathrm{d}\eta \, \mathrm{Tr}\Big(\partial_\tau (\tau \partial_\tau A_k) + \frac{ig}{\tau} [A_\eta, D_k A_\eta] + \tau D_j F_{kj} \Big) \delta A_k, \end{aligned} \tag{B.24}$$

and setting this equal to 0 leads to

$$\partial_\tau (\tau \partial_\tau A_i) + \frac{ig}{\tau} [A_\eta, D_i A_\eta] + \tau D_j F^{ij} = 0. \tag{B.25}$$

The three equations of motion, listed in Eqs. (B.17), (B.20) and (B.25), can be written in terms of α^η and α^i, which is done in Eq. (2.39). With the metric given by Eq. (B.8), the following relations can be found in region IV of Figure 2.1

$$\begin{aligned} \alpha^\eta &= g^{\eta\eta} A_\eta = -\frac{1}{\tau^2} A_\eta, \\ \alpha^i &= g^{ij} A_j = -A_i. \end{aligned} \tag{B.26}$$

The separate terms of Eq. (B.20) can be written as

$$\begin{aligned} \partial_\tau \Big(\frac{1}{\tau} \partial_\tau A_\eta \Big) &= \partial_\tau \Big(\frac{1}{\tau} \partial_\tau \big(-\tau^2 \alpha^\eta \big) \Big) \\ &= \partial_\tau \Big(\frac{1}{\tau} \big(-2\tau \alpha^\eta - \tau^2 \partial_\tau \alpha^\eta \big) \Big) \\ &= -3 \partial_\tau \alpha^\eta - \tau \partial_\tau^2 \alpha^\eta \\ &= -\frac{1}{\tau^2} \big(3\tau^2 \partial_\tau \alpha^\eta + \tau^3 \partial_\tau^2 \alpha^\eta \big) \\ &= -\frac{1}{\tau^2} \partial_\tau \big(\tau^3 \partial_\tau \alpha^\eta \big), \\ \frac{1}{\tau} D_i D^i A_\eta &= -\tau D_i D^i \alpha^\eta. \end{aligned} \tag{B.27}$$

and the whole equation thus becomes

$$\frac{1}{\tau^3}\partial_\tau\left(\tau^3\partial_\tau\alpha^\eta\right) + D_i D^i\alpha^\eta = 0. \tag{B.28}$$

The separate terms of Eq. (B.17) are

$$\begin{aligned}
\frac{1}{\tau}D_\eta F_{\tau\eta} &= \frac{1}{\tau}(\partial_\eta F_{\tau\eta} + ig[A_\eta, F_{\tau\eta}]) \\
&= \frac{ig}{\tau}[A_\eta, \partial_\tau A_\eta] \\
&= ig\tau\left[\alpha^\eta, \partial_\tau\left(\tau^2\alpha^\eta\right)\right] \\
&= ig\tau^3[\alpha^\eta, \partial_\tau\alpha^\eta], \\
\tau D_i F_{\tau i} &= \tau(\partial_i F_{\tau i} + ig[A_i, F_{\tau i}]) \\
&= \tau(\partial_i\partial_\tau A_i + ig[A_i, \partial_\tau A_i]) \\
&= \tau D_i\partial_\tau A_i \\
&= -\tau D_i\partial_\tau\alpha^i,
\end{aligned} \tag{B.29}$$

and the whole equation reads

$$ig\tau^2[\alpha^\eta, \partial_\tau\alpha^\eta] - D_i\partial_\tau\alpha^i = 0. \tag{B.30}$$

Equation (B.25) becomes

$$-\partial_\tau\left(\tau\partial_\tau\alpha^i\right) + \tau D_j F^{ij} + ig\tau^3[\alpha^\eta, D_i\alpha^\eta] = 0. \tag{B.31}$$

Appendix C

Bessel Functions

In Chapter 3, the search for a solution of the vector potential A_μ that describes the Glasma leads to Bessel differential equations. They are discussed in this appendix.

C.1 Transformation of the Bessel Differential Equation

The Bessel differential equation for $\eta(\xi)$ reads

$$\xi^2 \frac{\mathrm{d}^2\eta}{\mathrm{d}\xi^2} + \xi \frac{\mathrm{d}\eta}{\mathrm{d}\xi} + (\xi^2 - n^2)\eta = 0, \tag{C.1}$$

or, equivalently

$$\xi \frac{\mathrm{d}}{\mathrm{d}\xi}\left(\xi \frac{\mathrm{d}\eta}{\mathrm{d}\xi}\right) + (\xi^2 - n^2)\eta = 0. \tag{C.2}$$

Its solution is

$$\eta(\xi) = AJ_n(\xi) + BY_n(\xi), \tag{C.3}$$

with the Bessel functions of the first kind J_n and the ones of the second kind Y_n.

Consider the transformation of variables [20]

$$\begin{aligned} \eta &= \frac{y(x)}{x^\alpha}, \\ \xi &= \beta x^\gamma. \end{aligned} \tag{C.4}$$

The solution is

$$y(x) = x^\alpha (AJ_n(\beta x^\gamma) + BY_n(\beta x^\gamma)), \tag{C.5}$$

and the corresponding differential equation reads

$$\frac{\mathrm{d}^2 y}{\mathrm{d}x^2} - (2\alpha - 1)\frac{1}{x}\frac{\mathrm{d}y}{\mathrm{d}x} + \left(\frac{\alpha^2 - n^2\gamma^2}{x^2} + \beta^2\gamma^2 x^{2(\gamma-1)}\right) y = 0. \tag{C.6}$$

In the following, two special cases of this differential equation will be analysed. They are obtained by fixing the values for α, β, γ and n.

C.1.1 First Special Case: $\alpha = 0$, $\beta = \omega$, $\gamma = 1$, $n = 0$

With $\alpha = 0$, $\beta = \omega$, $\gamma = 1$ and $n = 0$, Eq. (C.6) becomes

$$\frac{\mathrm{d}^2 y}{\mathrm{d}x^2} + \frac{1}{x}\frac{\mathrm{d}y}{\mathrm{d}x} + \omega^2 y = 0. \tag{C.7}$$

Its solution is

$$y(x) = AJ_0(\omega x) + BY_0(\omega x). \tag{C.8}$$

Equation (C.7) is of the same form as the differential equation (3.76) for the field $\widetilde{\chi}$. One of the initial conditions, which are given in Eq. (3.78), is

$$\frac{\mathrm{d}y}{\mathrm{d}x}(x = 0) = 0. \tag{C.9}$$

This yields, after differentiating Eq. (C.8),

$$\begin{aligned} \frac{\mathrm{d}y}{\mathrm{d}x} &= -A\omega J_1(\omega x) - B\omega Y_1(\omega x), \\ B &= 0 \end{aligned} \tag{C.10}$$

because $Y_1(\omega x) \to -\infty$ for $x \to 0$ and $J_1(0) = 0$. The solution respecting Eq. (C.9) is therefore

$$y(x) = AJ_0(\omega x). \tag{C.11}$$

Due to the fact that $J_0(0) = 1$, the remaining constant A is simply the function $y(x)$ at $x = 0$. The solution is therefore

$$y(x) = y(0)J_0(\omega x). \tag{C.12}$$

This is exactly what was used to get Eq. (3.80).

C.1.2 Second Special Case: $\alpha = -1$, $\beta = \omega$, $\gamma = 1$, $n = 1$

If $\alpha = -1$, $\beta = \omega$, $\gamma = 1$ and $n = 1$, Eq. (C.6) becomes

$$\frac{\mathrm{d}^2 y}{\mathrm{d}x^2} + \frac{3}{x}\frac{\mathrm{d}y}{\mathrm{d}x} + \omega^2 y = 0. \tag{C.13}$$

Its solution is

$$y(x) = \frac{1}{x}(AJ_1(\omega x) + BY_1(\omega x)). \tag{C.14}$$

Equation (C.13) is of the same form as the field $\widetilde{\epsilon}_{(2)}$ in Eq. (3.75). One of the initial conditions, which are given in Eq. (3.77), reads

$$\frac{\mathrm{d}y}{\mathrm{d}x}(x = 0) = 0. \tag{C.15}$$

The derivate of $y(x)$ is calculated in the following

$$\frac{\mathrm{d}y}{\mathrm{d}x} = A\left(-\frac{J_1(\omega x)}{x^2} + \frac{\omega(J_0(\omega x) - J_2(\omega x))}{2x}\right) + B\left(-\frac{Y_1(\omega x)}{x^2} + \frac{\omega(Y_0(\omega x) - Y_2(\omega x))}{2x}\right). \tag{C.16}$$

Due to the fact that

$$\lim_{x\to 0}\left(-\frac{Y_1(\omega x)}{x^2}+\frac{\omega(Y_0(\omega x)-Y_2(\omega x))}{2x}\right)=\infty,$$
$$\lim_{x\to 0}\left(-\frac{J_1(\omega x)}{x^2}+\frac{\omega(J_0(\omega x)-J_2(\omega x))}{2x}\right)=0, \tag{C.17}$$

$B=0$. If one wants to give the solution in terms of $y(0)$, the value of the function at $x=0$, one gets

$$y(x)=\frac{2y(0)J_1(\omega x)}{\omega x}. \tag{C.18}$$

The factor of 2 occurs due to

$$\lim_{x\to 0}\frac{J_1(\omega x)}{\omega x}=\frac{1}{2}. \tag{C.19}$$

This was used to obtain Eq. (3.79).

C.2 The Inhomogeneous Bessel Differential Equation and its Transformation

The inhomogeneous Bessel differential equation

$$\xi^2\frac{\mathrm{d}^2\eta}{\mathrm{d}\xi^2}+\xi\frac{\mathrm{d}\eta}{\mathrm{d}\xi}+\xi^2\eta+a(\xi)=0 \tag{C.20}$$

has the solution

$$\begin{aligned}\eta(\xi)&=\eta_h(\xi)+\eta_p(\xi),\\ \eta_h(\xi)&=AJ_0(\xi)+BY_0(\xi),\\ \eta_p(\xi)&=J_0(\xi)\frac{\pi}{2}\int_1^\xi \mathrm{d}\zeta\, a(\zeta)Y_0(\zeta)-Y_0(\xi)\frac{\pi}{2}\int_1^\xi \mathrm{d}\zeta\, a(\zeta)J_0(\zeta).\end{aligned} \tag{C.21}$$

The same transformation of variables as before in Eq. (C.4) is made. One obtains

$$\frac{\mathrm{d}^2y}{\mathrm{d}x^2}-(2\alpha-1)\frac{1}{x}\frac{\mathrm{d}y}{\mathrm{d}x}+\left(\frac{\alpha^2-n^2\gamma^2}{x^2}+\beta^2\gamma^2x^{2(\gamma-1)}\right)y+a(\beta x^\gamma)=0 \tag{C.22}$$

and for $\alpha=0$, $\beta=\omega$, $\gamma=1$, $n=0$

$$\frac{\mathrm{d}^2y}{\mathrm{d}x^2}+\frac{1}{x}\frac{\mathrm{d}y}{\mathrm{d}x}+\omega^2y+a(\omega x)=0. \tag{C.23}$$

If the function $a(\tau)$ is not set to 0 during the calculation for χ one remains with Eq. (3.69)

$$\frac{1}{\tau}\partial_\tau(\tau\partial_\tau\chi)-\Delta_T\chi=a(\tau). \tag{C.24}$$

Its partial Fourier transform is

$$\frac{1}{\tau}\partial_\tau(\tau\partial_\tau\widetilde{\chi})+\omega^2\widetilde{\chi}=(2\pi)^2a(\tau)\delta(k_1)\delta(k_2), \tag{C.25}$$

with $\omega = \sqrt{k_T^2}$. This equation is not of the form of Eq. (C.23) because of the additional ω appearing in the argument of a. To solve this problem, Eq. (C.20) is written in a different way

$$\xi^2 \frac{\mathrm{d}^2\eta}{\mathrm{d}\xi^2} + \xi \frac{\mathrm{d}\eta}{\mathrm{d}\xi} + \xi^2\eta + a(\frac{\xi}{\beta}) = 0. \tag{C.26}$$

Analogous steps to before lead to

$$\frac{\mathrm{d}^2 y}{\mathrm{d}x^2} + \frac{1}{x}\frac{\mathrm{d}y}{\mathrm{d}x} + \omega^2 y + a(x) = 0, \tag{C.27}$$

without ω in the argument of a and with the solution

$$\begin{aligned} y(x) &= y_h(x) + y_p(x), \\ y_h(x) &= AJ_0(\omega x) + BY_0(\omega x), \\ y_p(x) &= J_0(\omega x)\frac{\pi}{2}\int_1^{\omega x} \mathrm{d}\zeta\, a(\frac{\zeta}{\omega})Y_0(\zeta) - Y_0(\omega x)\frac{\pi}{2}\int_1^{\omega x}\mathrm{d}\zeta\, a(\frac{\zeta}{\omega})J_0(\zeta). \end{aligned} \tag{C.28}$$

The solution of Eq. (C.25) is therefore

$$\begin{aligned} \widetilde{\chi}(\tau, k_T) = {} & AJ_0(\omega\tau) + BY_0(\omega\tau) - (2\pi)^2\delta(k_1)\delta(k_2) \\ & \times \left(J_0(\omega\tau)\frac{\pi}{2}\int_1^{\omega\tau}\mathrm{d}\zeta\, a\left(\frac{\zeta}{\omega}\right)Y_0(\zeta) - Y_0(\omega\tau)\frac{\pi}{2}\int_1^{\omega\tau}\mathrm{d}\zeta\, a\left(\frac{\zeta}{\omega}\right)J_0(\zeta)\right). \end{aligned} \tag{C.29}$$

The constants A and B have to be determined by the initial conditions, which are given in Eq. (3.78),

$$\begin{aligned} k_T^2\widetilde{\chi}(\tau = 0, k_T) &= \frac{ig\epsilon^{ij}}{(2\pi)^2}\int \mathrm{d}^2k'_T\,(k_i - k'_i)k'_j\left[\widetilde{\phi}_1^{LC}(k_T - k'_T), \widetilde{\phi}_2^{LC}(k'_T)\right], \\ k_i\partial_\tau\widetilde{\chi}(\tau = 0, k_T) &= 0. \end{aligned} \tag{C.30}$$

The force on the test parton of interest is determined by the field strength tensor, which is, to second order, determined by the fields $\epsilon_{(2)}$ and $\epsilon^i_{(2)}$. The latter is determined by spatial derivatives of the field χ. Hence, the function $a(\tau)$ has no influence on the forces that act on the test parton and can therefore be set to 0 to simplify the calculation.

The initial conditions of χ, which are derived from the initial conditions of $\epsilon^i_{(2)}$, also contain spatial derivatives. They can be neglected if $a(\tau)$ is set to 0, else they have to be kept to act on the inhomogeneous part of the solution of Eq. (C.29). In Fourier space, they produce a factor of the form of $x\delta(x)$, which vanishes. This way, the constants A and B can be determined even if $a(\tau)$ is not set to 0 because it drops out during the evaluation of the constants. The solution is

$$\begin{aligned} \widetilde{\chi}(\tau, k_T) = {} & \widetilde{\chi}(0, k_T)J_0(\omega\tau) - (2\pi)^2\delta(k_1)\delta(k_2) \\ & \times \left(J_0(\omega\tau)\frac{\pi}{2}\int_1^{\omega\tau}\mathrm{d}\zeta\, a\left(\frac{\zeta}{\omega}\right)Y_0(\zeta) - Y_0(\omega\tau)\frac{\pi}{2}\int_1^{\omega\tau}\mathrm{d}\zeta\, a\left(\frac{\zeta}{\omega}\right)J_0(\zeta)\right). \end{aligned} \tag{C.31}$$

Appendix D

Analysis of Occurring Integrals

In this appendix, some integrals that appear in this master's thesis are discussed in detail.

The φ integral of Eq. (4.74) reads

$$\begin{aligned}\int_0^{2\pi} \mathrm{d}\varphi \, \frac{\cos^2\varphi}{\omega^2} &= \int_0^{2\pi} \mathrm{d}\varphi \, \frac{\cos^2\varphi}{r_q^2 + r_l^2 + 2r_q r_l \cos\varphi} \\ &= \int_0^{2\pi} \mathrm{d}\varphi \, \frac{\cos^2\varphi}{a + b\cos\varphi} \\ &= \frac{1}{b}\int_0^{2\pi} \mathrm{d}\varphi \, \frac{\cos^2\varphi}{c + \cos\varphi},\end{aligned} \tag{D.1}$$

with

$$\begin{aligned}a &= r_q^2 + r_l^2, \\ b &= 2r_q r_l, \\ c &= \frac{a}{b}.\end{aligned} \tag{D.2}$$

$c \geq 1$, because

$$c = \frac{r_q^2 + r_l^2}{2r_q r_l} \geq 1 \leftrightarrow (r_q - r_l)^2 \geq 0. \tag{D.3}$$

The integrand of Eq. (D.1) is plotted in Figure D.1 for some $c \geq 1$. It is finite $\forall c > 1$, but infinite for $c = 1$, for which it has a pole of the form $\frac{2}{(\varphi-\pi)^2}$. $c = 1$ is realised in the diverging outer integrals of Eq. (4.74) because there, $r_q = r_l$ occurs. Therefore, $\langle p_z^2 \rangle_{\kappa\,(4)}$ diverges for $t \to \infty$.

The φ integral of Eq. (4.75) is

$$\int_0^{2\pi} \mathrm{d}\varphi \, \frac{\sin^2\varphi}{\omega^2} = \frac{1}{b}\int_0^{2\pi} \mathrm{d}\varphi \, \frac{\sin^2\varphi}{c + \cos\varphi}. \tag{D.4}$$

The integrand of Eq. (D.4) is plotted in Figure D.2 for some $c \geq 1$. It is finite $\forall c \geq 1$, but for $c = 1$, there is an undefined point at $\varphi = \pi$. This point is defined by identifying it with its limit

$$\lim_{\varphi\to\pi} \frac{\sin^2\varphi}{1 + \cos\varphi} = \lim_{\varphi\to\pi} \frac{2\sin\varphi\cos\varphi}{-\sin\varphi} = 2. \tag{D.5}$$

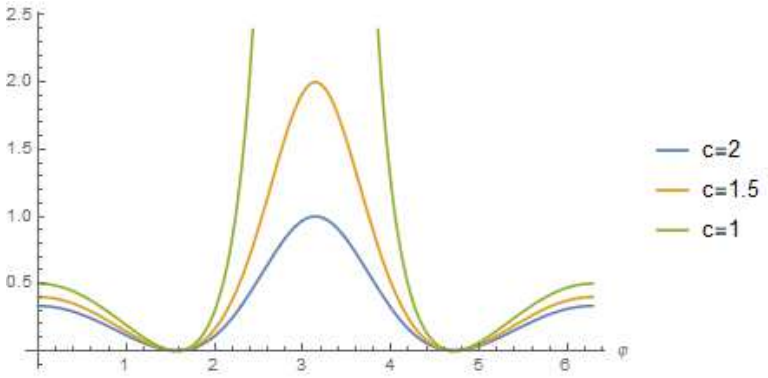

Figure D.1: $\frac{\cos^2\varphi}{c+\cos\varphi}$

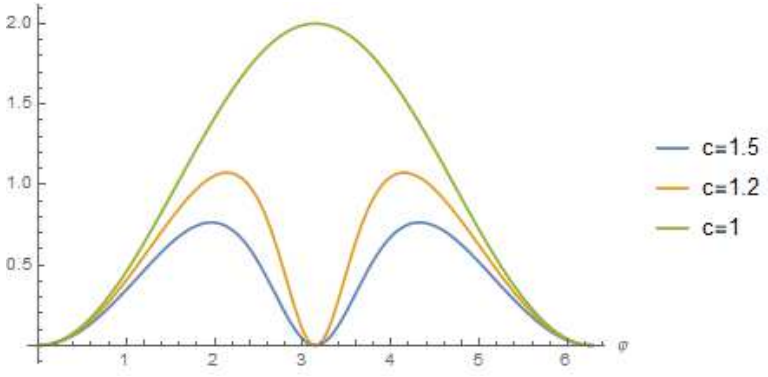

Figure D.2: $\frac{\cos^2\varphi}{c+\cos\varphi}$

Due to the symmetry of the integrand, one can write

$$\int_0^{2\pi} \mathrm{d}\varphi \, \frac{\sin^2\varphi}{c+\cos\varphi} = 2\int_0^{\pi} \mathrm{d}\varphi \, \frac{\sin^2\varphi}{c+\cos\varphi}. \tag{D.6}$$

For $c = 1$, Eq. (D.6) yields

$$2\int_0^{\pi} \mathrm{d}\varphi \, \frac{\sin^2\varphi}{1+\cos\varphi} = 2\pi, \tag{D.7}$$

for $c > 1$, the result is

$$\begin{aligned} 2\int_0^{\pi} \mathrm{d}\varphi \, \frac{\sin^2\varphi}{c+\cos\varphi} &= 2\left(c\varphi - 2\sqrt{c^2-1}\arctan\left(\frac{c-1}{\sqrt{c^2-1}}\tan\frac{\varphi}{2}\right) - \sin\varphi\right)\Bigg|_{\varphi=0}^{\pi} \\ &= 2\pi\left(c-\sqrt{c^2-1}\right). \end{aligned} \tag{D.8}$$

Taking the limit $c \to 1^+$

$$\lim_{c\to 1^+} 2\pi\left(c-\sqrt{c^2-1}\right) = 2\pi, \tag{D.9}$$

it can be seen that Eq. (D.8) $\to$ Eq. (D.7) for $c \to 1^+$. Therefore, Eq. (D.8) can not only be used for $c > 1$, but for $c \geq 1$.

Inserting Eq. (D.8) into Eq. (D.4) yields

$$\begin{aligned}\frac{1}{b}\int_0^{2\pi}\mathrm{d}\varphi\,\frac{\sin^2\varphi}{c+\cos\varphi} &= \frac{2\pi}{b}\left(c-\sqrt{c^2-1}\right)\\ &= \frac{\pi}{r_q r_l}\left(\frac{r_q^2+r_l^2}{2r_q r_l}-\sqrt{\left(\frac{r_q^2+r_l^2}{2r_q r_l}\right)^2-1}\right)\\ &= \frac{\pi}{r_q r_l}\left(\frac{r_q^2+r_l^2}{2r_q r_l}-\sqrt{\left(\frac{r_q^2-r_l^2}{2r_q r_l}\right)^2}\right)\\ &= \frac{\pi}{2}\frac{1}{(r_q r_l)^2}\left(r_q^2+r_l^2-\left|r_q^2-r_l^2\right|\right). \end{aligned} \tag{D.10}$$

To get the second line from the first one, Eq. (D.2) was used.

Now, one plugs Eq. (D.10) into Eq. (4.75), but before the limit $\Lambda_{UV}\to\infty$ was taken

$$\lim_{t\to\infty}\frac{\langle p_T^2\rangle_{\kappa(4)}}{2\pi B}m^2 = \frac{\pi}{2}\int_0^{\frac{\Lambda_{UV}}{m}}\mathrm{d}r_l\int_0^{\frac{\Lambda_{UV}}{m}}\mathrm{d}r_q\,r_l r_q\frac{r_q^2+r_l^2-\left|r_q^2-r_l^2\right|}{(r_q^2+1)^2(r_l^2+1)^2}. \tag{D.11}$$

The integrand is split to get rid of the absolute value

$$\begin{aligned} r_q\geq r_l \quad&\Rightarrow\quad r_q^2\geq r_l^2 \quad\Rightarrow\quad r_q^2+r_l^2-\left|r_q^2-r_l^2\right| = 2r_l^2,\\ r_q< r_l \quad&\Rightarrow\quad r_q^2< r_l^2 \quad\Rightarrow\quad r_q^2+r_l^2-\left|r_q^2-r_l^2\right| = 2r_q^2, \end{aligned} \tag{D.12}$$

and one obtains

$$\lim_{t\to\infty}\frac{\langle p_T^2\rangle_{\kappa(4)}}{2\pi B}m^2 = \frac{\pi}{2}\int_0^{\frac{\Lambda_{UV}}{m}}\mathrm{d}r_l\,\frac{r_l}{(r_l^2+1)^2}\left(\int_0^{r_l}\mathrm{d}r_q\,\frac{2r_q^3}{(r_q^2+1)^2}+\int_{r_l}^{\frac{\Lambda_{UV}}{m}}\mathrm{d}r_q\,\frac{2r_l^2 r_q}{(r_q^2+1)^2}\right). \tag{D.13}$$

The inner integrals are evaluated. The first one yields

$$\int_0^{r_l}\mathrm{d}r_q\,\frac{2r_q^3}{(r_q^2+1)^2} = -\frac{r_l^2}{r_l^2+1}+\ln(1+r_l^2), \tag{D.14}$$

and the second one gives

$$\int_{r_l}^{\frac{\Lambda_{UV}}{m}}\mathrm{d}r_q\,\frac{2r_l^2 r_q}{(r_q^2+1)^2} = -\frac{r_l^2}{1+\left(\frac{\Lambda_{UV}}{m}\right)^2}+\frac{r_l^2}{r_l^2+1}. \tag{D.15}$$

Note that the first term of Eq. (D.14) and the second term of Eq. (D.15) cancel each other. That leaves two terms in the outer integral remaining to be calculated

$$\begin{aligned}\int_0^{\frac{\Lambda_{UV}}{m}}\mathrm{d}r_l\,\frac{r_l}{(r_l^2+1)^2}\ln(1+r_l^2) &= -\frac{1+\ln\left(1+\left(\frac{\Lambda_{UV}}{m}\right)^2\right)}{2\left(1+\left(\frac{\Lambda_{UV}}{m}\right)^2\right)}+\frac{1}{2},\\ -\frac{1}{1+\left(\frac{\Lambda_{UV}}{m}\right)^2}\int_0^{\frac{\Lambda_{UV}}{m}}\mathrm{d}r_l\,\frac{r_l^3}{(r_l^2+1)^2} &= \frac{1}{2}\frac{1}{1+\left(\frac{\Lambda_{UV}}{m}\right)^2}\left(\frac{\left(\frac{\Lambda_{UV}}{m}\right)^2}{1+\left(\frac{\Lambda_{UV}}{m}\right)^2}-\ln\left(1+\left(\frac{\Lambda_{UV}}{m}\right)^2\right)\right). \end{aligned} \tag{D.16}$$

Putting everything together, one gets

$$\lim_{t\to\infty}\frac{\langle p_T^2\rangle_{\kappa\,(4)}}{2\pi B}m^2=\frac{\pi}{2}\frac{2\left(\frac{\Lambda_{UV}}{m}\right)^2+\left(\frac{\Lambda_{UV}}{m}\right)^4-2\left(1+\left(\frac{\Lambda_{UV}}{m}\right)^2\right)\ln\left(1+\left(\frac{\Lambda_{UV}}{m}\right)^2\right)}{2\left(1+\left(\frac{\Lambda_{UV}}{m}\right)^2\right)^2}. \tag{D.17}$$

This expression is finite $\forall\Lambda_{UV}$. Thus, $\langle p_T^2\rangle_{\kappa\,(4)}$ remains finite even for large times t, in contrast to $\langle p_z^2\rangle_{\kappa\,(4)}$, which diverges for $t\to\infty$.

Bibliography

[1] Edmond Iancu and Raju Venugopalan. The Color Glass Condensate and High Energy Scattering in QCD. In Rudolph C. Hwa and Xin-Nian Wang, editors, *Quark-gluon plasma 4*, pages 249–3363. 2003.

[2] Francois Gelis, Edmond Iancu, Jamal Jalilian-Marian, and Raju Venugopalan. The Color Glass Condensate. *Ann. Rev. Nucl. Part. Sci.*, 60:463–489, 2010.

[3] Daniil Gelfand, Andreas Ipp, and David Müller. Simulating collisions of thick nuclei in the color glass condensate framework. *Phys. Rev.*, D94(1):014020, 2016.

[4] T. Lappi. Production of gluons in the classical field model for heavy ion collisions. *Phys. Rev.*, C67:054903, 2003.

[5] F. Gelis. Color Glass Condensate and Glasma. *Int. J. Mod. Phys.*, A28:1330001, 2013.

[6] Raju Venugopalan. From Glasma to Quark Gluon Plasma in heavy ion collisions. *J. Phys.*, G35:104003, 2008.

[7] Alex Kovner, Larry D. McLerran, and Heribert Weigert. Gluon Production at High Transverse Momentum in the McLerran-Venugopalan Model of Nuclear Structure Functions. *Phys. Rev.*, D52:3809–3814, 1995.

[8] Miklos Gyulassy and Michael Plumer. Jet quenching in dense matter. *Phys. Lett.*, B243:432–438, 1990.

[9] David A. Appel. Jets as a probe of quark-gluon plasmas. *Phys. Rev. D*, 33:717–722, Feb 1986.

[10] Rolf Baier and Yacine Mehtar-Tani. Jet quenching and broadening: the transport coefficient $\hat{q}$ in an anisotropic plasma. *Phys. Rev.*, C78:064906, 2008.

[11] M. E. Carrington, St. Mrówczyński, and B. Schenke. Momentum broadening in unstable quark-gluon plasma. *Phys. Rev.*, C95(2):024906, 2017.

[12] David Müller. *Simulations of the Glasma in 3+1D*. PhD thesis, TU Wien, 2019.

[13] Axel Polaczek. The JIMWLK equation: Fundamentals and weak field expansion. Master's thesis, TU Wien, 2018.

[14] Larry D. McLerran and Raju Venugopalan. Computing Quark and Gluon Distribution Functions for Very Large Nuclei. *Phys. Rev.*, D49:2233–2241, 1994.

[15] Larry D. McLerran and Raju Venugopalan. Gluon Distribution Functions for Very Large Nuclei at Small Transverse Momentum. *Phys. Rev.*, D49:3352–3355, 1994.

[16] S. K. Wong. Field and Particle Equations for the Classical Yang-Mills Field and Particles with Isotopic Spin. *Il Nuovo Cimento A (1965-1970)*, 65(4):689–694, Feb 1970.

[17] M. E. Carrington, St. Mrówczyński, and B. Schenke. Momentum broadening in unstable quark-gluon plasma. *Phys. Rev.*, C95(2):024906, 2017.

[18] Daniel F. Litim and Cristina Manuel. Semi-classical transport theory for non-Abelian plasmas. *Phys. Rept.*, 364:451–539, 2002.

[19] Michael Peskin and Dan Schroeder. *An Introduction to Quantum Field Theory*. Westview Press, 1995.

[20] F. Bowman. *Introduction to Bessel Functions*. Dover Books on Mathematics. Dover Publications, 1958.